CONFIDENTIAL

Copy
RM L50A13

NACA RM L50A13

NACA

RESEARCH MEMORANDUM

PRELIMINARY INVESTIGATION OF A SUBMERGED AIR SCOOP UTILIZING BOUNDARY-LAYER SUCTION TO OBTAIN INCREASED PRESSURE RECOVERY

By Mark R. Nichols and P. Kenneth Pierpont

Langley Aeronautical Laboratory
Langley Air Force Base, Va.

NATIONAL ADVISORY COMMITTEE FOR AERONAUTICS

WASHINGTON
March 17, 1950

CONFIDENTIAL

NACA RM L50A13

NATIONAL ADVISORY COMMITTEE FOR AERONAUTICS

RESEARCH MEMORANDUM

PRELIMINARY INVESTIGATION OF A SUBMERGED AIR SCOOP UTILIZING BOUNDARY-LAYER SUCTION TO OBTAIN INCREASED PRESSURE RECOVERY

By Mark R. Nichols and P. Kenneth Pierpont

SUMMARY

A submerged air scoop consisting essentially of a conventional scoop located in a dimple in the fuselage surface has been investigated preliminarily at low speeds. The inlet had an entrance width-height ratio of about 3.7 and a steep approach ramp (19° at the entrance) which provided a short and compact installation. The internal and external flow characteristics of the basic inlet without boundary-layer control were studied by means of pressure and tuft surveys over a wide range of inlet-velocity ratio. Studies were then conducted to determine the effects of boundary-layer control, suction-slot location and model configuration, and variations of boundary-layer thickness on inlet performance. A self-activating boundary-layer bypass was incorporated in the final arrangement tested. An indication of the external drag was obtained by wake surveys downstream of the scoop and by pressure surveys in the boundary-layer suction flow.

In the presence of a thin initial turbulent boundary layer representative for a fighter airplane in the high-speed high-altitude flight condition, the peak total-pressure recovery at the end of the 2:1 area ratio diffuser of the basic inlet without boundary-layer control was $0.83q_0$ and occurred at an inlet-velocity ratio of 1.1. Application of boundary-layer control increased the pressure recovery markedly over the entire inlet-velocity-ratio range and shifted the peak pressure recovery to a much lower value of inlet-velocity ratio. In the final arrangement tested, a suction quantity of 11.7 percent of the entering flow produced calculated increases in maximum net thrust of 6.2 percent or greater and calculated reductions in specific fuel consumption of 3.1 percent or greater (compared to the basic inlet without boundary-layer control) for a typical jet-engine installation operating at a flight speed of 600 miles per hour. It appears that the flow instability frequently encountered in the case of twin internally coupled inlets will be avoided with this arrangement for design high-speed inlet-velocity ratios as low as 0.5.

Appreciable increases in the thickness of the initial boundary layer caused significant decreases in inlet performance which cannot be overcome simply by increasing the suction quantity. Hence, the inlet appears desirable for application only at forward locations on the fuselage where the boundary layer is relatively thin.

INTRODUCTION

In modern thin-winged fighter aircraft, equipment such as the radar scanner and guns must be located on the fuselage nose. This placement of equipment frequently rules out the nose inlet and necessitates the use of either the wing-root inlet or the fuselage scoop. The submerged version of the fuselage scoop, the subject of this paper, is of interest in such cases because installation usually can be accomplished without increasing the frontal area or changing the basic lines of the body and, presumedly, without increasing the drag of the body importantly. A secondary advantage of the submerged scoop is that the ingestion of foreign material into the ducting is reduced as compared to other types of inlets by external inertia separation.

A satisfactory internal-flow pressure recovery is more difficult to achieve with a submerged inlet than with a conventional protruded inlet for two reasons: (1) the submerged approach ramp tends to confine the boundary layer approaching the entrance and to prevent it from being swept outboard around the entrance, as happens to an important extent in the case of the protruded inlet (see reference 1); and (2) the flow ahead of the entrance must turn inward where the floor of the approach ramp diverges from the basic fuselage contour. This turning of the flow decreases the surface pressures in this region and thus, by increasing the magnitude of the over-all pressure rise along the ramp, causes the boundary layer on the ramp to thicken more rapidly and to separate farther upstream than in the case of the protruded inlet. The increased flow velocity in this region also may cause important decreases in internal-flow pressure recovery due to boundary-layer-shock interaction at free-stream Mach numbers appreciably lower than those for the protruded inlet.

One type of submerged inlet, described in references 2 and 3, has been investigated previously by the National Advisory Committee for Aeronautics. This inlet has an approach ramp which diverges from the basic fuselage surface at an angle of about 7° and is bounded at the sides by trumpet-shaped walls which are approximately perpendicular to the fuselage surface. As described in reference 3, vortices originating at the tops of these ramp walls prevent most of the boundary layer outboard of the ramp walls from entering the ramp in the high-speed range of inlet-velocity ratio. Thus, as in the case of the protruded

inlet, a large proportion of the fuselage boundary layer bypasses the entrance in this range of inlet-velocity ratio. As stated in reference 3, the effectiveness of this self-activating boundary-layer control decreases as the inlet-velocity ratio is increased to values typical for climbing flight because a large proportion of the vortex flow then enters the inlet.

A second type of submerged inlet is the subject of the present investigation. This inlet, designated a submerged scoop, consists essentially of a conventional scoop located in a dimple in the fuselage surface deep enough to permit complete submergence of the air inlet and wide enough to provide "gutters" on each side of the scoop. If a large proportion of the ramp boundary layer can be made to bypass the entrance through these gutters, this arrangement, in the absence of shock waves, should provide internal-flow pressure recoveries only slightly lower than those obtained with conventional protruded inlets.

Inasmuch as a suitable high-speed facility was not immediately available for this type of research, the present preliminary phase of the investigation was conducted at low speeds in the $\frac{1}{15}$-scale model of the full-scale tunnel, which is described in reference 4. The results obtained obviously are directly applicable only to subcritical flight Mach numbers. Large changes in the performance characteristics of the inlet might occur at flight speeds appreciably exceeding those corresponding to the initial attainment of sonic velocity on the approach ramp.

The model was installed in a groundboard curved in the transverse direction to simulate the side of a typical fuselage. The test inlet had a width-height ratio of about 3.7 and incorporated a steep approach ramp (19° at the entrance) which provided a short and compact installation at the expense of an increase in the magnitude of the negative pressure peak at the start of the approach ramp. The internal and external flow characteristics of the basic inlet without boundary-layer control were studied by means of pressure and tuft surveys over a wide range of inlet-velocity ratio. Studies were then conducted to determine the effects of boundary-layer control, suction-slot location, and model configuration, and variations of boundary-layer thickness on inlet performance. A self-activating boundary-layer bypass was incorporated in the final arrangement tested. The benefits obtained by the use of boundary-layer control are discussed quantitatively in terms of the performance of a typical jet-engine installation.

External drag could not be determined directly in the present tests because of the obvious limitations of the experimental apparatus. An indication of the drag characteristics of the inlet at subcritical speeds

was obtained, however, by means of wake surveys downstream of the scoop and by pressure surveys in the boundary-layer suction flow.

SYMBOLS

C_D drag coefficient $\left(\frac{\text{Drag}}{q_o A_i}\right)$

C_Q suction-flow coefficient based on boundary-layer thickness 20 inches ahead of scoop lip $\left(\frac{Q_s}{V_o \delta^* b}\right)$

C_q suction-flow coefficient based on inlet area of main duct $\left(\frac{Q_s}{A_i V_o} = \frac{Q_s}{Q_d}\left(\frac{V_i}{V_o}\right)\right)$

V_i/V_o inlet-velocity ratio $\left(\frac{Q_d}{A_i V_o}\right)$

A area

b span of suction slot

H total pressure

H' boundary-layer shape parameter $\left(\frac{\delta^*}{\theta}\right)$

h inlet height of boundary-layer slot

M_{cr} predicted critical Mach number

p static pressure

P static-pressure coefficient $\left(\frac{p - p_o}{q_o}\right)$

Q volume rate of flow

q dynamic pressure $\left(\frac{1}{2}\rho V^2\right)$

V flow velocity

x distance parallel to surface of fuselage (see table I; station 0 corresponds to lip leading edge of configuration I)

y distance from plane tangent to fuselage at center line of inlet (See table I.)

y' distance measured perpendicular to surface

z distance from plane of symmetry of inlet (See table I.)

ρ mass density of air

δ total thickness of boundary layer

δ^* displacement thickness of boundary layer $\left(\int_0^{\delta} \left(1 - \frac{V}{V_b}\right) dy'\right)$

θ momentum thickness of boundary layer $\left(\int_0^{\delta} \frac{V}{V_b}\left(1 - \frac{V}{V_b}\right) dy'\right)$

Subscripts:

av average value weighted according to mass flow in case of main duct and according to area in case of suction ducts

b point just outside boundary layer

d end of diffuser of main duct

i point of minimum area near entrance of main duct

o free stream

s boundary-layer suction flow

1 suction slot in ramp ahead of entrance

2 suction slot in duct floor downstream of entrance

APPARATUS AND TESTS

A schematic diagram of the test setup is shown in figure 1 and views of typical scoops are shown in figure 2. Line drawings comparing the six scoop configurations are presented as figure 3; details of the boundary-layer-removal systems are given in figures 4 and 5; and surface ordinates are given in tables I and II.

The minimum area near the entrance of the main duct was 25.1 square inches for configurations I, II, and III and 24.7 square inches for configurations IV, V, and VI. The measuring station in the inlet was located in the diffuser 3.4 inches downstream of the lip. The upper and lower walls of the internal diffuser diverged at an included angle of 6° from the minimum area station to an area of 49.7 square inches at the rear measuring station so that an area expansion ratio of about 2 was provided.

The internal-flow system (fig. 1) included an axial-flow fan and a butterfly-type valve in the main duct and in each boundary-layer-removal duct to permit testing over wide ranges of flow rates. The quantity of internal flow in each duct was measured by means of a calibrated venturi. In the final configuration tested, a part of the boundary-layer suction flow was not carried outside the tunnel but was ducted to exits at the sides of the scoop as might be desirable in an actual installation. (See figs. 2(d), 2(e), and 5.) In this case, the suction flow was determined from the readings of total-pressure and static-pressure tubes located just inside the exits of the bypass ducting. (See fig. 6(e).)

Pressures at the entrance and end of the diffuser of the main duct and at the ends of the diffusers of the boundary-layer slots were measured by means of the rakes of total-pressure and static-pressure tubes located as shown in figure 6. The inlet rake of the main duct was always removed when measuring pressures at the end of the diffuser of this duct. Surface pressure measurements were obtained by the use of flush orifices. Boundary-layer surveys ahead of the inlet were conducted using a total-pressure and static-pressure probe suspended from a rigid frame above the test section. The total-pressure tube in this probe was of 0.040-inch-outside-diameter tubing (0.002-inch wall thickness) flattened so that the over-all thickness of the front end of the tube was 0.012 inch. A micrometer screw at the top of the boundary-layer-probe support strut permitted accurate positioning of this total-pressure tube with respect to the surface of the model. The static-pressure tube in the probe was located 1/2 inch above the total-pressure tube. Boundary-layer surveys aft of the scoop lip were made by the use of rakes of total-pressure and static-pressure tubes shown in figure 2(b).

All pressure measurements on the model were recorded by photographing a multitube manometer. The differential pressures of the several venturis and the survey-probe pressures were read visually from micromanometers. Tufts were used to observe the direction and stability of the flow. Plexiglass windows were installed at several points in the ducting to facilitate observation of the flow within the diffuser.

Each of the inlet configurations was investigated in conjunction with one or more of the turbulent boundary layers 20 inches ahead of the scoop lip shown in figure 7. Boundary layer A was the boundary layer on the groundboard surface without artificial thickening. Boundary layer B, which is considered to be approximately representative of full-scale conditions just ahead of the wing of a fighter airplane in the high-speed high-altitude flight condition with regard to its thickness relative to the inlet height, was obtained by shellacking a 9-inch-wide band of coarse sand to the groundboard surface 40 inches ahead of the scoop lip. Boundary layer C, which was tested to determine the effects of locating this type of inlet in a region of thick boundary layer, was obtained by laying turbulence rods transversely on either side of the sand strip used to generate boundary layer B. The displacement thicknesses (δ^*) of the three boundary layers at station -20 were 0.073, 0.085, and 0.169 inch in alphabetical order. The corresponding shape parameters $\left(H' = \frac{\delta^*}{\theta}\right)$ were 1.36, 1.29, and 1.24, as compared to the value of 1.286 for the $\frac{1}{7}$-power variation.

All tests were conducted at a tunnel speed of about 100 feet per second which corresponds to a Reynolds number of approximately 1.4×10^5 based on the inlet height.

RESULTS AND DISCUSSION

The quantity of boundary-layer suction flow usually is expressed in the present paper in terms of the suction-flow coefficient $C_Q = \frac{Q_s}{V_o \delta^* b}$. This coefficient has physical significance in that it is the ratio of the quantity of flow entering the suction slot to the quantity of flow displaced by the boundary layer at station -20 over a transverse distance equal to the suction-slot span b. The value of this coefficient required to obtain a given total-pressure recovery in the main duct would be expected to remain nearly constant over a broad range of initial boundary-layer thickness. The ratio of the quantity of suction flow to the flow quantity of the main duct may be readily determined by converting the

form of flow coefficient from C_Q to the equivalent value of $C_q = \frac{Q_s}{A_i V_o}$ by use of figure 8. For an inlet-velocity ratio of unity, the value of C_q gives the flow ratio Q_s/Q_d directly; for other inlet-velocity ratios $\frac{Q_s}{Q_d} = \frac{C_q}{V_i/V_o}$.

All results discussed are those obtained with initial boundary layer B (fig. 7) unless otherwise noted. In the case of arrangements using two boundary-layer suction slots in tandem, the downstream slot always was faired out if a suction-flow coefficient is given for the upstream slot only.

Study of Basic Inlet without Suction

Flow along ramp and duct bottom.- Static-pressure distributions along the center line of the ramp and duct bottom of slotless configuration I (figs. 2(a) and 3) are shown in figure 9(a). The negative pressure peak in the region of substream pressure required to turn the flow ahead of the entrance occurred about 4 inlet heights ahead of the scoop lip. This negative pressure peak increased in value from $-0.15q_c$ to $-0.30q_o$ and moved slightly aft as the inlet-velocity ratio was increased from 0.31 to 1.54. Downstream of this negative pressure peak the surface pressure increased to a point $1\frac{1}{2}$ to 2 inlet heights ahead of the scoop lip as the flow diffused along the ramp and then changed rapidly to the entrance pressure which was determined by the inlet-velocity ratio, the inlet-velocity distribution, and the total-pressure losses ahead of the inlet.

Static-pressure distributions in the valley approaching the inner corner of the inlet and along the edge of the dimple are presented in figures 10(a) and 11(a), respectively. In each case, the negative pressure peak near the crest of the ramp off the center line never exceeded that at the ramp center line. The pressures in the valley near station 0 were much more negative at the higher inlet-velocity ratios than those at the ramp center line because of the large induced velocities at the inner side of the scoop lip. (See fig. 12(a).)

At inlet-velocity ratios below about 0.5, tuft observations showed that the boundary layer on the approach ramp separated ahead of the inlet somewhat downstream of the stations where the surface pressure distributions flatten out. (See distribution for $\frac{V_i}{V_o} = 0.31$, fig. 9(a).) As the inlet-velocity ratio was increased, the point of separation

moved progressively downstream and passed the measuring station at the end of the diffuser at an inlet-velocity ratio of about 1.0. The flow into the inner corner of the inlet was observed to be appreciably rougher than the entering flow at the center line. Tuft observations showed that this roughness was caused mainly by some of the boundary layer outside the span of the inlet flowing down the approach valley and entering the inlet rather than passing outboard through the gutter as was desired.

The boundary-layer thickness at the center line of the entrance measuring station decreased rapidly with increases in inlet-velocity ratio as the point of initial flow separation moved downstream along the ramp and duct bottom, figure 13(a). An inlet-velocity ratio greater than 0.6 was required to obtain an H' value as low as 2.6, the approximate upper limiting value for unseparated flow. (See reference 5.)

Total-pressure recovery.- The average total-pressure recovery at the entrance measuring station increased rapidly with inlet-velocity ratio from $0.67q_0$ at $\frac{V_i}{V_o} = 0.26$ to $0.88q_0$ at $\frac{V_i}{V_o} = 0.75$, as the ramp boundary layer thinned rapidly, and then increased more slowly to $0.92q_0$ at $\frac{V_i}{V_o} = 1.54$. (See fig. 14(a).) The average total-pressure recovery at the end of the diffuser likewise increased from a value of $0.53q_0$ at an inlet-velocity ratio of 0.26 to a value of $0.83q_0$ at an inlet-velocity ratio of about 1.1, but then dropped off again with further increases in inlet-velocity ratio because of an increase in the diffuser losses.

External flow.- The surface pressures at the edge of the dimple aft of the scoop lip (fig. 11(a)) generally were more negative than the surface pressures in the intersection of the scoop lip with the gutter floor (fig. 12(a)). As a result, the boundary layer on the floor of the gutter tended to flow outward over the edge of the gutter at all inlet-velocity ratios.

Tuft observations showed that the approaching flow was approximately alined with the base, top-center-line, and top-corner sections of the scoop lip at inlet-velocity ratios of the order of 0.5. At higher inlet-velocity ratios, the flow approached these sections from the outside at an angle which increased gradually with increases in the inlet-velocity ratio. The top portion of the scoop lip, figure 3(a), was well suited to this flow pattern since it incorporated reverse camber and a thick internal fairing.

Comparison of Arrangements Utilizing Boundary-Layer Control

Inasmuch as the internal-flow pressure recoveries obtained with configuration I were undesirably low, a study of arrangements utilizing boundary-layer suction to obtain increased pressure recovery was undertaken.

Configurations II and III.- In configuration II, a flush suction slot shaped in accordance with the principles of reference 6 was installed in the approach ramp 3.82 inches (1.40 inlet heights) ahead of the scoop lip. This slot (figs. 3 and 4) was similar to that illustrated in figure 2(a) and had a width of 0.187 inch and a span of 14 inches compared to the entrance width of 10 inches. The location of the suction slot corresponds approximately to the most forward separation point observed for slotless configuration I for $\frac{V_i}{V_o} = 0.4$.

The original version of configuration III, figure 2(a) was identical to that for configuration II except that the suction slot was located 5 inches (1.83 inlet heights) ahead of the scoop lip. In the course of preliminary tests, however, it was found necessary to relieve the central portion of the ramp ahead of this slot and to extend the center of this slot lip forward to 5.2 inches (1.90 inlet heights) ahead of station 0 (thus providing a submerged scoop-type slot at the center line) in order to obtain reasonable spanwise uniformity of the suction flow at the lower suction-flow coefficients. (See figs. 2(b), 3, and 4.) At the same time, the span of this slot was reduced to 12.24 inches inasmuch as this small reduction in span had no measurable effect on the inlet flow, and the gutter was deepened a small amount (fig. 3) in an attempt to improve the flow into the corners of the inlet. The camber of the scoop lip also was increased positively (fig. 3(a)) to allow for the change in flow direction at the lip that was observed to occur when boundary-layer control was applied to the ramp.

The application of boundary-layer suction to the approach ramp caused large increases in static pressure and large decreases in boundary-layer displacement thickness downstream of the suction slot at the lower inlet-velocity ratios. (Compare results for configurations I and III, figs. 9 and 13(b).) In both configurations II and III, a suction-flow coefficient of about 0.7 was required to obtain a reasonably uniform flow into the suction slot. As illustrated for configuration III in figure 15(a), a suction-flow coefficient of 0.8 caused large increases in the average total-pressure recovery at the end of the diffuser compared to the recoveries for slotless configuration I (about $0.1q_o$ at a typical high-speed inlet-velocity ratio of 0.6). Above this value,

the average total-pressure recoveries at the inlet and end of the diffuser continued to increase with further increases in suction-flow coefficient, but at a decreasing rate. Doubling the suction-flow coefficient produced an additional increase of only about $0.03q_o$ at the end of the diffuser at $\frac{V_i}{V_o} = 0.6$; however, the minimum inlet-velocity ratio for the same total-pressure recovery was reduced to about 0.48. The increases in total-pressure recovery obtained by use of the suction were large at the lower inlet-velocity ratios, but were small at inlet-velocity ratios of 1.0 and greater for which the entering boundary layer for slotless configuration I was already thin and unseparated. (See fig. 13(a).) It is noted that the total-pressure recoveries given for the inlet of configuration III at inlet-velocity ratios above 1.0, which are shown to be less than those for slotless configuration I in some cases, are believed to be lower than the true values.

At the maximum suction-flow coefficients investigated (1.5 for configuration II and 1.6 for configuration III) the average total-pressure recoveries at the inlets of configurations II and III were about equal. (See fig. 14(a).) The average total-pressure recoveries at the end of the diffuser of configuration III were somewhat larger than those for configuration II $\left(0.04q_o \text{ at } \frac{V_i}{V_o} = 0.6\right)$. It is believed that the lower recovery for configuration II resulted from a break in the duct floor at station 0.51 (fig. 3(a)) which may have caused flow separation; this break was faired out with a larger radius in configuratio III. The near equality of the entrance total-pressure recoveries shows that the two suction slots were about equally effective and that the pressure-recovery characteristics of this type of inlet are not critically sensitive to small variations in suction-slot location.

Tuft observations of configurations II and III showed that neither suction slot was effective in eliminating the flow roughness at the inner corners of the inlet which had been observed in the flow studies of configuration I. In each case some of the boundary layer outboard of the slot ends was drawn into the slot. Some of the boundary layer still further outboard then flowed into the ramp and entered the inlet. Additional arrangements were investigated, therefore, to determine if the rough flow into the corner of the inlet could be eliminated by changes in the scoop configuration. Inasmuch as the average total-pressure recoveries measured in the suction slots after diffusion, figures 16(a) and 16(d), were undesirably low, all succeeding suction slots were designed for lower slot inlet-velocity ratios. Raised scoop-type slots were used in most cases in an attempt to recover a larger percentage of the dynamic pressure in the boundary-layer flow.

Configuration IV.- In configuration IV, figures 2(c), 3, and 4, the point of divergence of the ramp from the basic fuselage contour was varied in the transverse direction from the original position at the center line to about half the original distance ahead of the entrance at the ends of the scoop. As shown in figure 2(c) the divergence of the crest lines of the revised dimple was similar in shape to the divergence of the ramp walls of the submerged inlet of references 2 and 3. The present arrangement differed greatly from this submerged inlet, however, in that the surface was smoothly faired at all points and that the divergence terminated at the edges of the original dimple outboard of the scoop ends rather than at the scoop ends themselves. It was hoped that this change in dimple shape would provide transverse gradients between the positive pressures at the center line of the ramp and the negative pressures along the ramp crest lines ahead of the scoop ends large enough to cause most of the ramp boundary layer to flow around the ends of the scoop at low inlet-velocity ratios.

With boundary layer A, the average total-pressure recovery measured at the end of the diffuser of configuration IV with a suction-flow coefficient of 1.7 was higher than that for configuration III with a suction-flow coefficient of 1.6 at inlet-velocity ratios below 0.7. (See upper graph of fig. 14(b).) Tuft observations at and below this value of inlet-velocity ratio showed that the flow separated from the dimple crest 3 to 5 inches on each side of the center line and that strong vortices originated at the points of flow separation. These vortices, which were similar to those observed for the NACA submerged inlet (reference 3), entrained large amounts of boundary layer from the ramp floor, passed down the gutters, and then drifted outboard into the flow above the fuselage surface. It was found possible to fair over the outer quarters of the suction slot (thereby reducing the over-all suction quantity by one-half) without affecting the pressure recovery at the end of the diffuser.

The total-pressure recovery for configuration IV was less than that for configuration III in the higher range of inlet-velocity ratio, figure 14(b). Also it appeared that the vortices shed at low inlet-velocity ratios might cause large increments in pressure drag on the aft portions of the fuselage and wing in the high-speed flight condition. The drag of these vortices could not be evaluated in the present setup; further investigation of this arrangement was therefore discontinued pending the obtainance of drag data in future complete-model tests.

Configuration V.- In configuration V (figs. 2(d), 2(e), 3, and 4) the ends of the scoop were slanted forward to the lip of a raised scoop-type boundary-layer slot which was long enough to extend into the gutters slightly outboard of these scoop lip extensions. This suction slot was located 3.81 inches (1.39 inlet heights) ahead of station 0 and had an inlet height of 0.35 inch and a span of 11.88 inches. A

second suction slot installed in the duct floor 3.09 inches (1.13 inlet heights) downstream of station 0 also was investigated to see if additional boundary-layer removal at this point would yield major gains in pressure recovery at the lower inlet-velocity ratios. This second slot (figs. 2(e) and 3(a)) was a flush scoop-type slot and had a height of 0.22 inch over the floor of the duct. The height of the slot tapered to 0.1 inch at the tops of the 0.5-inch-radius fillets in the bottom corners of the duct.

Most of the gutters aft of the scoop lip extensions were faired out. This partial fairing out of the gutters increased the amount of gutter boundary layer flowing over the scoop lip extensions into the inlet. It was considered desirable, however, because it provided smooth flow outboard of the scoop ends and greatly reduced the amount of fuselage surface distorted by the scoop installation. The tendency of the gutter boundary layer to flow outward over the edge of the dimple was eliminated apparently because of the changes in the surface pressures along the edge of the dimple relative to the surface pressures at the base of the scoop lip. (See figs. 11, 12(a), and 12(b).)

Use of the raised scoop-type suction slot increased the surface pressures on the ramp ahead of the slot a small amount over those observed for the arrangements with flush suction slots. (Compare fig. 9(b) with fig. 9(c) and fig. 10(b) with fig. 10(c).) However, a static-pressure peak existed on the lip of this slot for most operating conditions, figures 9(c) and 10(c). This type of pressure peak is characteristic of raised scoop-type slots operating at low value of slot inlet-velocity ratio, but does not occur in the case of flush slots, figures 9(b) and 10(b). The boundary-layer-displacement thickness at the center line of the entrance was slightly greater at a typical high-speed inlet-velocity ratio of 0.52 than those for configurations II and III, probably because of the presence of this pressure peak, figure 13(b).

Tuft observations showed that the flow into the corners of the inlet of configuration V was much smoother than that for configuration III. This improvement in the flow approximately compensated for the increased thickness of the boundary layer entering the center portion of the inlet. At comparable suction-flow coefficients, the average total-pressure recoveries for configuration V with only the ramp suction slot operating were slightly higher than those for configuration III at inlet-velocity ratios above 0.7 and somewhat lower than those for configuration III at inlet-velocity ratios below 0.7, figure 14(a).

Operation of the second suction slot in conjunction with the ramp slot caused a further increase in the static pressures downstream of the second slot (compare figs. 9(c) and 9(d)) and an appreciable increase

in average total-pressure recovery at the end of the diffuser over most of the test range of inlet-velocity ratio, figure 14(c). Total-pressure recoveries measured at the end of the diffuser at $\frac{V_i}{V_o} = 0.52$ are presented in figure 17 as a function of the suction-flow coefficients of the ramp and second slots. An examination of the lines of constant $\left(C_{Q_1} + C_{Q_2}\right)$ superimposed on this plot shows that the total-pressure recovery was essentially independent of the distribution of suction between the two slots so long as the ramp slot was operating at a suction-flow coefficient greater than about 1.4, apparently the minimum value required to prevent flow separation between the two slots. This insensitivity of the total-pressure recovery to the distribution of suction between the two slots prevailed over most of the inlet-velocity-ratio range. (See fig. 14(c).) Thus, for a given suction quantity, no gain in effectiveness of the boundary-layer removal system was obtained by the addition of the second slot.

The average total-pressure recoveries in the ramp suction slot of configuration V (after an area expansion of 2:1) at a suction-flow coefficient of 1.7 were about $0.11q_o$ greater than those for configuration III at a suction-flow coefficient of 1.6 over the entire test range of inlet-velocity ratio, figure 16(d). These total-pressure recoveries were not changed to a major extent by large increases in suction-flow coefficient or by operation of the second slot, figure 16(b).

With a suction-flow coefficient of 1.7 into the ramp slot, the total-pressure recovery in the second suction slot of configuration V (also after an area expansion of 2:1) was much higher at a suction-flow coefficient of 0.9 than that for the ramp slot in the high-speed range of inlet-velocity ratio (compare figs. 16(d) and 16(e)). The total-pressure recovery in the second slot decreased rapidly, however, with increases in suction coefficient and with increases in inlet-velocity ratio. In all cases, the total-pressure recovery became negative at inlet-velocity ratios above about 1.2. The rapid decrease of the total-pressure recovery of the second slot with increasing inlet-velocity ratio was caused apparently by the slot being located in a region where the static pressure decreased rapidly with increases in inlet-velocity ratio, figure 9(a).

Inasmuch as the average total-pressure recovery at the end of the diffuser of configuration V was about the same as that for configuration III, configuration V is considered to be definitely preferable to configuration III because of: (1) the much greater pressure recovery in the suction flow of the ramp slot after diffusion; (2) the greater smoothness of the external flow; and (3) the reduced distortion of the

fuselage surface. The use of the second suction slot of configuration V is not considered desirable, however, because: (1) the gain in total-pressure recovery obtained by its use is no greater than that obtained by increasing the suction quantity of the ramp slot an equal amount; and (2) the total-pressure recovery in the suction flow entering this slot becomes negative or undesirably low at the higher inlet-velocity ratios which are encountered in take-off and climbing flight.

Configuration VI.- A total-pressure recovery at the end of the diffuser of $0.9q_0$ is usually considered to be the minimum value acceptable for modern turbojet aircraft in the high-speed and cruise flight conditions. The results for configuration V show that suction quantities of 15 to 25 percent of the entering flow were required to obtain this value in the high-speed range of inlet-velocity ratio. Only 5 to 10 percent of the air flow to the engine is required usually for engine and tail-pipe cooling. The problem of efficiently handling and disposing the suction flow in excess of the amount required for cooling therefore arises in the process of applying configuration V to an actual airplane.

It appeared that a possible solution to this problem would be an arrangement in which all or part of the suction flow entering the ramp slot is bypassed to the fuselage surface as close as possible to the slot inlet as was done for a protruded scoop in reference 7. This type of arrangement was investigated in configuration VI (figs. 2 to 4), which was exactly the same as configuration V except for the ducting and exits of the ramp suction slot (fig. 5).

The suction-flow coefficient provided by the bypass, figure 18, varied from a maximum of 1.97 at the lowest inlet-velocity ratio of 0.31 to a minimum of 0.8 at the highest inlet-velocity ratio of 1.54. This decrease in suction-flow coefficient with increasing inlet-velocity ratio was caused mainly by the corresponding decrease of static pressure in the region of the slot inlet. (See fig. 9.)

As shown by a comparison with the results for configuration V for a constant suction-flow coefficient of 1.7, figure 14(d), the effect of the variable suction flow provided by the bypass of configuration VI was to increase the average total-pressure recoveries at the lower inlet-velocity ratios and to decrease these recoveries at the higher inlet-velocity ratios. The maximum total-pressure recovery at the end of the diffuser of configuration VI was about $0.03q_0$ greater than that for configuration V although the suction coefficients were nearly the same for the two arrangements at the inlet-velocity ratio corresponding to peak recovery for configuration VI. It was found that the pressure recoveries obtained with configuration VI were consistently higher than those for configuration V at equal suction-flow coefficients. This

difference may have been caused by a dissymmetry in the suction flow entering the ramp slot of configuration VI. Tuft observations showed that appreciably more flow entered the outer quarters of the slot than entered in the central half.

The peak total-pressure recovery at the end of the diffuser of configuration VI with only the ramp suction slot operating was $0.905q_o$ as compared to $0.83q_o$ for slotless configuration I, and the suction shifted the inlet-velocity ratio for peak pressure recovery from 1.1 for configuration I to about 0.83 for configuration VI. (See fig. 15(c).) At this inlet-velocity ratio the suction-flow coefficient for configuration VI was about 1.66 (fig. 18) or about 8 percent of the entering flow (fig. 8).

The total-pressure recovery at the exit of the bypass ducting of configuration VI, figure 16(c), was only $0.10q_o$ to $0.18q_o$ over the test range of inlet-velocity ratio; thus, on the basis of the results for configuration V, fig. 16(b), the losses in the additional ducting used in this arrangement amounted to about $0.15q_o$. This loss is regarded as excessive. It probably could be reduced appreciably by more careful design of the bypass ducting.

Performance of Configurations V and VI with Boundary Layer B

Configurations V and VI are considered to be the most desirable arrangements investigated. The results obtained with these arrangements are summarized in this section of the paper and are analyzed to indicate the optimum design conditions and the benefits obtained through the use of boundary-layer control. At the present time, the over-all performance of these inlets cannot be compared with the over-all performance of other types of fuselage scoops and wing-root inlets because comprehensive external-drag data are not available either for the present inlets or for any other inlet of this general class.

Total-pressure recovery.- The average total-pressure recoveries in the main ducts and boundary-layer removal systems of configurations V and VI are summarized in figures 15(b), 15(c), and 16. As previously noted, the use of the second slot inside the inlet is not considered desirable because of the low total-pressure recovery in the suction flow entering this slot at the higher inlet-velocity ratios. However, it has been shown also that the total-pressure recovery at the end of the diffuser of the main duct was essentially independent of the distribution of suction between the ramp and second slots so long as the ramp slot was operating at a suction-flow coefficient greater than

about 1.4. Thus, the total-pressure recoveries at the ends of the main-duct diffusers of the two-slot versions of configurations V and VI, given in figures 15(b) and 15(c), furnish an acceptably accurate indication of the total-pressure recoveries that would be obtained at the end of the diffusers of the single-slot versions of these configurations at suction-flow coefficients greatly exceeding the maximum values investigated.

It is noted in figure 15 that when sufficient suction flow was provided to obtain a peak total-pressure recovery at the end of the diffuser of $0.90q_o$ or greater, the total-pressure recovery at this point remained above $0.85q_o$ over a range of inlet-velocity ratio broad enough to cover the more important flight conditions. It also is noted in figure 15 that the peak total-pressure recovery at the end of the diffuser with the maximum suction-flow coefficient investigated was lower than that which would be obtained by a well-designed nose inlet even without boundary-layer control. The use of the present type of inlet can be justified, therefore, only on the basis of a design compromise.

The over-all induction losses measured at the end of the diffuser of configuration V at an inlet-velocity ratio of infinity (V_i = 100 ft/sec, V_o = 0) are presented as a function of the inlet dynamic pressure in the following table:

Condition	$\frac{H_o - H_d}{q_i}$
Both slots sealed and faired	0.033
Both slots vented to room pressure	.034
$\frac{Q_1}{Q_d} = 0.066$, $\frac{Q_2}{Q_d} = 0.032$	.036

These small induction losses indicate that an auxiliary inlet (or "blow-in door") would not be required to increase the take-off thrust of a jet airplane utilizing this type of air inlet.

Diffusion effectiveness.- The static-pressure recovery at the end of the diffuser, figure 19, is the lower limit of the total-pressure recovery that would be obtained after any additional amount of diffusion and also is a direct measure of the over-all diffusion effectiveness of the inlet-diffuser combination. As shown in this figure, the static-pressure recovery for slotless configuration I was $0.4q_o$ to $0.5q_o$ less

than the theoretical value for uniform frictionless flow, the differences being chargeable to the total-pressure losses and the nonuniformity of the flow at the measuring station. The effectiveness of boundary-layer suction in increasing the over-all diffusion effectiveness is shown by the large increases in static-pressure recovery obtained by the application of suction. A total suction coefficient $\left(C_{Q_1} + C_{Q_2}\right)$ of 2.6 provided a gain in static-pressure recovery throughout the high-speed range of inlet-velocity ratio equal to about one-half of the differences between the values for slotless configuration I and the ideal values which are approached closely by a well-designed nose inlet.

Velocity distributions in internal flow.- Representative distributions of the flow velocity at the inlet and end-of-the-diffuser measuring stations of configuration V are presented in figures 20(a) and 20(b), respectively. As previously noted, the inlet measuring station actually was located in the diffuser after appreciable area expansion; hence the velocity ratios given for this station are lower than those for the minimum area station of the entrance on which the nominal inlet-velocity ratios were based. With an inlet-velocity ratio of 0.52 and a suction-flow coefficient of 1.7, the flow-velocity distributions at both stations were very nonuniform, mainly because of the thick residual boundary layer entering along the ramp. (See fig. 13(b).) Inasmuch as the entering boundary layer thinned rapidly with increasing inlet-velocity ratio (for example, see fig. 13(a)), the flow distributions became appreciably more uniform as the inlet-velocity ratio was increased to 1.03 (fig. 20). The improvement in uniformity of the flow distribution caused by increasing the inlet velocity from 0.52 to 1.03 was much greater than that obtained at an inlet-velocity ratio of 0.52 by increasing the suction-flow coefficient from 1.7 to 2.6, for which the improvement in flow uniformity was negligible. It appears that a prohibitively high suction-flow coefficient would be required to obtain a near-uniform velocity distribution at the end of the diffuser at low inlet-velocity ratios.

External drag.- Boundary-layer surveys were conducted at station 8.0 both before and after installation of the scoops. Section wake-drag increments for configurations V and VI calculated from these measurements are presented in figure 21. In each case, installation of the scoop reduced the drag over the span of the entrance and increased the drag at the spanwise location of the gutter. The increase in drag behind the gutter of configuration VI was much greater than for configuration V because of the low energy air flowing out of the bypass exit of configuration VI just ahead of the measuring station.

The section-wake-drag increments of figure 21 were integrated in the spanwise direction to obtain the over-all increments in wake drag at station 8 caused by installation of these two scoops. As shown by

the lowest curve of figure 22, the installation of scoop configuration V reduced the wake drag at station 8 throughout the test range of inlet-velocity ratio. Installation of scoop configuration VI also reduced the wake drag at station 8 for inlet-velocity ratios above 1.0, but increased the wake drag by a small amount in the high-speed range of inlet-velocity ratio. Inasmuch as the wake drag of configuration V was essentially unaffected by suction quantity, consideration of the effects of suction quantity on the friction drag of the fuselage would not appear necessary in the determination of the optimum suction quantity.

The increment in external drag caused by installation of the scoop in the basic body is considered to be the sum of the change in body friction drag and the drag of the suction flow. In order to obtain an indication of the external drag increment chargeable to scoop configuration V, the drag equivalent of the suction flow of this arrangement, calculated from the suction-flow quantity and the total-pressure recovery in the suction flow after diffusion, was added to the friction-drag increment determined from the wake surveys at station 8 to obtain the two corrected drag-increment curves given in figure 22. In the case of configuration IV, no correction was necessary because the surveys at station 8 covered the wakes of the bypass exits as well as the wake of the scoop. The external drag increments for configuration V obviously are slightly lower than the values which would be obtained if a small additional total-pressure loss of $0.1q_o$ or less was assumed to occur in the suction ducting between the measuring station and the duct exit. The external drag increments for configuration VI also are slightly higher than the values which would be obtained if the bypass ducting of this arrangement was redesigned to reduce the previously noted excessive ducting loss of about $0.15q_o$.

The external-drag-increment data of figure 22 indicate that installation of an air scoop of this type in a region of comparable boundary-layer thickness will not increase the external drag importantly above an inlet-velocity ratio of about 0.5, provided that the suction-flow coefficient is less than about 2.0 and provided that the bypass exits are properly located so that they do not upset the flow in a critical region such as the wing-fuselage juncture. This conclusion is applicable only to subcritical Mach numbers. Further research is required to establish the drag and other performance characteristics of this type of inlet at supercritical Mach numbers.

Critical Mach number.- Representative surface pressure measurements for configuration V are given in figures 9 to 12. Critical Mach numbers, figure 23, were predicted from these and similar measurements by means of the Von Kármán relation (reference 8). This relation is strictly applicable only to the two-dimensional case; however, results reported in reference 9 for nose inlets show that this relation also is reasonably accurate for the three-dimensional case so long as the critical Mach

number is not predicted from a sharp local pressure peak. The values given are unconservative in that the induced velocities due to the fuselage, wing, and so forth, were not simulated in the test setup. The results of reference 9, however, also show that the actual critical Mach number is appreciably higher than the critical Mach number predicted from low-speed pressure measurements and that a further margin of the order of 0.05 exists between the actual critical Mach number and the force-break Mach number. Similar results have been observed in numerous airfoil and wing investigations. It is believed that these effects approximately counterbalance the unconservatism of the pressure measurements so that no losses in pressure recovery or drag rises due to shocks would occur at flight Mach numbers below the values presented.

The predicted critical Mach numbers of configuration V were not affected importantly by variations in suction quantity. (Compare parts (a) and (b) of fig. 23.) The critical Mach number of the installation was established by the top surface of the scoop lip at the inlet-velocity ratios below about 0.6, by the center section of the ramp at inlet-velocity ratios between about 0.6 and 0.8, and by the inner surface of the side of the scoop lip at inlet-velocity ratios above about 0.8. The limitation imposed by the top surface of the scoop lip is not regarded as important because of the large delay in the force break which would occur for this component and because shocks in this region would not affect the internal flow. Hence, the center section of the ramp also is considered to be the limiting factor at the inlet-velocity ratios below 0.6.

The results of figure 23 indicate that in the high-speed range of inlet-velocity ratio the scoop would perform essentially as at low speeds up to a Mach number of at least 0.81. An appreciable delay in adverse effects due to shocks appears possible through modifications to the transition curvature at the crest of the ramp. A further delay could be obtained by reducing the inclination of the ramp.

Design inlet-velocity ratio.- The inlet-velocity ratio for maximum total-pressure recovery at the end of the diffusers of configurations V and VI was approximately 0.8 at the lowest suction-flow coefficients investigated. (See figs. 15(b) and 15(c).) A much lower value of inlet-velocity ratio is desirable for the high-speed design condition so that the corresponding inlet-velocity ratios for take-off and climb will not be so large as to cause excessively low pressure recoveries. An inspection of figures 15(b) and 15(c) shows that the total-pressure recovery at the lowest suction-flow coefficients decreased only a small amount ($0.025q_o$ or less) when the inlet-velocity ratio was decreased to 0.6; but appreciable further reductions resulted in significant losses. At the higher suction-flow coefficients, decreases in total-pressure recovery greater than $0.025q_o$ did not occur down to an

inlet–velocity ratio of 0.5. It appears, therefore, that single scoops of this type should be designed for an inlet–velocity ratio in the high–speed condition of 0.5 to 0.6.

The flow into twin internally coupled inlets has been observed to be unstable in a number of installations when the inlets were operated at an inlet–velocity ratio below that for peak total–pressure recovery at the end of the diffuser. This flow instability apparently arises when some disturbance changes the flow quantity into one inlet. Inasmuch as the flow quantity to the engine tends to remain fixed, the flow quantity into the second inlet undergoes an opposite and approximately equal change. Then, since the total–pressure recovery in each duct increases with flow rate, the flow quantity continues to increase into one inlet and to decrease into the other inlet.

Results obtained in an investigation currently under way at the Ames Laboratory show that the divergence in flow rates of twin ducts just described ceases when the static pressures in the two ducts become equal at their juncture. This research also shows that this type of flow instability cannot occur if the static pressure in each duct at its juncture with the other duct decreases continuously with increasing inlet–velocity ratio. Thus, as shown in figure 19, twin–duct installations using the single–suction–slot version of scoop configuration V or VI can be designed safely for high–speed inlet–velocity ratios as low as 0.5, the minimum value recommended for single scoops. An inspection of the surface pressure distributions along the duct bottom, figure 9(c), shows that the surface pressure for $\frac{V_i}{V_o} = 0.31$ is more positive than that for $\frac{V_i}{V_o} = 0.52$ for all longitudinal stations between the inlet and the end of the diffuser; hence, this design value is satisfactory regardless of the amount of area expansion that has been obtained between the duct entrances and the point of juncture.

Optimum suction quantity.– In order to obtain an indication of the optimum suction quantity, the effects of the suction flow in increasing the maximum net thrust and reducing the corresponding specific fuel consumption of an installation incorporating a typical jet engine rated at 4000 pounds static thrust at sea level were computed for a typical high–speed design condition, V_o = 600 miles per hour and $\frac{V_i}{V_o} = 0.6$. The results of reference 10 were used to determine the effects of changes in total–pressure recovery at the end of the diffuser on the performance of the engine itself. The drag of the suction flow, computed from the suction–flow quantities and the estimated total–pressure recoveries in the suction flows at the exits of the suction ducts, was subtracted

from the increase in net thrust indicated in reference 10 to obtain the over-all increase in net thrust. In the case of the ramp suction slot of configuration VI, the total-pressure recoveries in the exiting suction flow assumed were those given in figure 16(c). For all other suction slots, a factor of $0.15q_0$ was subtracted from the values given in figure 16 to allow for additional losses in the suction ducts between the measuring stations and the duct exits. The results of the computations, figure 24, represent the gains in performance obtained by the use of boundary-layer control relative to the performance of the installation using scoop configuration I. Boundary-layer control would be expected to effect appreciable gains in performance in this case or in any other case in which flow separation occurs ahead of the inlet.

The application of boundary-layer suction is shown in figure 24 to cause important increases in maximum net thrust and important decreases in specific fuel consumption for all altitudes between sea level and 40,000 feet. The calculated specific fuel consumption decreased regularly with increases in suction-flow coefficient for both the single and two-slot arrangements. The calculated gain in maximum net thrust, however, reached maximum values for both the single and two-slot arrangements and then decreased as the drag of the suction flow began to increase more rapidly than the gain in thrust due to the suction. At a total suction coefficient $C_{Q_1} + C_{Q_2}$ of 2.6, the specific fuel consumptions for the single-slot and two-slot versions of configuration V were the same and the maximum net thrust for the two-slot version was only about 1 percent greater than that for the single-slot version. Thus, in view of the low total-pressure recoveries obtained in the second suction slot at higher values of inlet-velocity ratio, the use of a second suction slot of the type investigated again does not appear justified.

As shown by the data for configuration III, the peak value of maximum net thrust for the single-slot versions of the present type of submerged scoop apparently occurs at a suction-flow coefficient of 0.8 or below. However, inasmuch as the net thrust decreases only slowly as the suction-flow coefficient is increased above this value, a much larger value of suction-flow coefficient is desirable in order to realize a further decrease in specific fuel consumption. The results for configuration V indicate that a suction-flow coefficient as high as 3 may be desirable. It is noted that the decrease in net thrust caused by the increase in suction-flow coefficient above the value for peak net thrust probably can be minimized by redesigning the suction slot to obtain a lower slot entry velocity ratio. Several investigations, such as that of reference 6, have shown that an average flow velocity into the slot entry of 0.6 of the local flow velocity is approximately optimum. With a main duct inlet-velocity ratio of 0.6, the inlet-velocity ratio of

the ramp suction slot of configuration VI was about 0.53 based on the local flow velocity at a suction-flow coefficient of 1.8.

For the single-slot version of configuration VI, a suction-flow coefficient of 1.8 (11.7 percent of the entering flow) produced calculated increases of 6.2 and 6.4 percent in maximum net thrust at sea level and 40,000-foot altitude, respectively. The corresponding decreases in specific fuel consumption were 5.1 and 3.1 percent.

Variation of Boundary-Layer Thickness

Average total-pressure recoveries in the main ducts of configurations III and V are presented in figure 25 for the three initial boundary-layer thicknesses investigated (fig. 7). The results for boundary layers A and B, which had displacement thicknesses of 0.074 and 0.085 inch, respectively, were very nearly the same for comparable suction-flow coefficients. Doubling the displacement thickness of the boundary layer, however, produced losses of as much as $0.08q_o$. (Compare recoveries at the ends of the diffusers for boundary layers B and C at equal values of the total suction-flow coefficient $C_{Q_1} + C_{Q_2}$.) This result shows that the suction-flow coefficient required to obtain a given total-pressure recovery is not independent of the initial boundary-layer thickness, but instead increases rapidly with increases in the initial boundary-layer thickness.

Average total-pressure recoveries in the ramp and second suction slots of configuration V after area expansions of 2:1 are presented in figure 26 for the three initial boundary-layer thicknesses. It has been shown previously that the total-pressure recovery in the ramp slot was essentially independent of the suction-flow coefficient. The results of figure 26(b) indicate, therefore, that the total-pressure recovery in this slot is changed only a small amount by variations in the initial boundary-layer thickness. It should be noted, however, that even though the total-pressure recovery in this slot remains constant, the drag equivalent of its suction flow will increase continuously with increases in initial boundary-layer thickness at a constant suction-flow coefficient because the absolute quantity of suction flow for a constant suction-flow coefficient varies directly with the boundary-layer thickness.

Results of calculations of the effect of boundary-layer thickness on the maximum net thrust and corresponding specific fuel consumption of a jet-engine installation using scoop configuration III are presented in figure 27. The operating conditions considered are the same as those considered in the preceding section of the paper. The calculation procedure also was identical except that the differences in wake drag aft

of the inlet for the three boundary layers was taken into account. Increases in the thickness of the initial boundary layer are shown to cause important decreases in maximum net thrust and important increases in the corresponding specific fuel consumption. These adverse effects cannot be eliminated by merely increasing the suction-flow coefficient because attending increases in the drag of the suction system would offset any gain in total-pressure recovery obtained at the end of the diffuser. Hence, the present type of inlet appears desirable for application only at forward locations on the fuselage where the boundary layer is relatively thin and not at aft locations such as might be desirable for an engine installed in the rear part of the fuselage.

SUMMARY OF RESULTS AND CONCLUSIONS

A submerged air scoop consisting essentially of a conventional scoop located in a dimple in the fuselage surface has been investigated preliminarily at low speeds both without and with boundary-layer control. The more important results of the tests of this inlet in the presence of an initial turbulent boundary layer approximately representative of full-scale conditions just ahead of the wing of a fighter-type airplane in the high-speed high-altitude flight conditions are summarized as follows:

1. Without boundary-layer control, the peak total-pressure recovery at the end of the 2:1 area ratio diffuser was $0.83q_0$ and occurred at an inlet-velocity ratio of 1.1. Application of boundary-layer control increased the pressure recovery markedly over the entire inlet-velocity-ratio range and shifted the peak pressure recovery to a much lower value of inlet-velocity ratio.

2. When sufficient suction flow was provided to obtain a peak total-pressure recovery at the end of the diffuser of $0.90q_0$ or greater, the total-pressure recovery at this point remained above $0.85q_0$ over a range of inlet-velocity ratio broad enough to cover the more important flight conditions.

3. The total-pressure recovery was not critically sensitive to small variations in suction-slot location and, for a given total suction quantity, was not increased by the use of two slots in tandem.

4. It is indicated that installation of an inlet of this type will not increase the external drag importantly above an inlet-velocity ratio of about 0.5 provided that the suction flow is exited in a region which is not critical with respect to flow separation.

5. In the final arrangement tested, a suction quantity of 11.7 percent of the entering flow produced calculated increases in maximum net thrust of 6.2 percent or greater and calculated reductions in specific fuel consumption of 3.1 percent or greater (compared to the basic inlet without boundary-layer control) for a typical jet-engine installation operating at a flight speed of 600 miles per hour.

6. It appears that the flow instability frequently encountered in the case of twin internally coupled inlets will be avoided with this arrangement for design high-speed inlet-velocity ratios as low as 0.5.

Appreciable increases in the thickness of the initial boundary layer caused significant decreases in inlet performance which cannot be overcome simply by increasing the suction quantity. Hence, the present type of inlet appears desirable for application only at forward locations on the fuselage where the boundary layer is relatively thin and not at aft locations such as might be desirable for an engine installed in the rear part of the fuselage.

Further research on the present type of inlet, including in particular measurements of the total drag, appears desirable. Tests at transonic speeds to establish the high-speed characteristics and complete model tests to establish the effects of pitch and yaw are necessary before the inlet can be recommended for application.

Langley Aeronautical Laboratory
National Advisory Committee for Aeronautics
Langley Air Force Base, Va.

REFERENCES

1. Smith, Norman F., and Baals, Donald D.: Wind-Tunnel Investigation of a High-Critical-Speed Fuselage Scoop Including the Effects of Boundary Layer. NACA ACR L5B01a, 1945.

2. Mossman, Emmet A., and Randall, Lauros M.: An Experimental Investigation of the Design Variables for NACA Submerged Duct Entrances. NACA RM A7I30, 1947.

3. Delany, Noel K.: An Investigation of Submerged Air Inlets on a $\frac{1}{4}$-Scale Model of a Typical Fighter-Type Airplane. NACA RM A8A20, 1948.

4. Thoedorsen, Theodore, and Silverstein, Abe: Experimental Verification of the Theory of Wind-Tunnel Boundary Interference. NACA Rep. 478, 1934.

5. Von Doenhoff, Albert E., and Tetervin, Neal: Determination of General Relations for the Behavior of Turbulent Boundary Layers. NACA Rep. 772, 1943.

6. Pierpont, P. Kenneth: Investigation of Suction-Slot Shapes for Controlling a Turbulent Boundary Layer. NACA TN 1292, 1947.

7. Nichols, Mark R., Keith, Arvid L., Jr., and Boswinkle, Robert W., Jr.: Wind-Tunnel Investigation of Carburetor-Air Scoops for the XTB2D-1 Airplane with Emphasis on Means for Bypassing the Boundary Layer. NACA MR, June 7, 1944.

8. Von Kármán, Th.: Compressibility Effects in Aerodynamics. Jour. Aero. Sci., vol. 8, no. 9, July 1941, pp. 337-356.

9. Pendley, Robert E., and Smith, Norman F.: An Investigation of the Characteristics of Three NACA 1-Series Nose Inlets at Subcritical and Supercritical Mach Numbers. NACA RM L8L06, 1949.

10. Hanson, Frederick H., Jr., and Mossman, Emmet A.: Effect of Pressure Recovery on the Performance of a Jet-Propelled Airplane. NACA TN 1695, 1948.

CONFIDENTIAL

TABLE I

ORDINATES OF EXTERNAL SURFACES OF THE SEVERAL SCOOPS

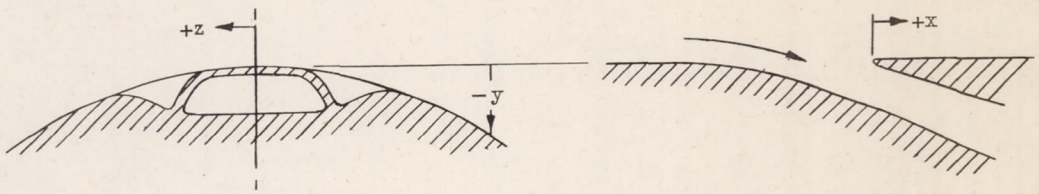

(a) Configurations I and II.

x / z	-9.73	-7.06	-5.34	-3.73	-2.0	0		1.0	3.0	5.0
						Ramp	Lip			
0	[a]-0.38	-0.92	-1.39	-1.93	-2.53	-3.22	-0.10	0	0	0
2.00	-.43	-.99	-1.44	-1.93	-2.53	-3.22	-.18	-.07	-.07	-.07
4.00	-.62	-1.18	-1.59	-2.05	-2.56	-3.16	-.42	-.31	-.30	-.29
4.50	------	-----	-----	-----	-----	-3.08	-.74	-.50	-.42	-.38
4.75	------	-----	-----	-----	-----	-3.00	-1.00	-.68	-.53	-.44
5.00	-.75	-1.26	-1.70	-2.13	-2.48	-2.75	-1.40	-.99	-.69	-.52
5.25	------	-----	-----	-----	-----	-2.46	-1.92	-1.32	-.89	-.60
5.50	------	-----	-----	-----	-----	-2.25	-2.25	-1.69	-1.10	-.69
5.75	------	-----	-----	-----	-----	-2.14	-2.14	-1.81	-1.24	-.75
6.00	-.84	-1.29	-1.65	-1.92	-2.08	-2.03	-2.03	-1.80	-1.30	-.77
7.00	-.94	-1.26	-1.42	-1.57	-1.66	-1.60	-1.60	-1.54	-1.22	-.90
8.00	-1.17	-1.26	-1.30	-1.33	-1.34	-1.30	-1.30	-1.28	-1.21	-1.17

(b) Configuration III.

x / z	-9.73	-7.06	-5.93	-4.93	-2.93	-0.93	0	0.16	1.1	3.1	5.1	7.1
0	-0.38	-0.92	-1.23	-1.53	-2.22	-2.91	-3.22	-0.15	0.22	0.20	0.11	0.02
2.00	-.43	-.99	-1.27	-1.53	-2.22	-2.91	-3.22	-.23	.05	.07	-.05	-.10
4.00	-.62	-1.13	-1.38	-1.68	-2.29	-2.92	-3.16	-.52	-.18	-.17	-.26	-.31
4.50	-----	-----	-1.44	-----	-----	-----	-3.08	-.74	-.34	-.29	-.36	-.39
4.75	-----	-----	-1.48	-----	-----	-----	-3.02	-.96	-.46	-.38	-.41	-.42
5.00	-.75	-1.23	-1.50	-1.80	-2.34	-2.83	-2.94	-1.30	-.67	-.52	-.50	-.48
5.25	-----	-----	-1.52	-----	-----	-----	-2.85	-1.82	-.95	-.69	-.62	-.55
5.50	-----	-----	-1.53	-----	-----	-----	-2.76	-2.25	-1.36	-.95	-.78	-.65
5.75	-----	-----	-1.53	-----	-----	-----	-2.66	-2.58	-1.95	-1.30	-1.01	-.77
6.00	-.84	-1.29	-1.52	-1.77	-2.14	-2.42	-2.53	-2.52	-2.37	-1.80	-1.34	-.92
6.25	-----	-----	-----	-----	-----	-----	-2.40	-2.40	-2.33	-2.00	-1.54	-1.00
7.00	-.94	-1.26	-1.39	-1.55	-1.80	-1.97	-2.00	-2.00	-1.97	-1.78	-1.43	-1.06
8.00	-1.17	-1.25	-1.30	-1.33	-1.42	-1.51	-1.54	-1.55	-1.55	-1.53	-1.27	-1.20

[a]Ordinate (y).

All linear dimensions are in inches.

TABLE I

ORDINATES OF EXTERNAL SURFACES OF THE SEVERAL SCOOPS – Concluded

(c) Configuration IV.

z \ x	−9.84	−6.84	−3.84	−2.84	−1.84	−0.84	0	0.16	1.16	3.16	5.16	7.16
0	[a]−0.35	−0.97	−2.08	−2.54	−2.40	−2.83	−3.18	−0.15	0.23	0.19	0.10	0.02
2.00	−.31	−.90	−2.07	−2.54	−2.40	−2.83	−3.18	−.23	.05	.06	−.05	−.10
4.00	−.34	−.62	−1.98	−2.52	−2.40	−2.83	−3.18	−.52	−.18	−.17	−.26	−.32
4.50	−.39	−.57	−1.81	−2.43	−2.40	−2.81	−3.17	−.74	−.33	−.29	−.36	−.39
4.75	−.43	−.55	−1.62	−2.34	−2.40	−2.79	−3.16	−.96	−.45	−.38	−.41	−.43
5.00	−.48	−.55	−1.45	−2.14	−2.37	−2.74	−3.14	−1.30	−.66	−.52	−.50	−.49
5.25	−.51	−.56	−1.31	−1.92	−2.29	−2.65	−3.08	−1.82	−.94	−.69	−.61	−.55
5.50	−.56	−.58	−1.18	−1.72	−2.15	−2.55	−2.97	−2.25	−1.36	−.95	−.78	−.65
5.75	−.60	−.61	−1.05	−1.53	−1.97	−2.42	−2.74	−2.58	−1.94	−1.29	−1.00	−.77
6.00	−.66	−.66	−.93	−1.35	−1.78	−2.21	−2.50	−2.52	−2.37	−1.78	−1.34	−.91
6.25	−.71	−.71	−.85	−1.18	−1.60	−2.00	−2.25	−2.27	−2.23	−2.00	−1.53	−.99
6.50	−.76	−.76	−.82	−1.04	−1.42	−1.80	−2.06	−2.07	−2.08	−1.94	−1.54	−1.03
7.00	−.88	−.88	−.88	−.94	−1.15	−1.46	−1.74	−1.77	−1.82	−1.78	−1.43	−1.06
7.50	−1.01	−1.01	−1.01	−1.01	−1.07	−1.25	−1.47	−1.51	−1.62	−1.60	−1.31	−1.11
8.00	−1.17	−1.17	−1.17	−1.17	−1.17	−1.20	−1.34	−1.37	−1.42	−1.42	−1.27	−1.20

(d) Configurations V and VI.

Configuration	V and VI										V
z \ x	−9.73	−6.80	−4.73	−2.73	−1.73	−0.73	0	0.16	1.27	3.27	5.27
0	−0.38	−0.98	−1.67	−2.03	−2.45	−2.87	−3.18	−0.15	0.23	0.19	0.10
2.00	−.41	−1.06	−1.72	−2.03	−2.45	−2.87	−3.18	−.23	.14	.11	.02
4.00	−.62	−1.21	−1.79	−2.03	−2.45	−2.87	−3.18	−.34	−.07	−.09	−.18
4.75	-----	-----	-----	−1.97	−2.39	−2.81	−3.12	-----	-----	-----	-----
5.00	−.75	−1.30	−1.85	−1.53	(−1.95) (−1.22)	(−2.37) (−.89)	(−2.68) (−.72)	−.44	−.30	−.28	−.36
5.25	−.77	−1.31	−1.86	−1.29	−.96	−.65	-----	-----	-----	-----	-----
5.50	−.80	−1.31	−1.85	−1.35	−1.00	−.72	-----	−.53	−.43	−.40	−.46
6.00	−.84	−1.30	−1.77	−1.46	−1.16	−.88	-----	−.65	−.55	−.54	−.58
7.00	−.94	−1.28	−1.63	−1.51	−1.38	−1.16	-----	−.96	−.84	−.82	−.87
8.00	−1.16	−1.27	−1.52	−1.50	−1.43	−1.32	-----	−1.21	−1.13	−1.12	−1.17
9.00	−1.47	−1.50	−1.53	−1.53	−1.51	−1.50	-----	−1.50	−1.49	−1.47	−1.50

[a]Ordinate (y).

All dimensions are in inches.

TABLE II

ORDINATES OF CENTER-LINE SECTION OF LIP OF

SCOOP CONFIGURATIONS III TO VI

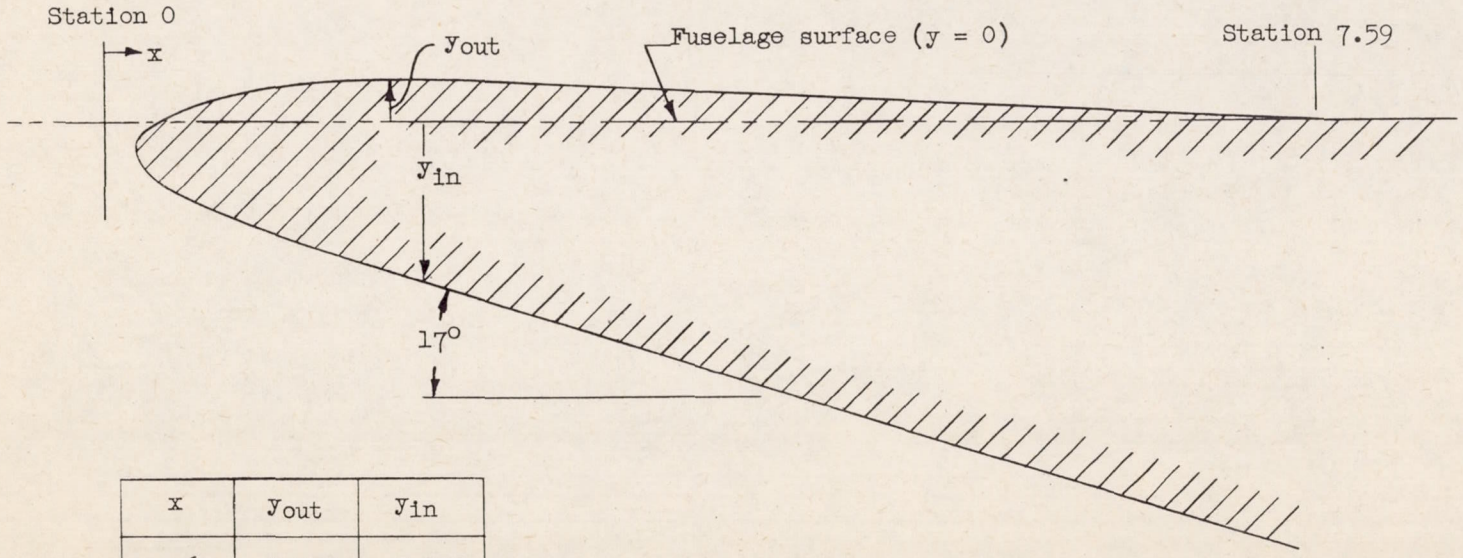

x	y_{out}	y_{in}
0.160	−0.150	−0.150
.200	−.080	−.230
.240	−.050	−.280
.320	.000	−.360
.490	.070	−.460
.650	.130	−.530
.820	.175	−.600
.980	.197	−.658
1.145	.223	−.720
1.470	.250	−.845
1.800	.250	−.955
2.000	.240	−1.023
2.500	.225	−1.183

All linear dimensions are inches.

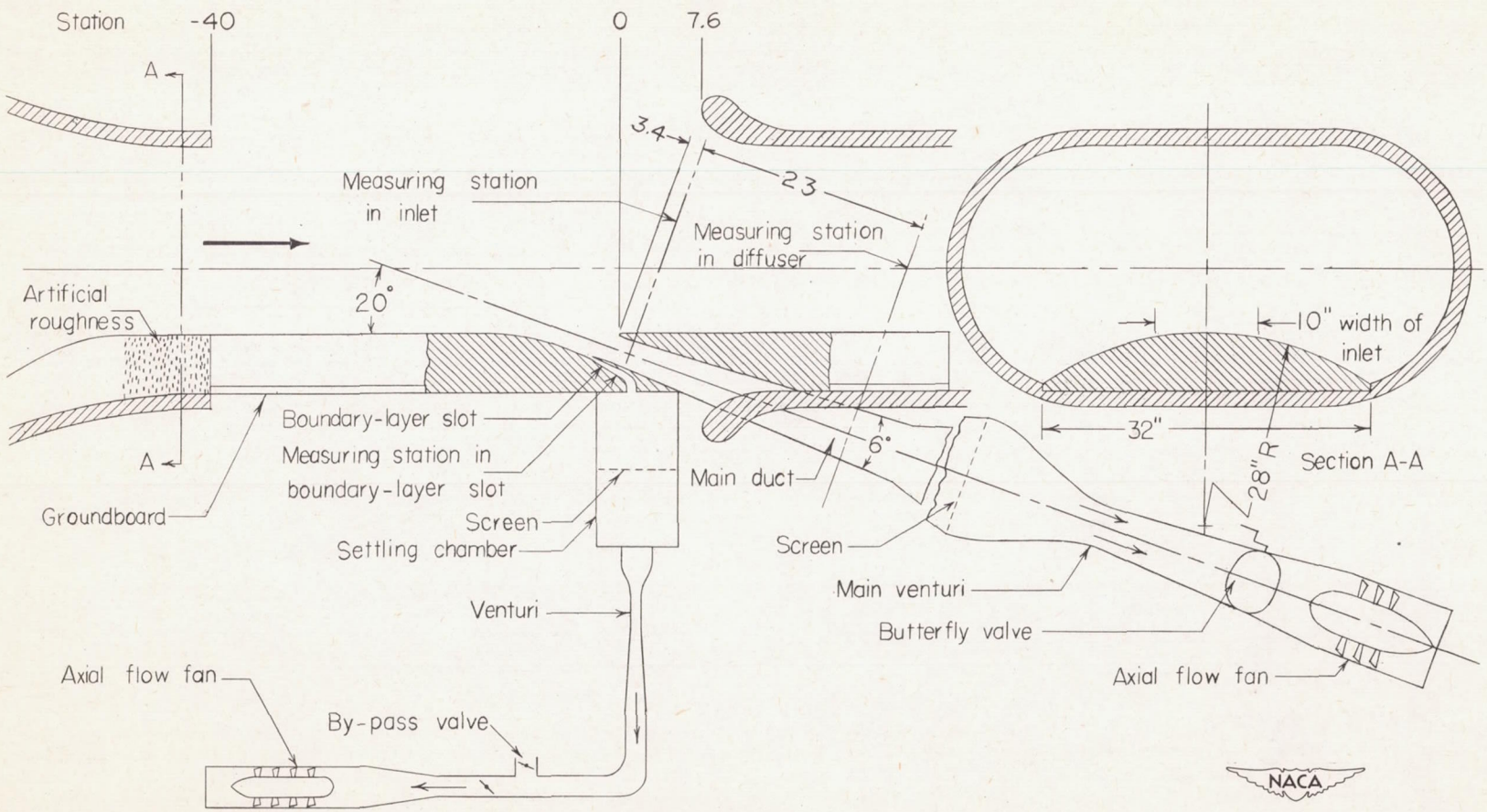

Figure 1.- Schematic diagram of test setup. All linear dimensions are in inches.

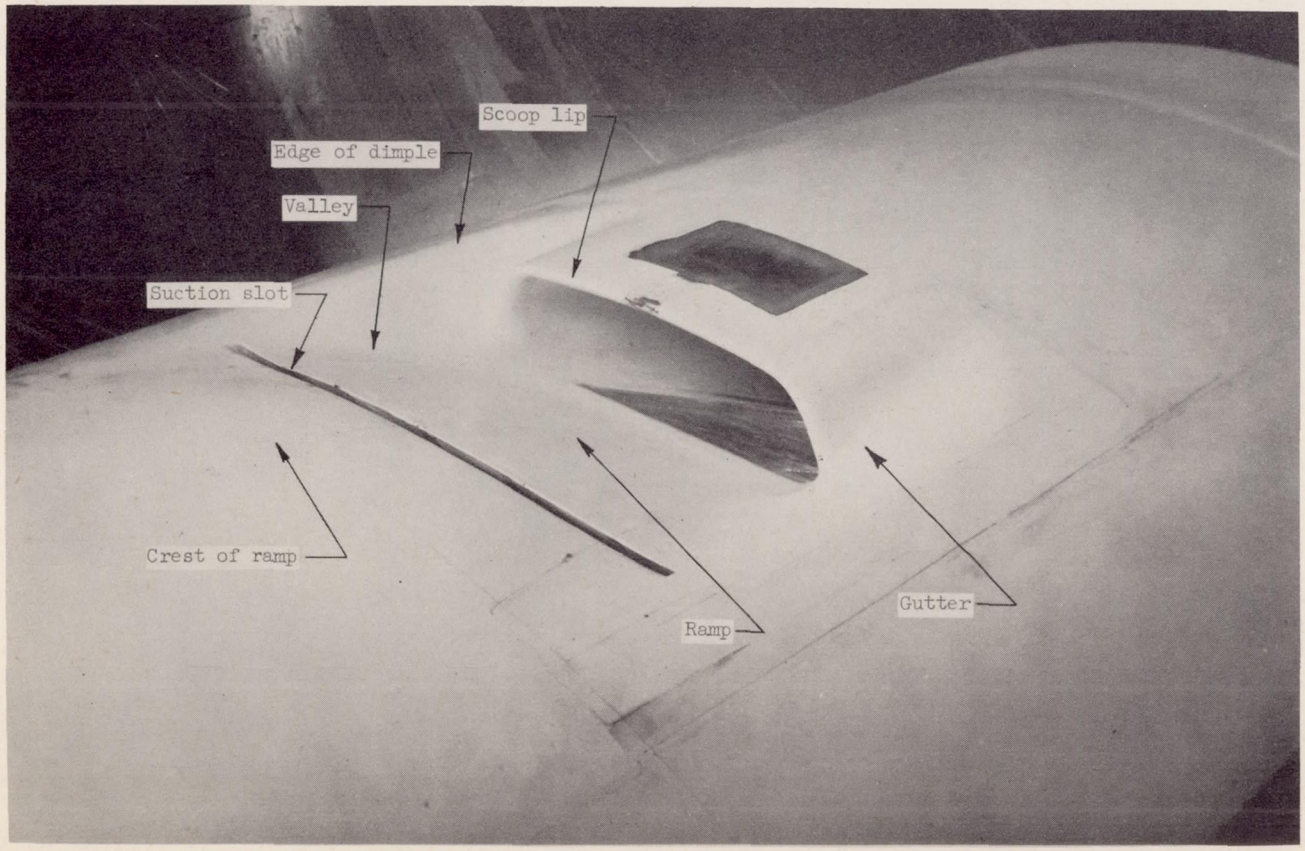

(a) Original version of configuration III. Configuration I was identical except for absence of slot. Configuration II also was identical except that slot was 0.43 inlet heights further aft.

Figure 2.- Views of typical scoops.

L-55969.1

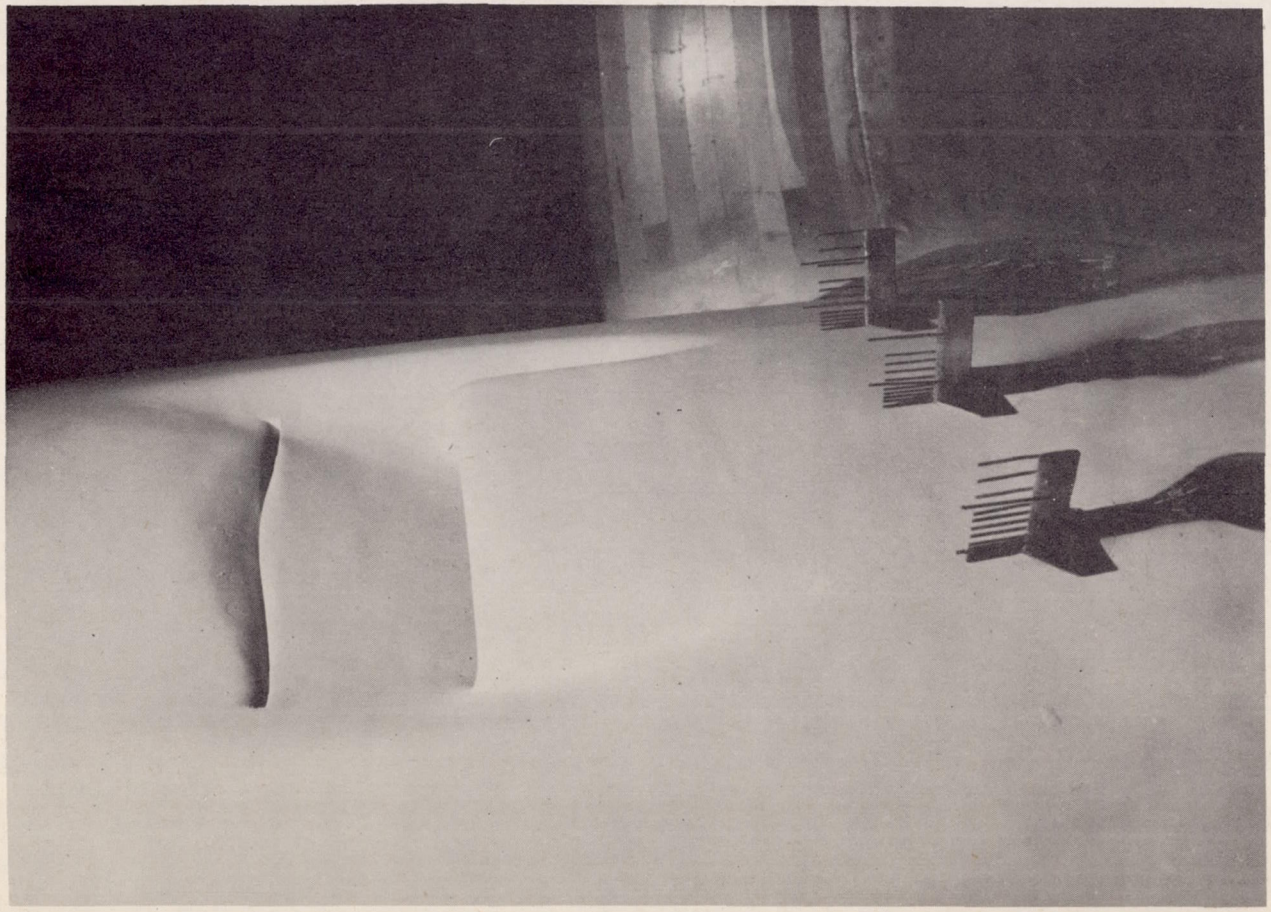

(b) Final version of configuration III with modified slot, scoop lip, and gutters.

NACA

L-57206

Figure 2.- Continued.

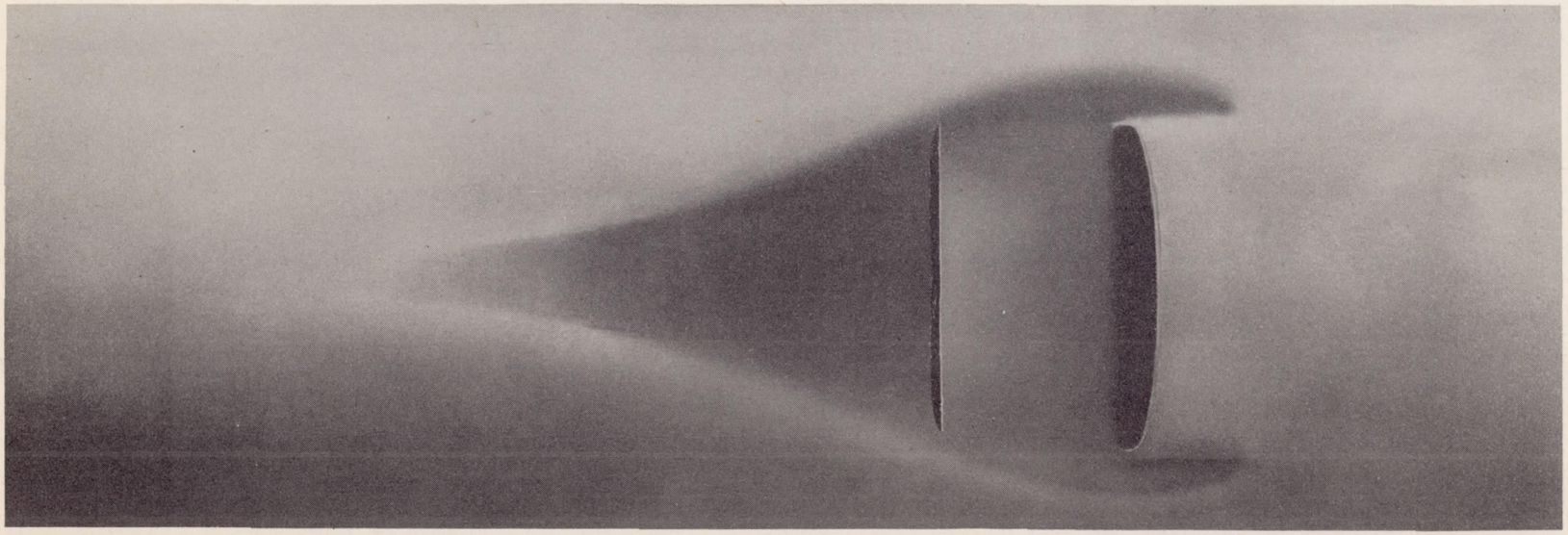

(c) Configuration IV.

NACA

L-63578

Figure 2.- Continued.

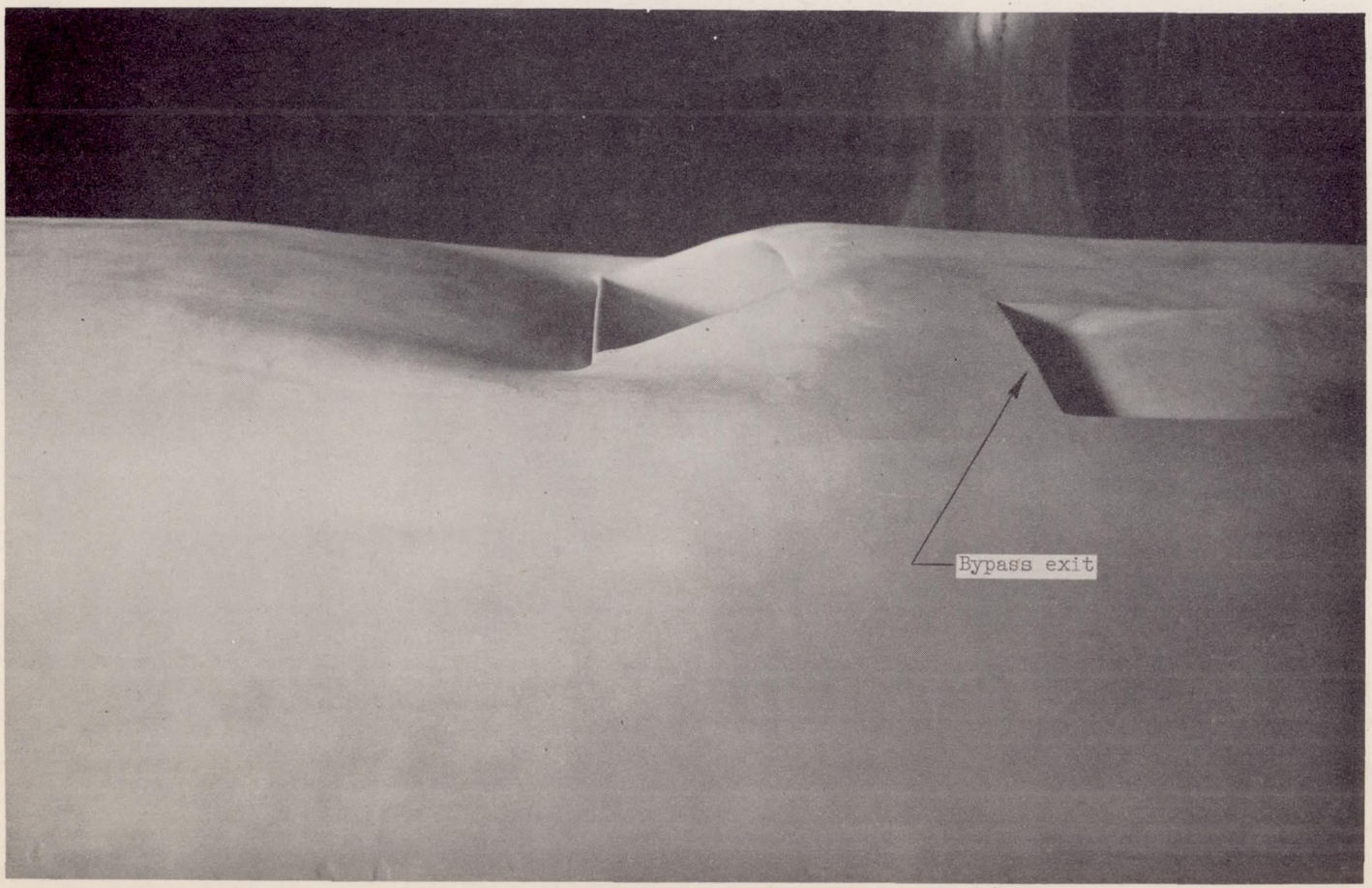

(d) Configuration VI, side view. Configuration V was identical except for absence of bypass exits.

Figure 2.- Continued.

NACA L-59942.1

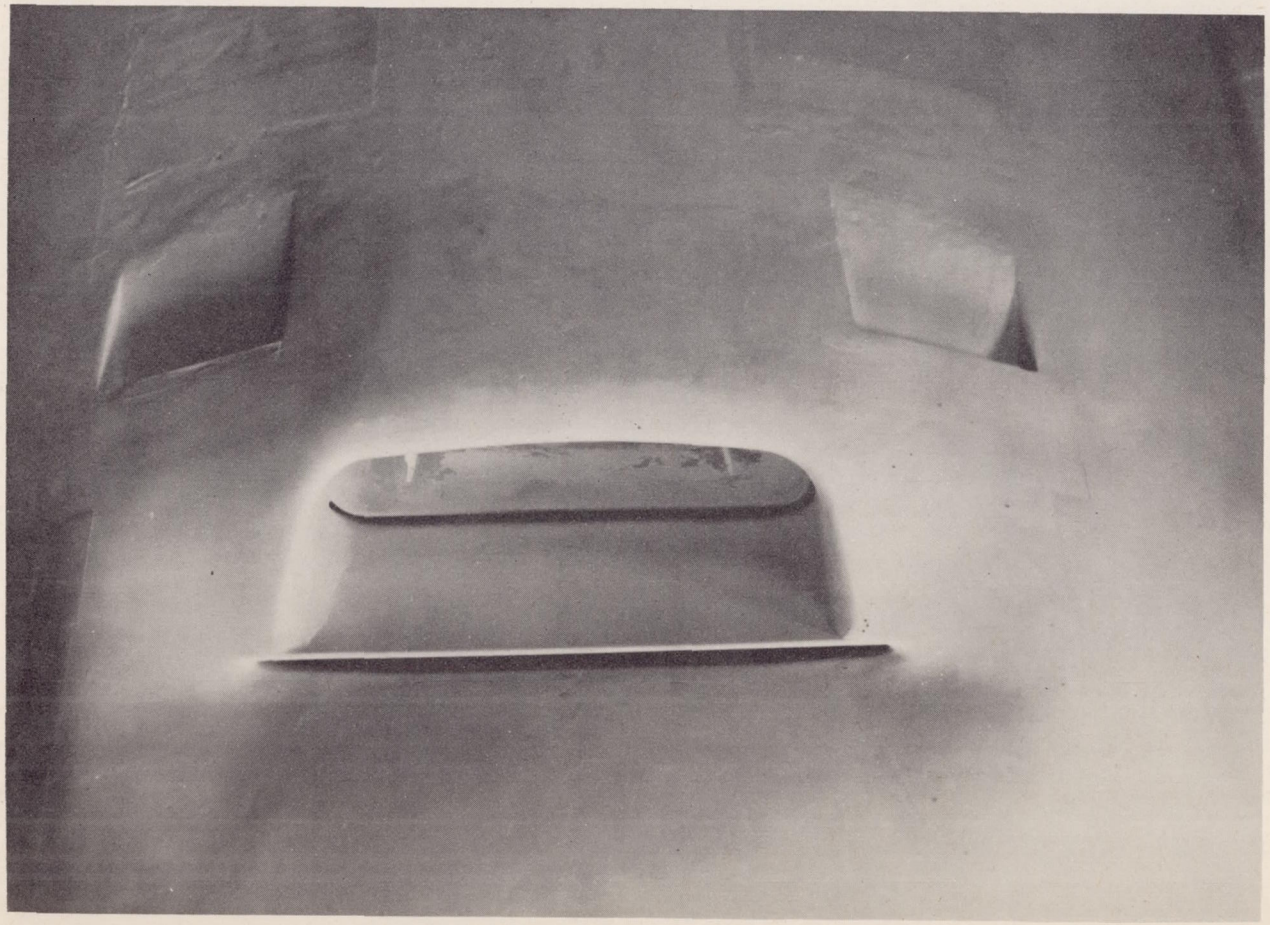

(e) Configuration VI, plan view. Configuration V was identical except for absence of bypass exits.

Figure 2.- Concluded.

NACA

L-59943

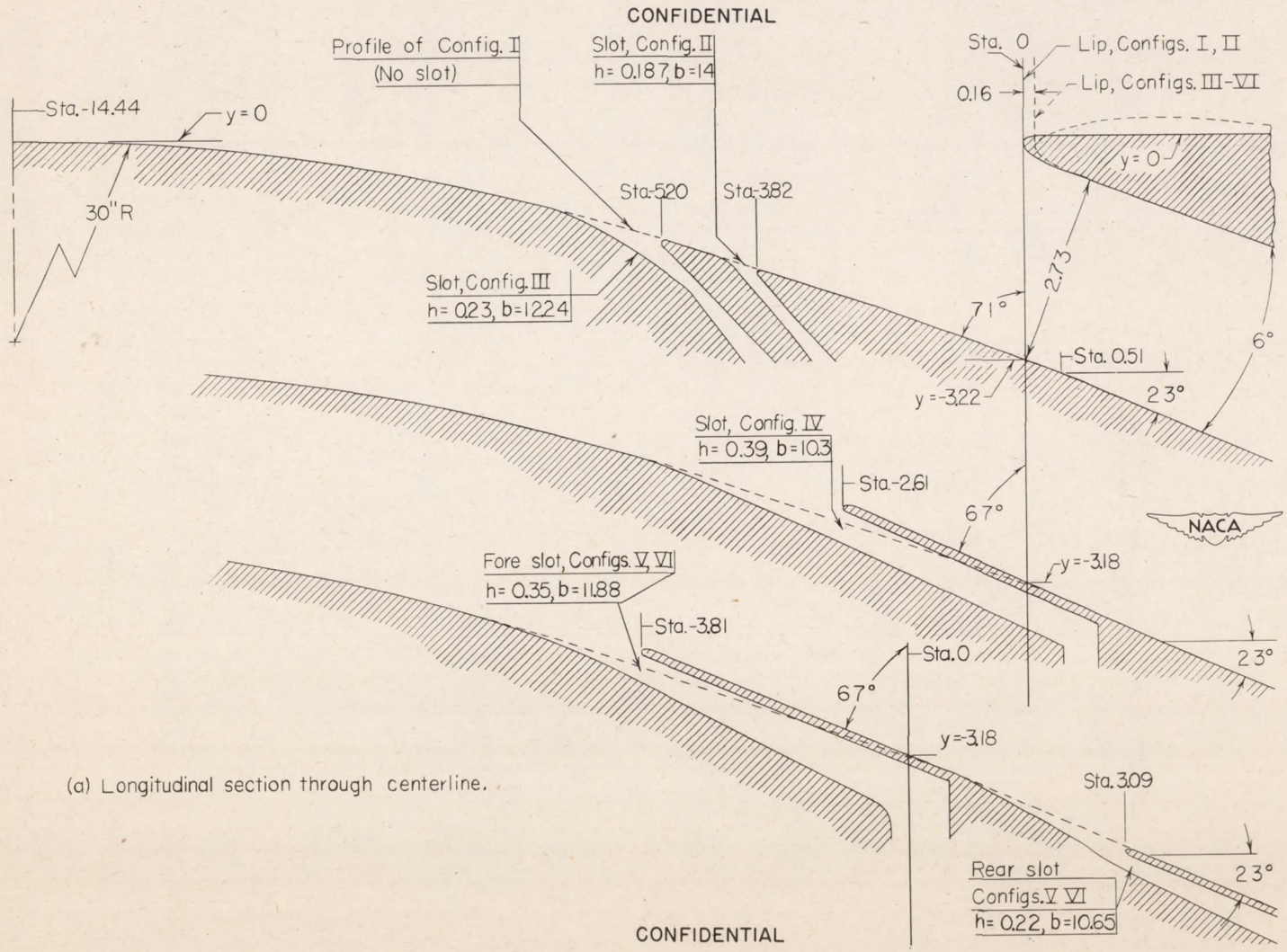

(a) Longitudinal section through centerline.

Figure 3.- Line drawings comparing the several configurations. All linear dimensions are in inches. See figure 4 for slot dimensions and tables I and II for surface ordinates.

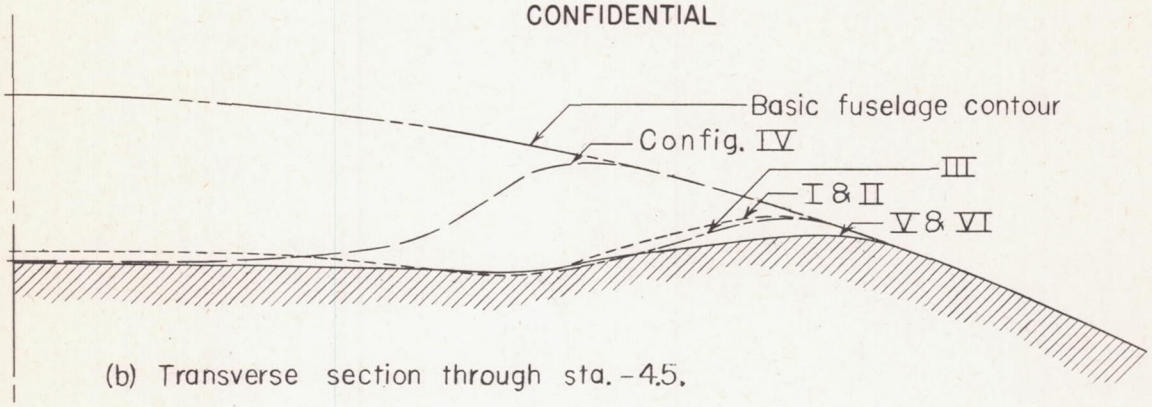

(b) Transverse section through sta. -4.5.

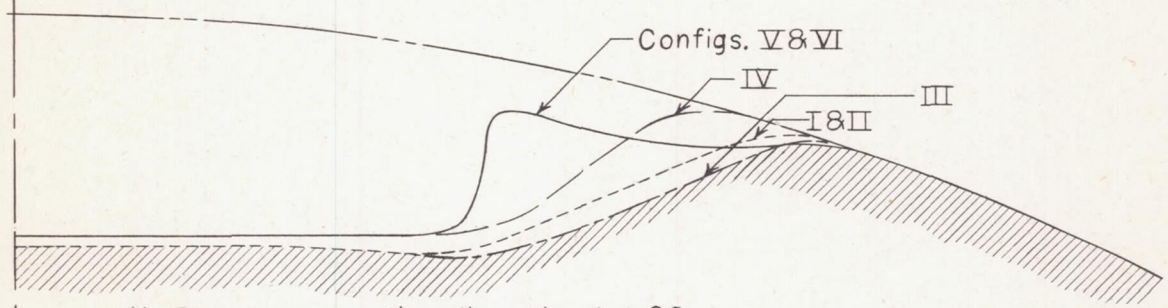

(c) Transverse section through sta. -2.0.

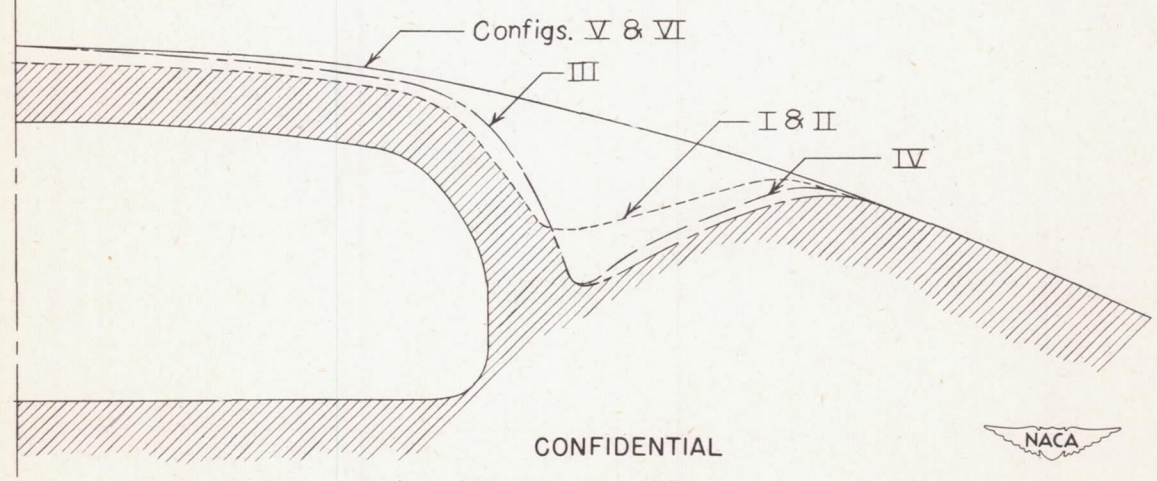

(d) Transverse section through sta. 1.0.

Figure 3.- Concluded.

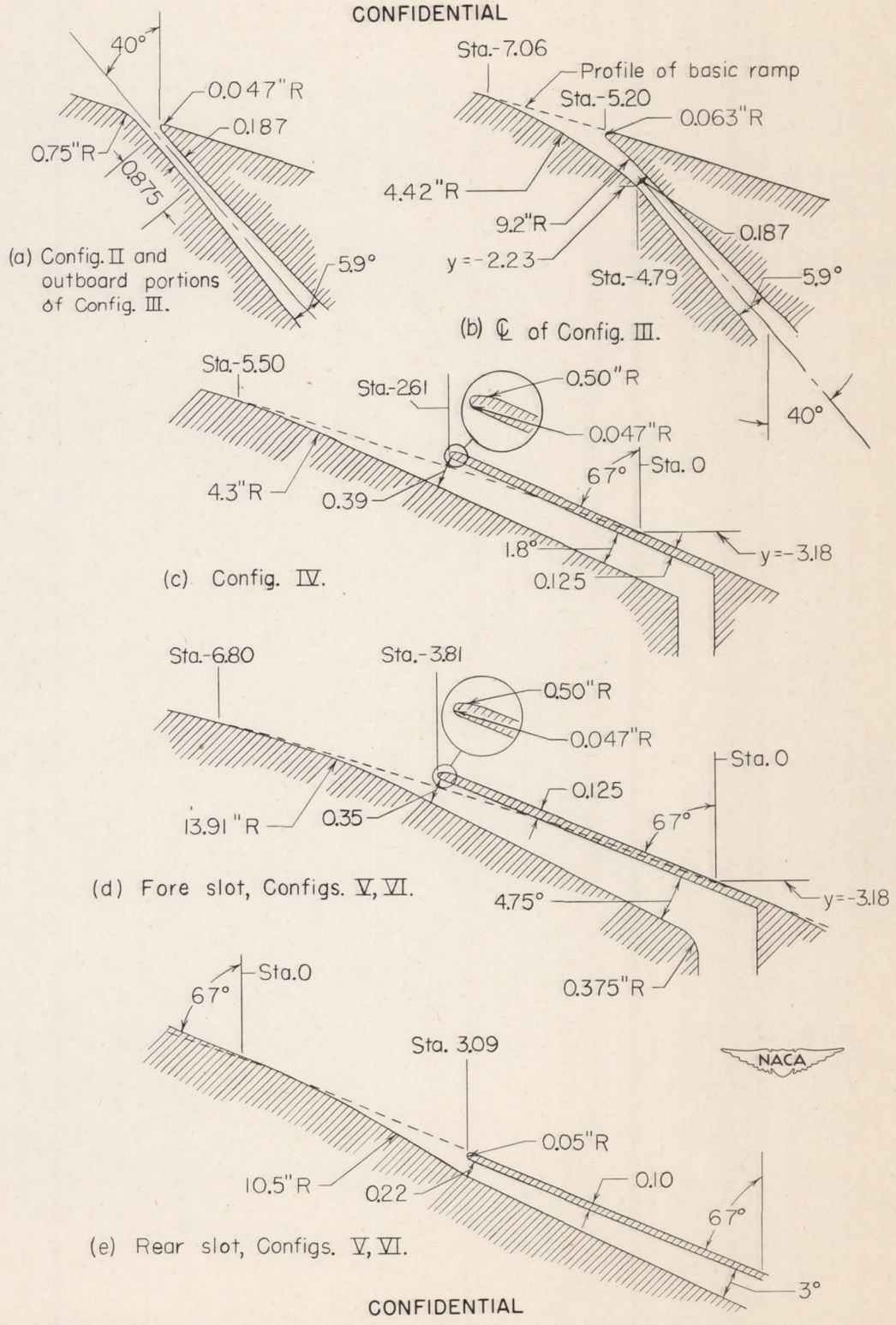

Figure 4.- Dimensions of boundary-layer slots.

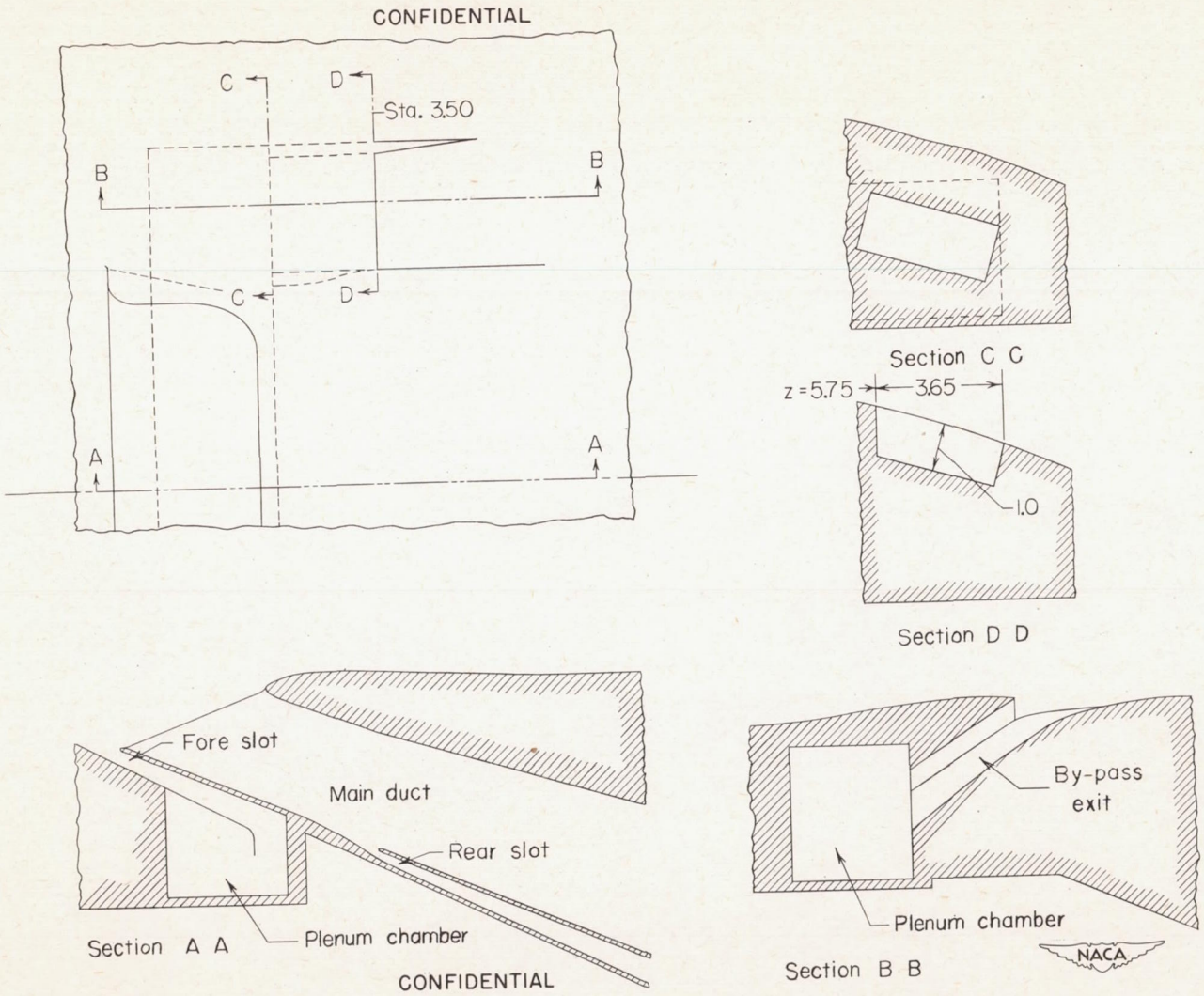

Figure 5.- Bypass ducting of configuration VI.

CONFIDENTIAL

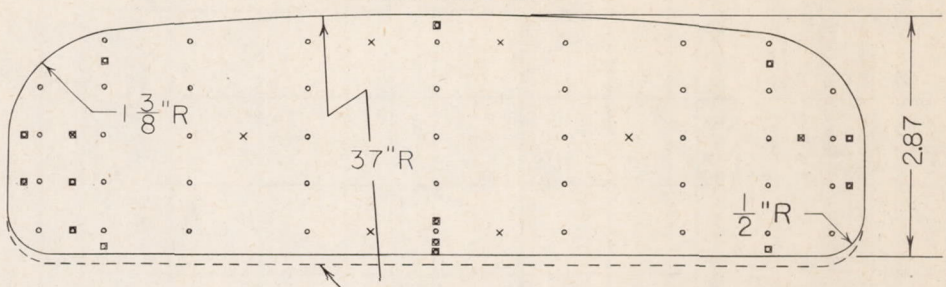

(a) Inlet of main duct.

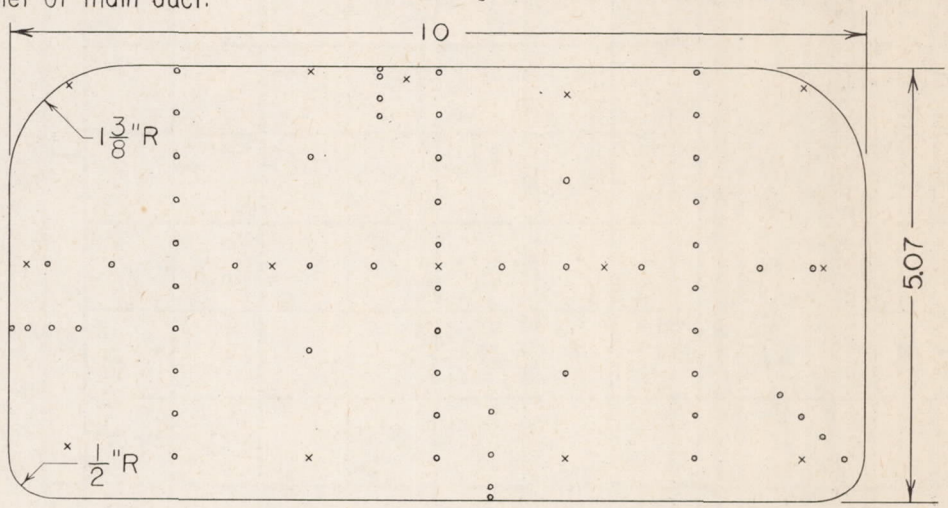

(b) End of diffuser of main duct.

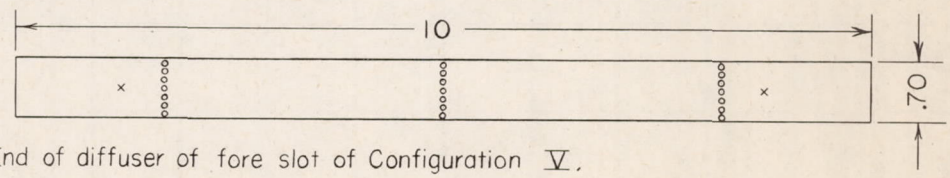

(c) End of diffuser of fore slot of Configuration V.

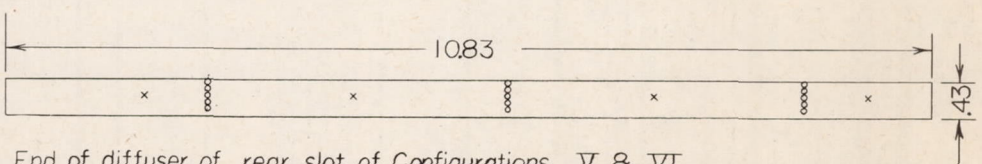

(d) End of diffuser of rear slot of Configurations V & VI.

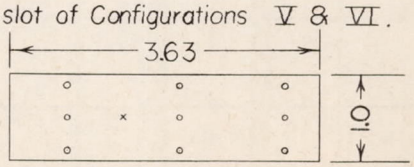

(e) By pass exit (sta. 2.85) of Configuration VI

NACA

CONFIDENTIAL

Figure 6.- Dimensions and instrumentation of measuring stations in ducting.

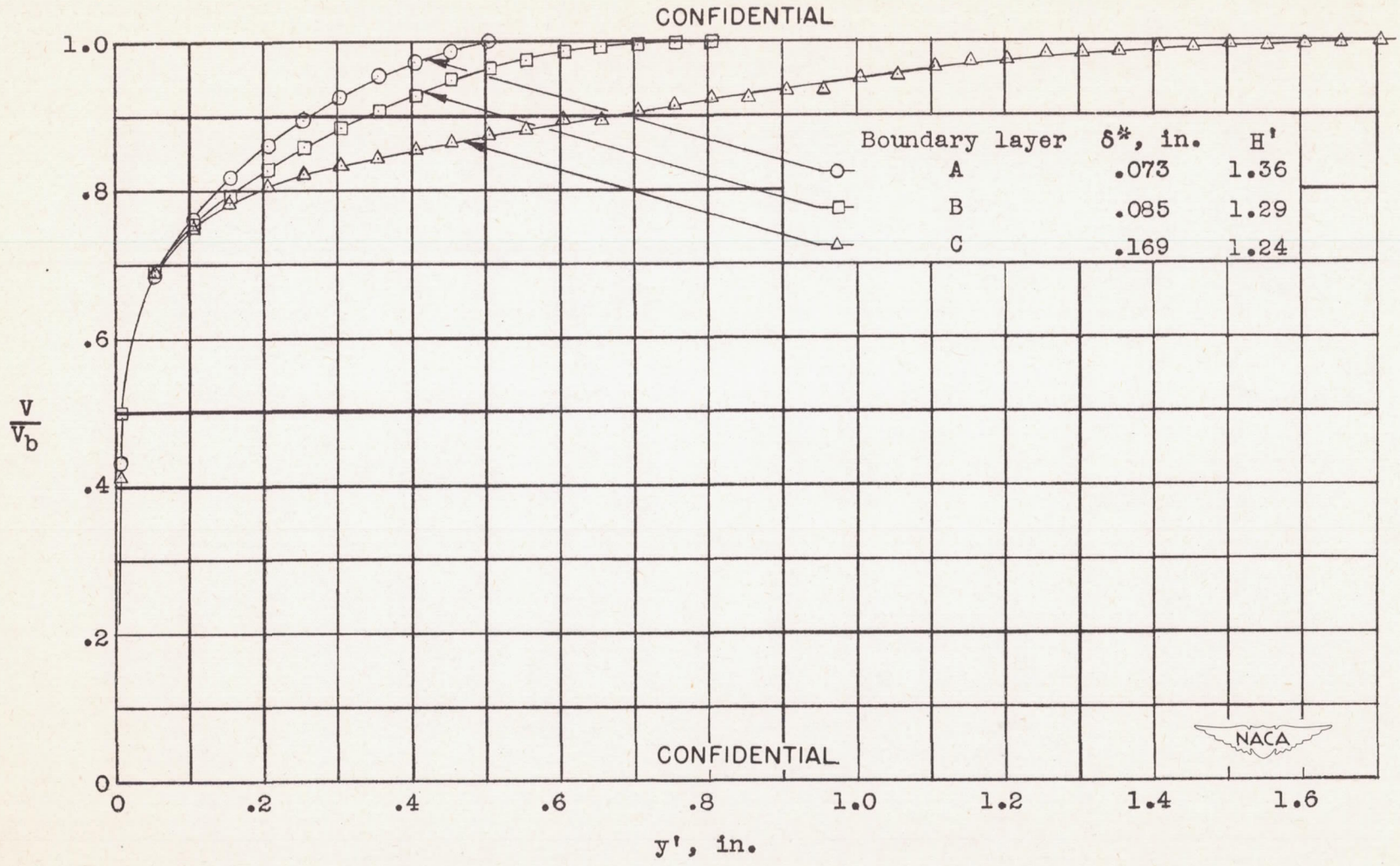

Figure 7.- Velocity distributions in boundary layer 20 inches ahead of inlet.

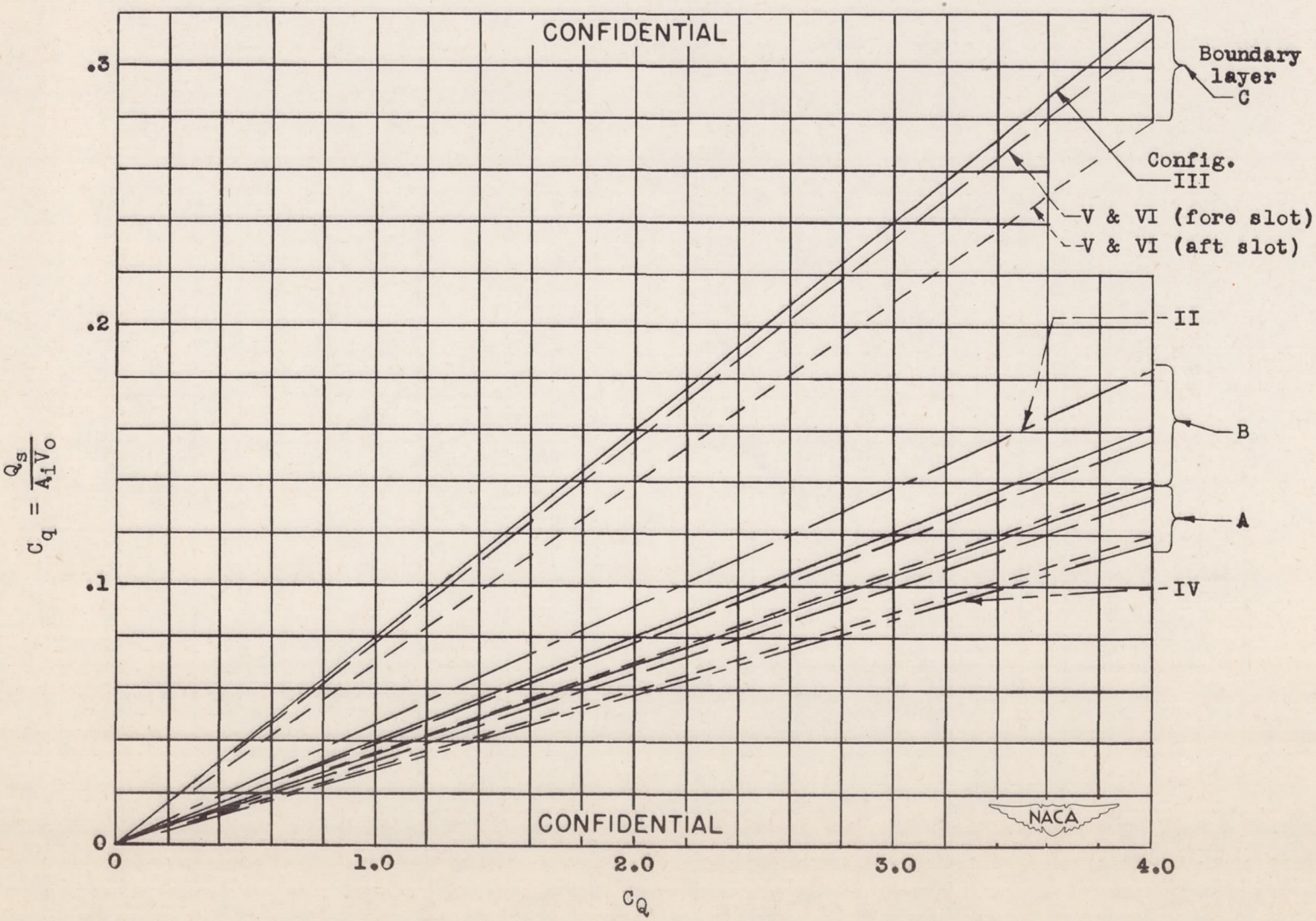

Figure 8.- Relationship of C_Q to C_q.

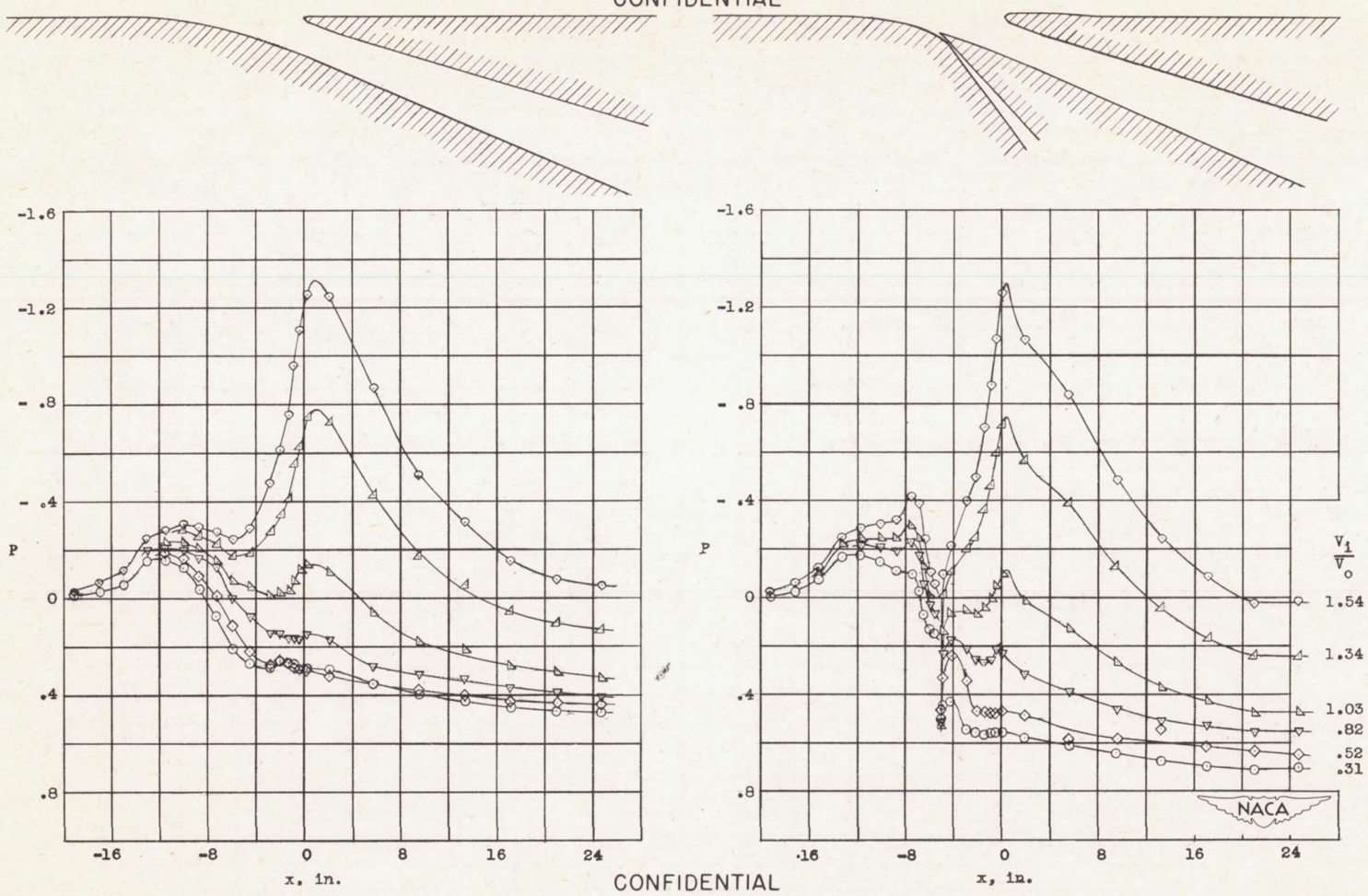

CONFIDENTIAL

(a) Configuration I, no slot.

(b) Configuration III, $C_{Q_1} = 1.6$.

Figure 9.- Static-pressure distributions along center line of ramp and duct bottom. Boundary layer B.

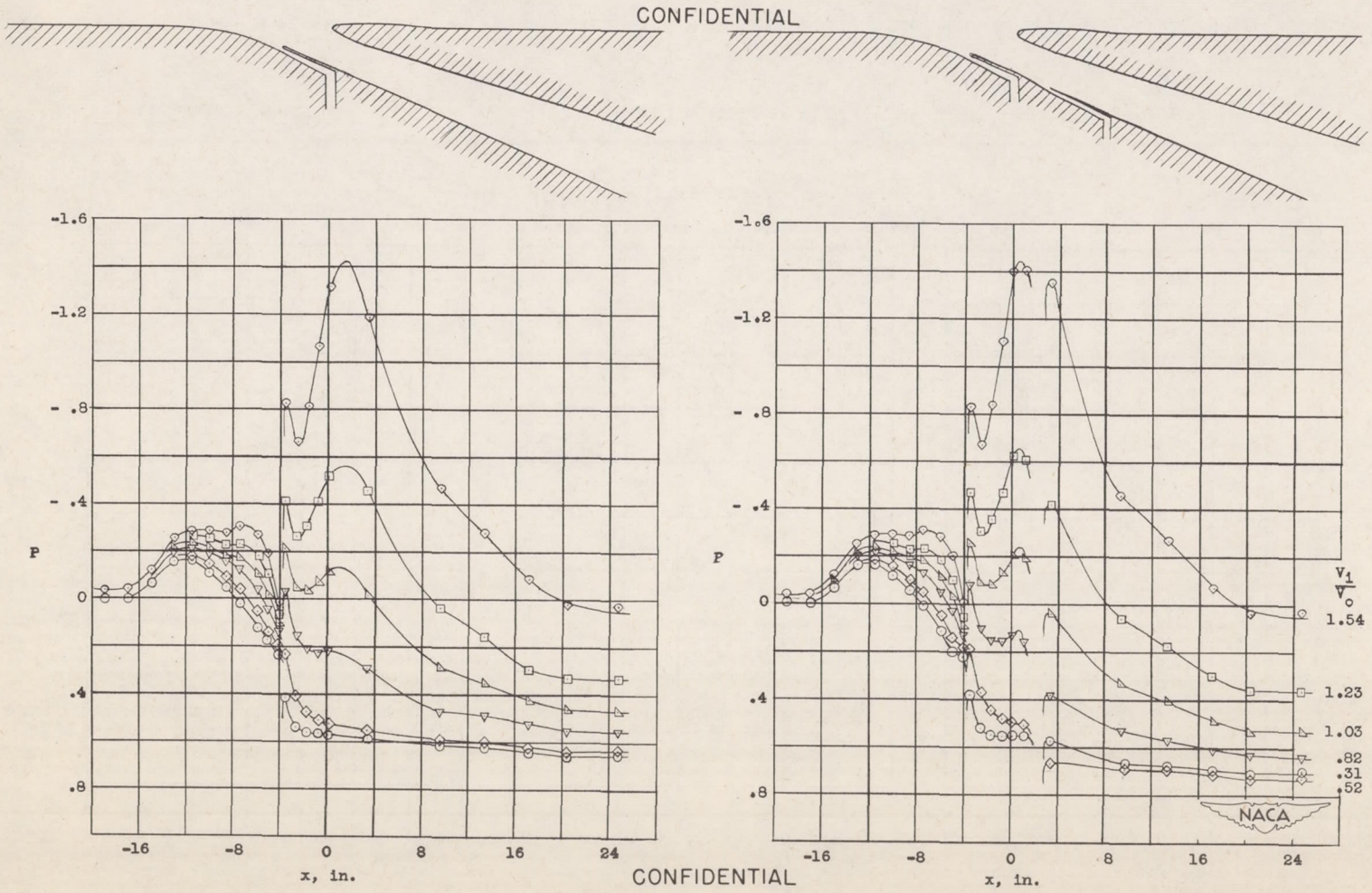

(c) Configuration V, C_{Q_1} = 1.7.

(d) Configuration V, C_{Q_1} = 1.7, C_{Q_2} = 0.9.

Figure 9.- Concluded.

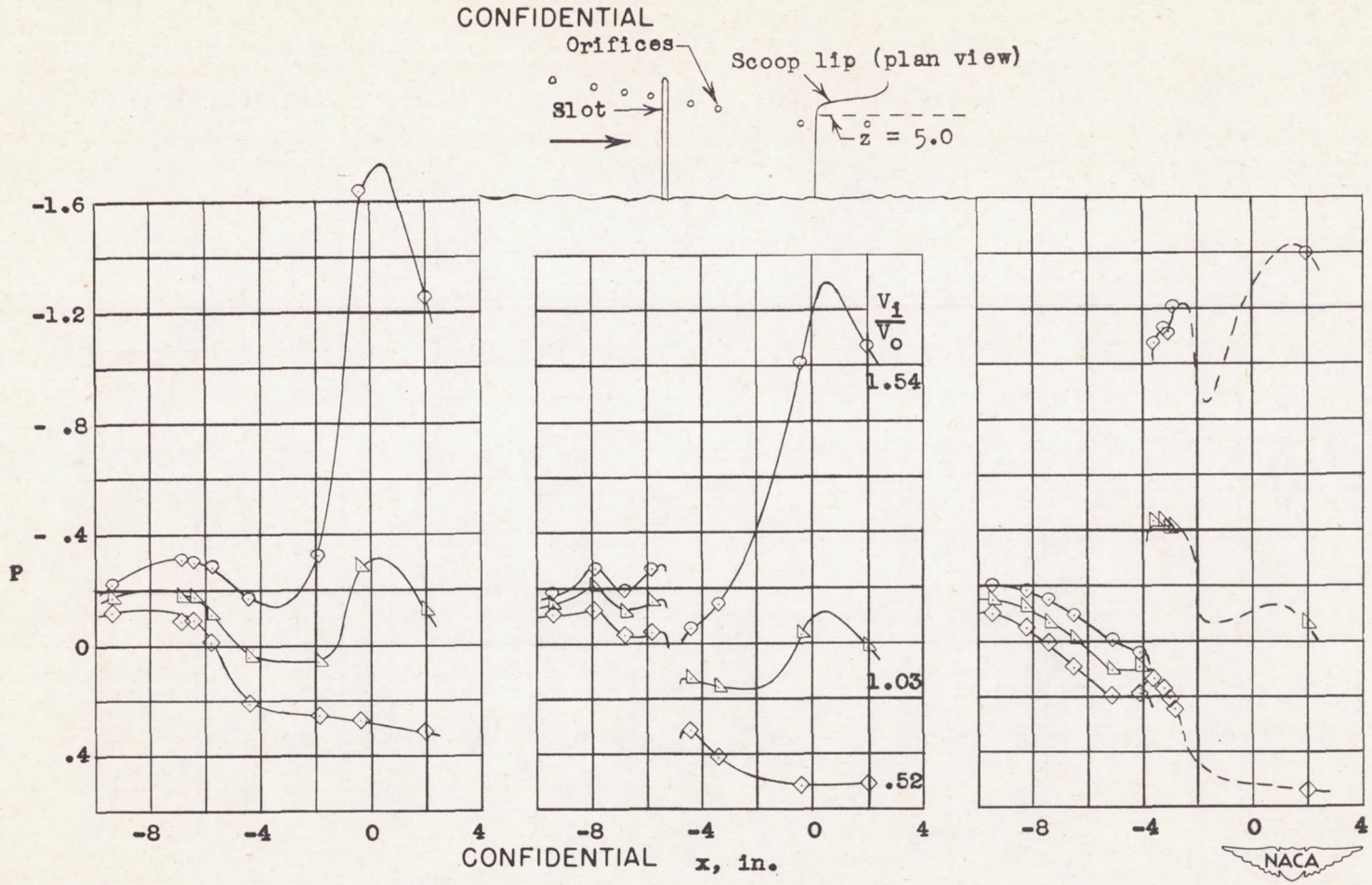

(a) Configuration I.

(b) Configuration III, $C_{Q_1} = 1.6$.

(c) Configuration V, $C_{Q_1} = 1.7$.

Figure 10.- Static-pressure distributions in valley approaching inner corner of entrance. Boundary layer B.

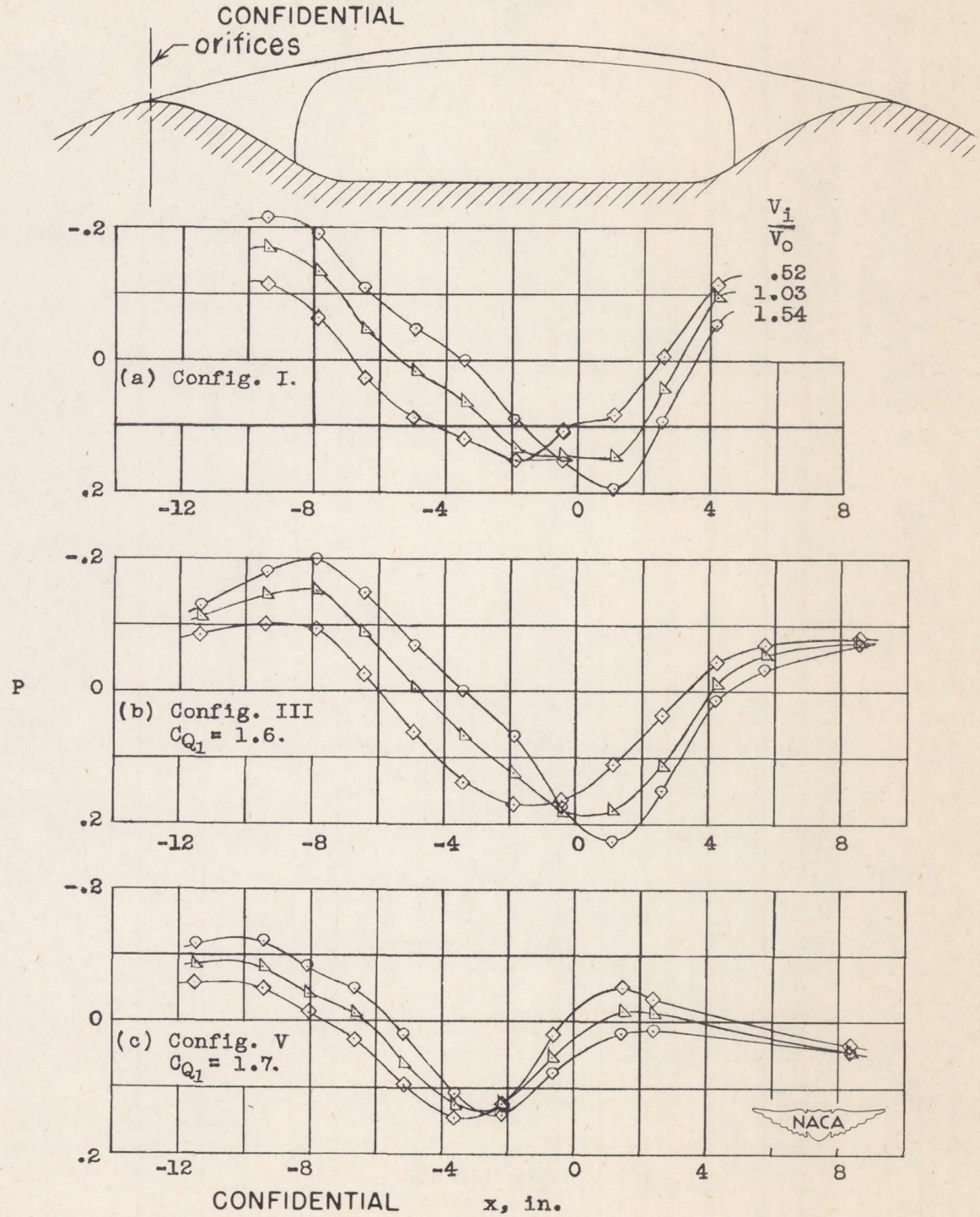

Figure 11.- Static-pressure distributions along edge of dimple. Boundary layer B.

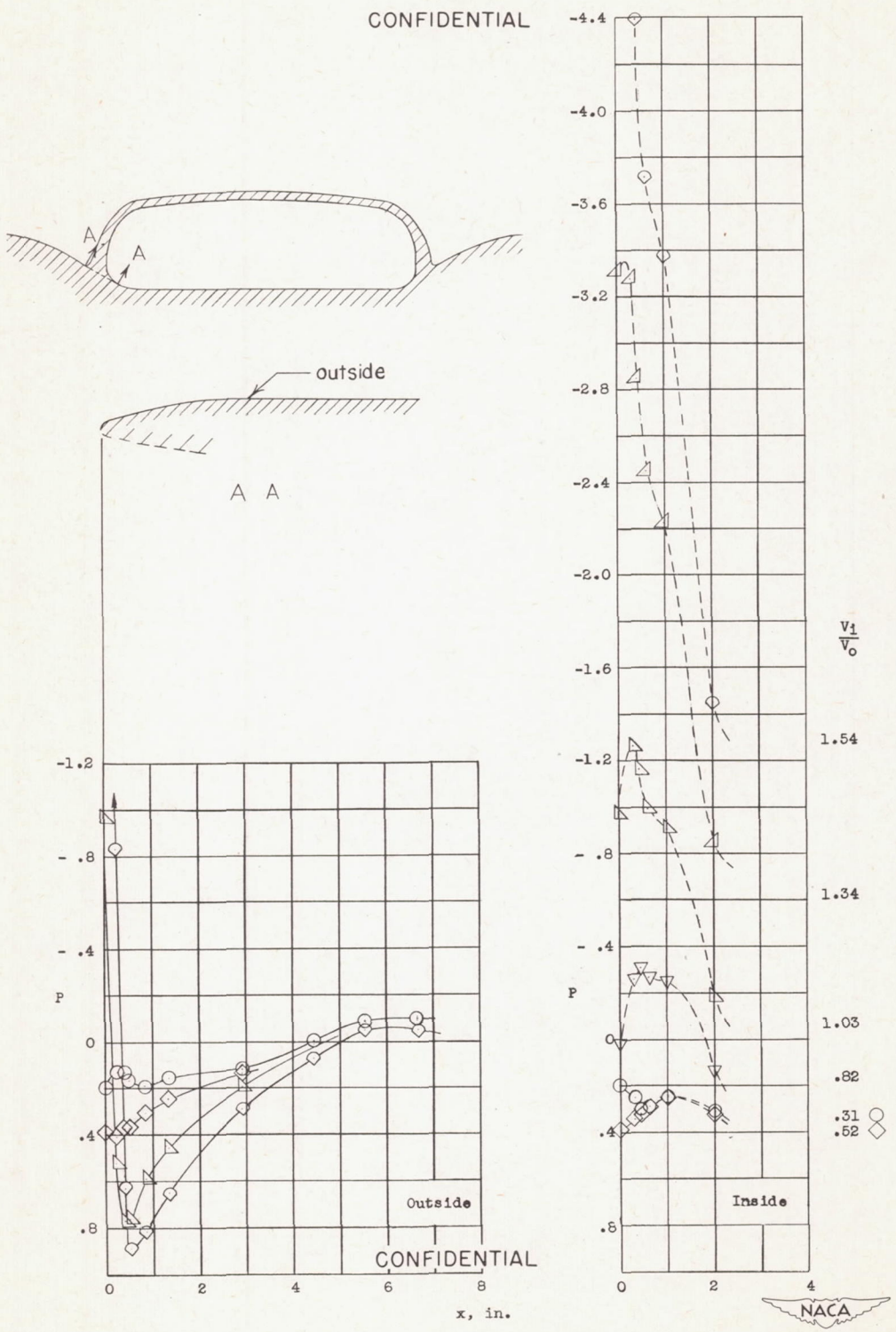

(a) Base section - configuration I.

Figure 12.- Static-pressure distributions around scoop lip. Boundary layer B.

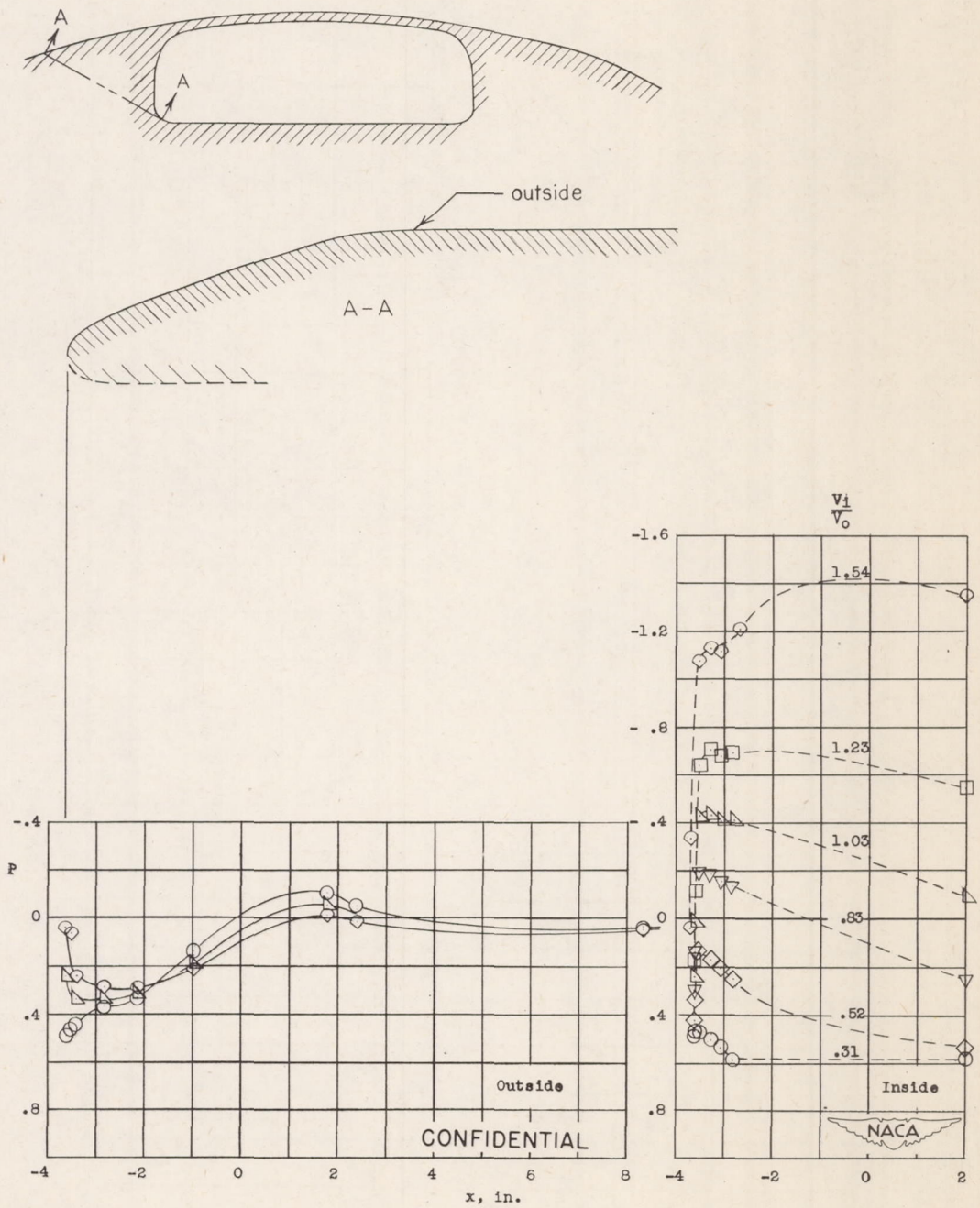

(b) Base section - configuration V, $C_{Q_1} = 1.7$.

Figure 12.- Continued.

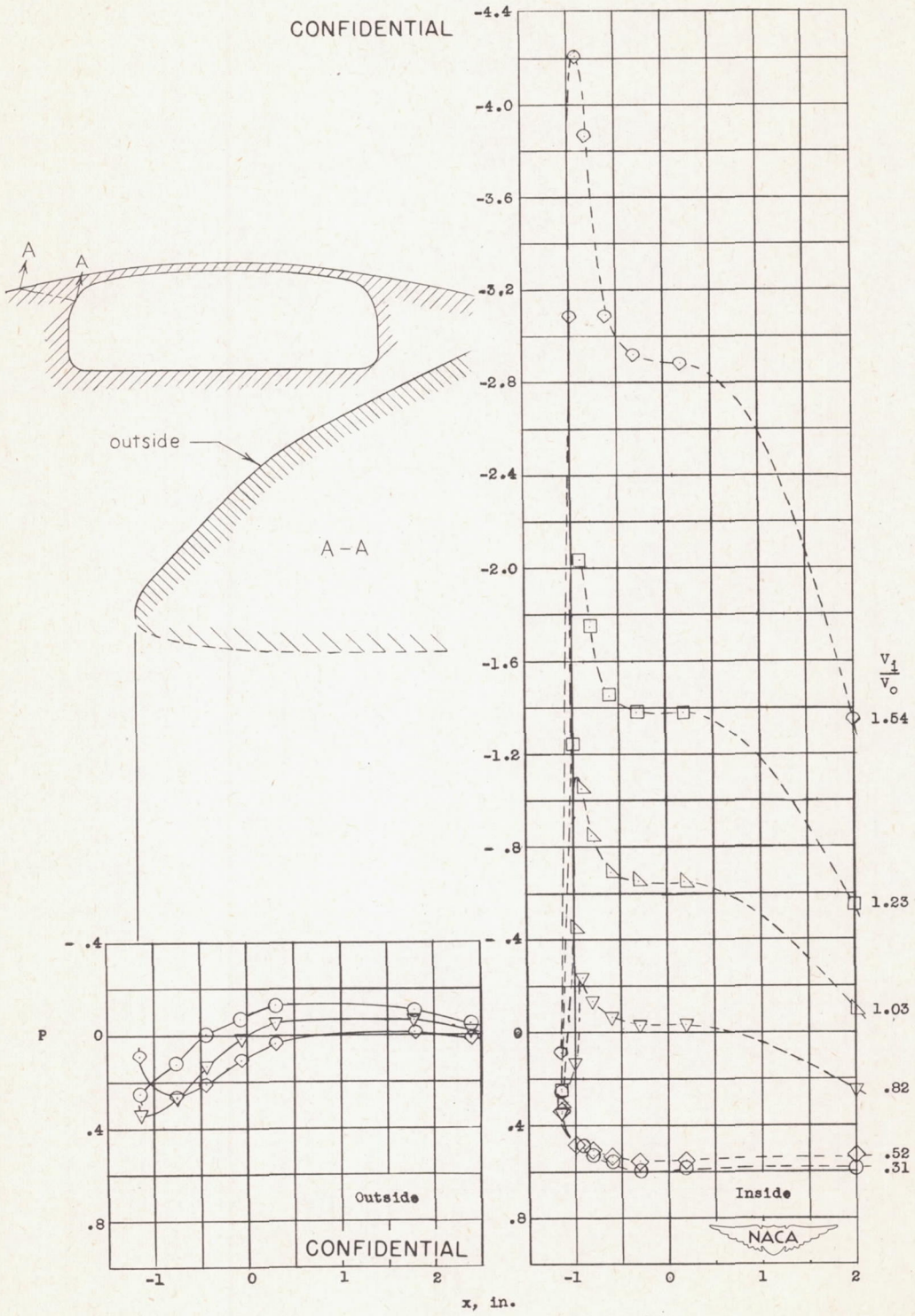

(c) Top corner section - configuration V, $C_{Q_1} = 1.7$.

Figure 12.- Continued.

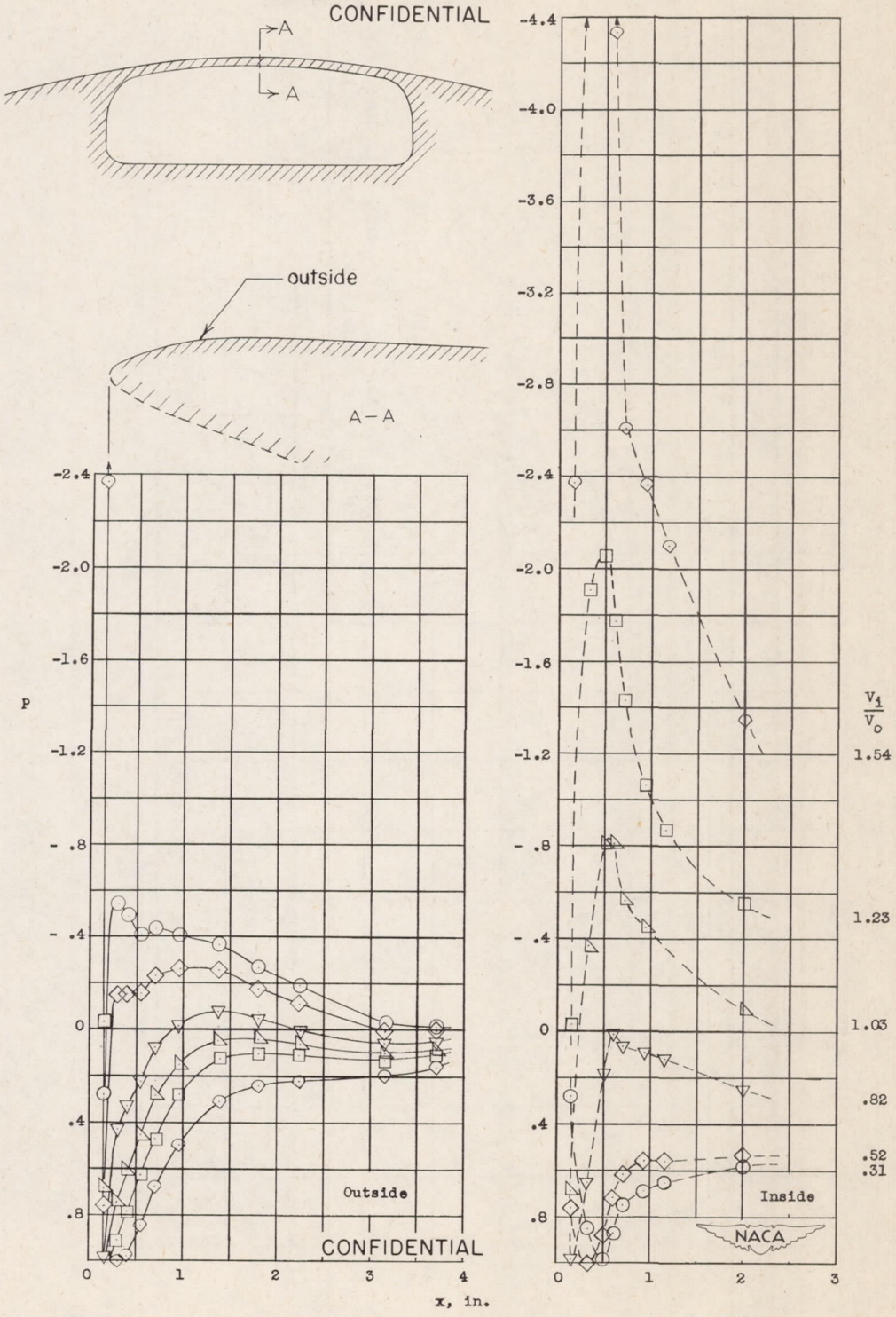

(d) Center-line section - configuration V, $C_{Q_1} = 1.7$.

Figure 12.- Concluded.

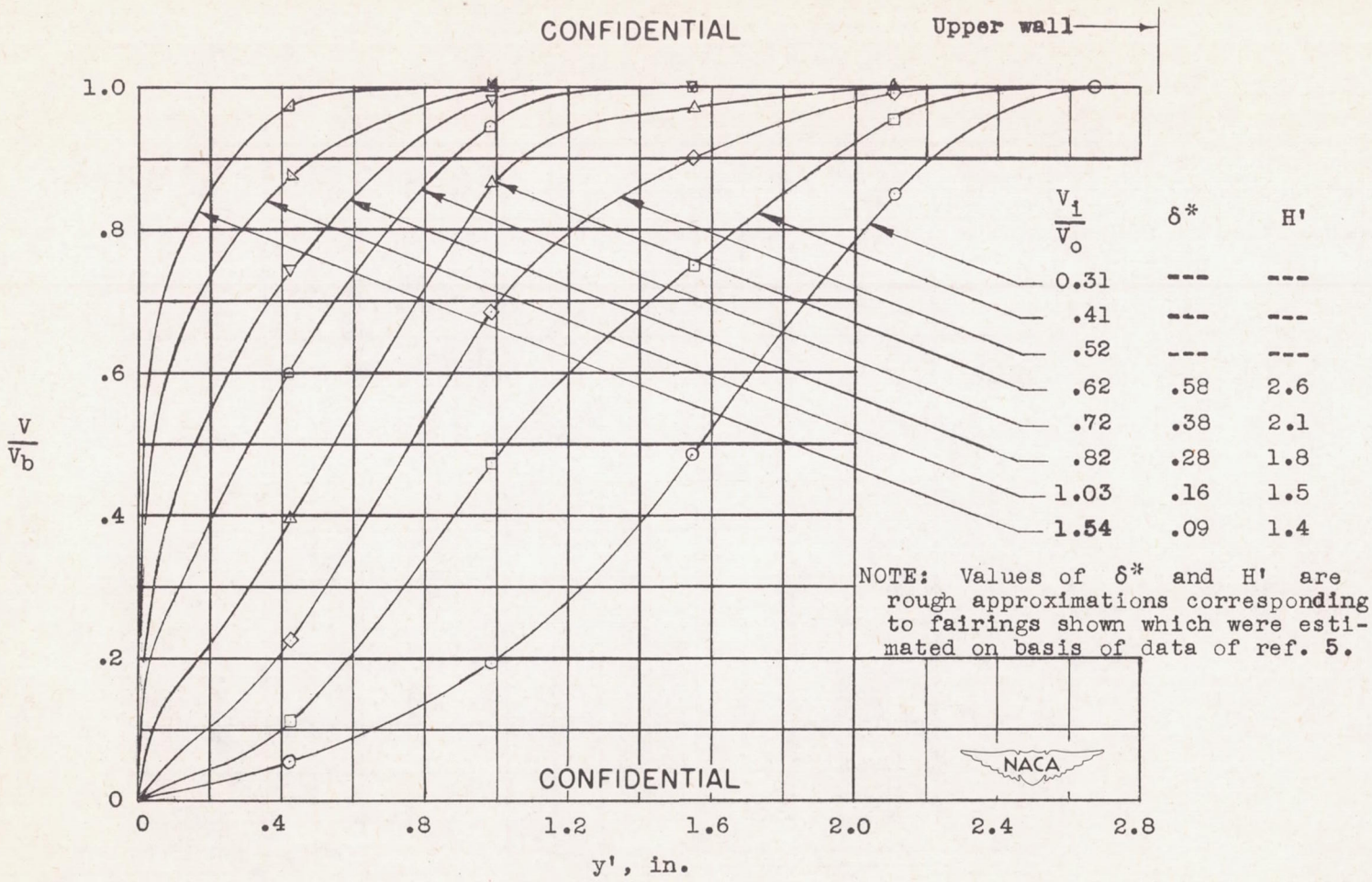

(a) Effect of inlet-velocity ratio. Slotless configuration I.

Figure 13.- Velocity profiles of boundary layer on duct floor at center line of entrance measuring station.

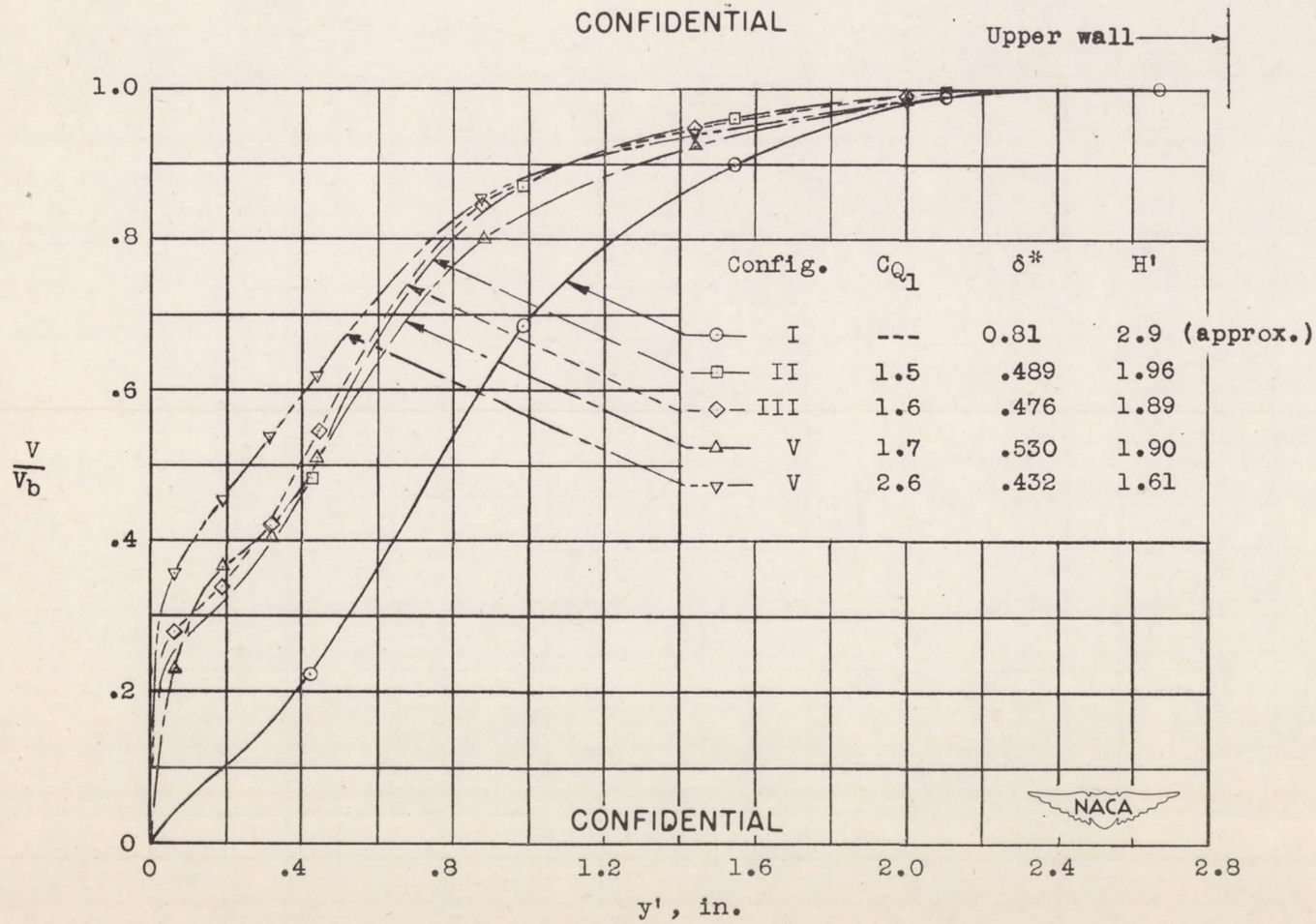

(b) Effects of slot arrangement and suction quantity, $\frac{V_i}{V_o} = 0.52$.

Figure 13.- Concluded.

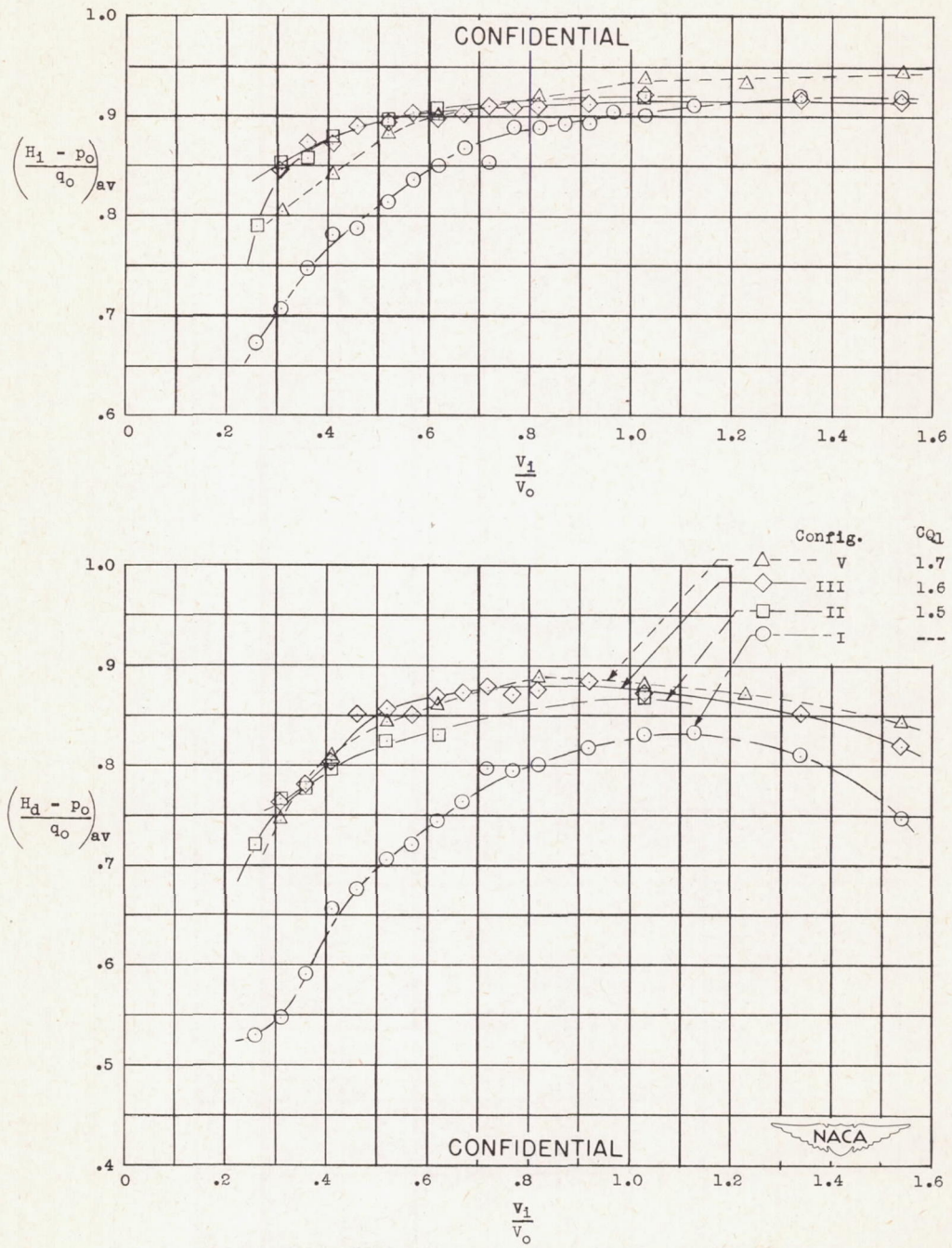

(a) Configurations I, II, III, and V. Effect of ramp slot configuration. Standard ramp without sidewalls, no second slot, boundary layer B.

Figure 14.- Comparison of average total-pressure recoveries at inlets and ends of diffusers of the several scoop configurations.

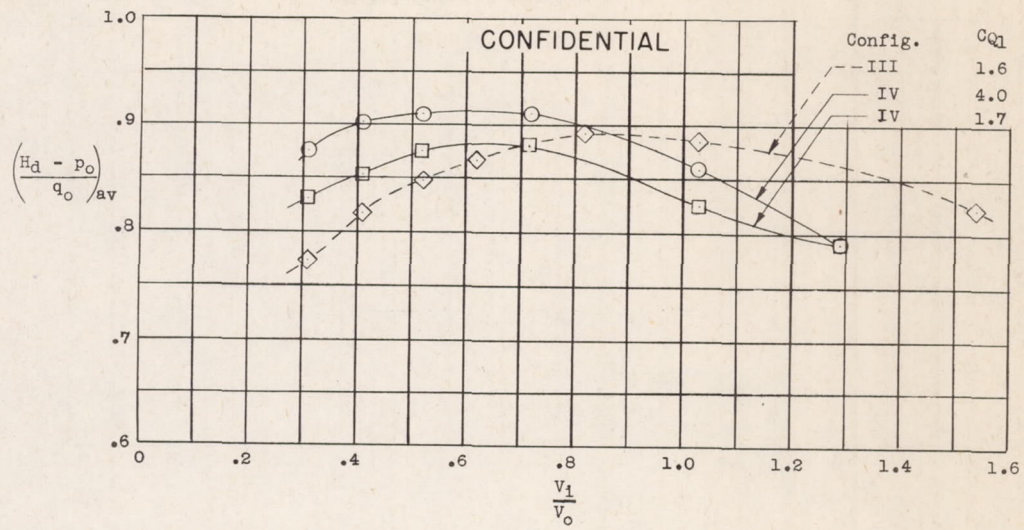

(b) Configurations III and IV. Effect of diverging ramp sidewalls, boundary layer A.

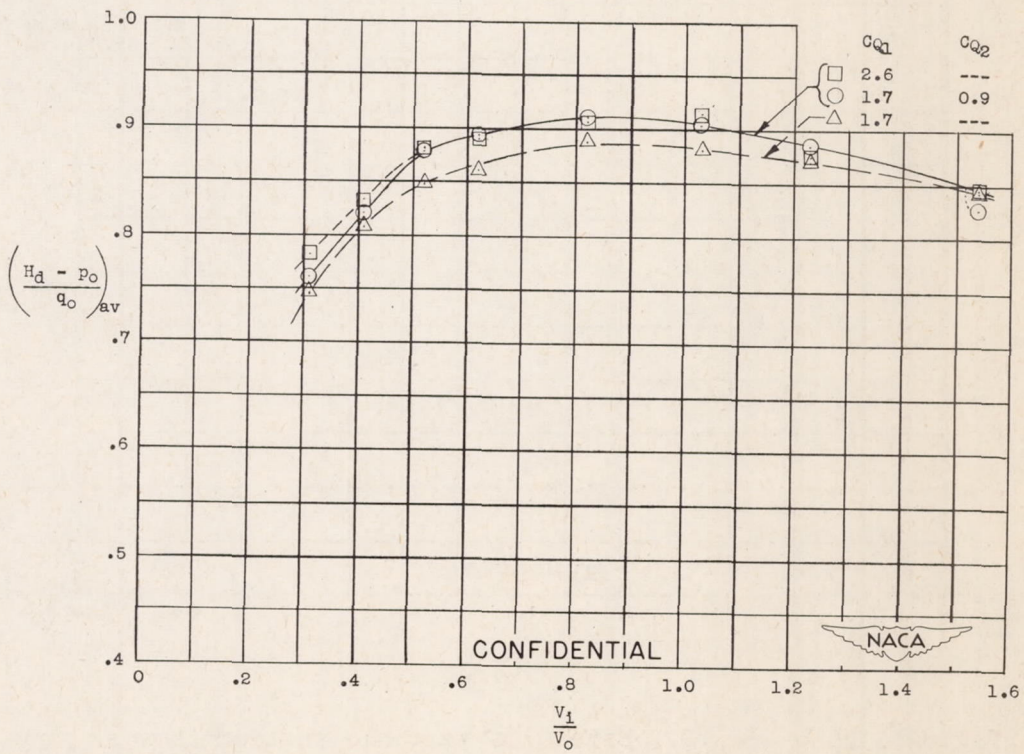

(c) Configuration V. Effect of addition of second slot inside inlet, boundary layer B.

Figure 14.- Continued.

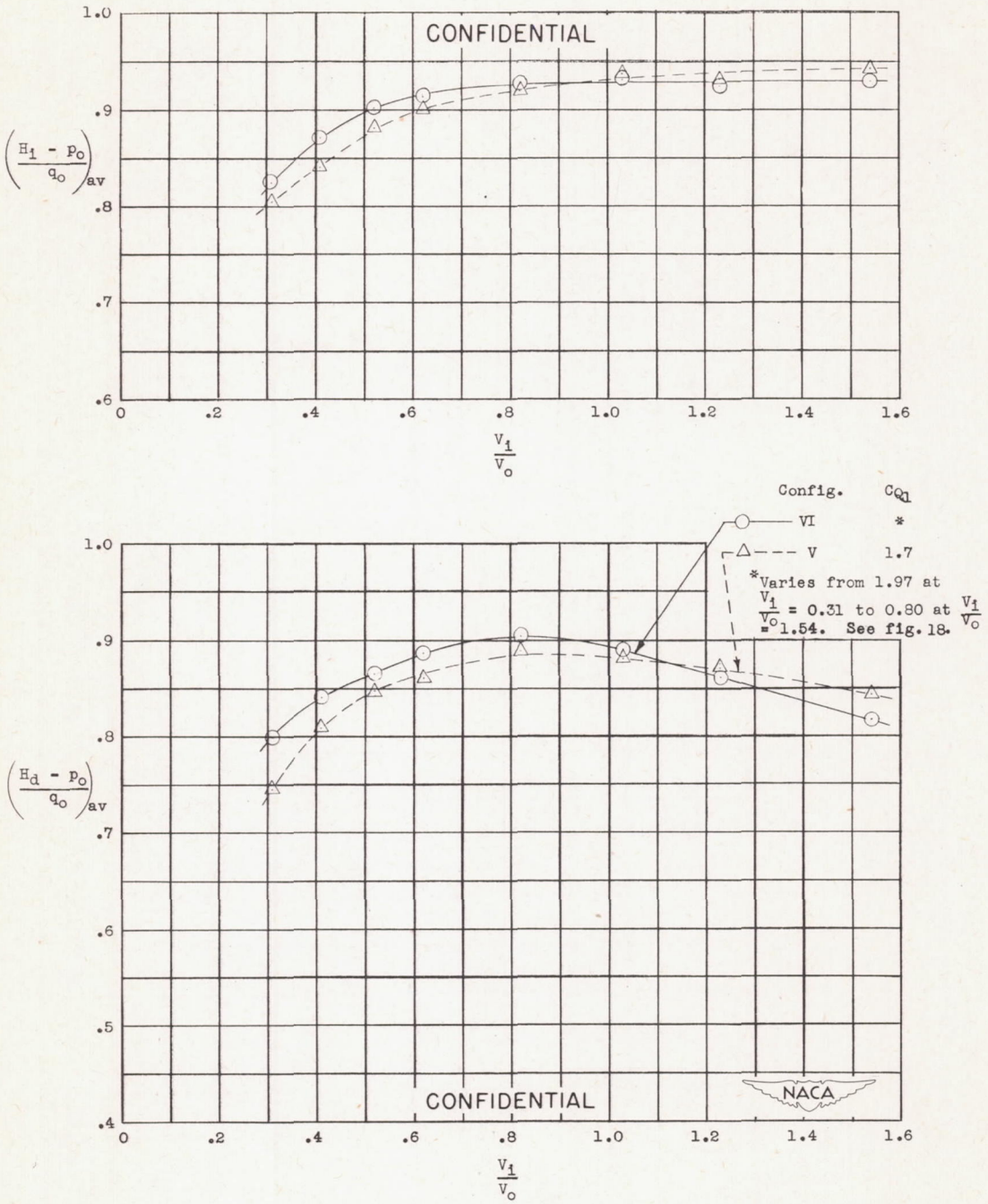

(d) Configurations V and VI. Effect of variable suction flow as provided by bypass of configuration VI; no second slot, boundary layer B.

Figure 14.- Concluded.

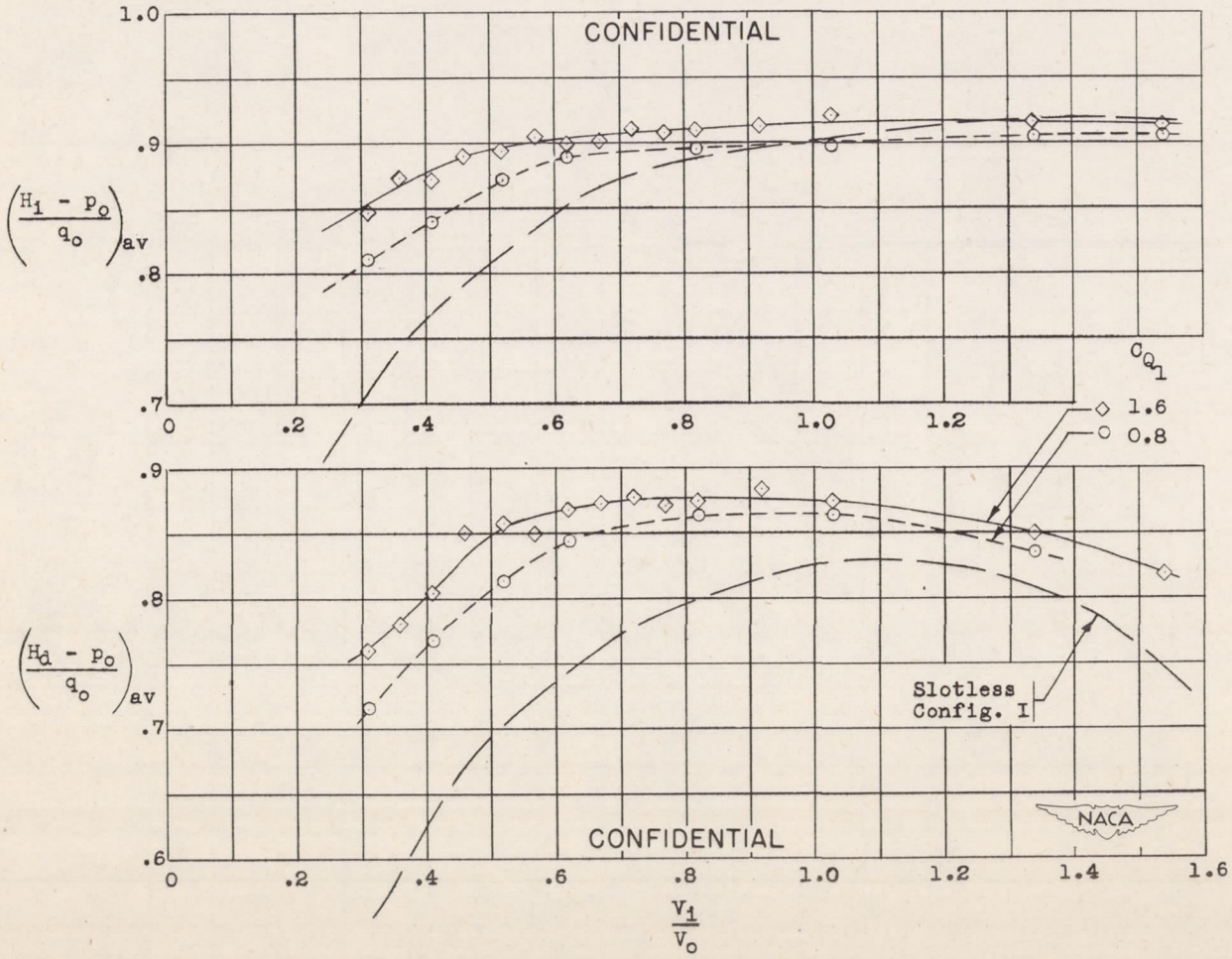

(a) Configuration III.

Figure 15.- Average total-pressure recovery at inlet and end of diffuser as a function of inlet-velocity ratio and suction quantity. Boundary layer B.

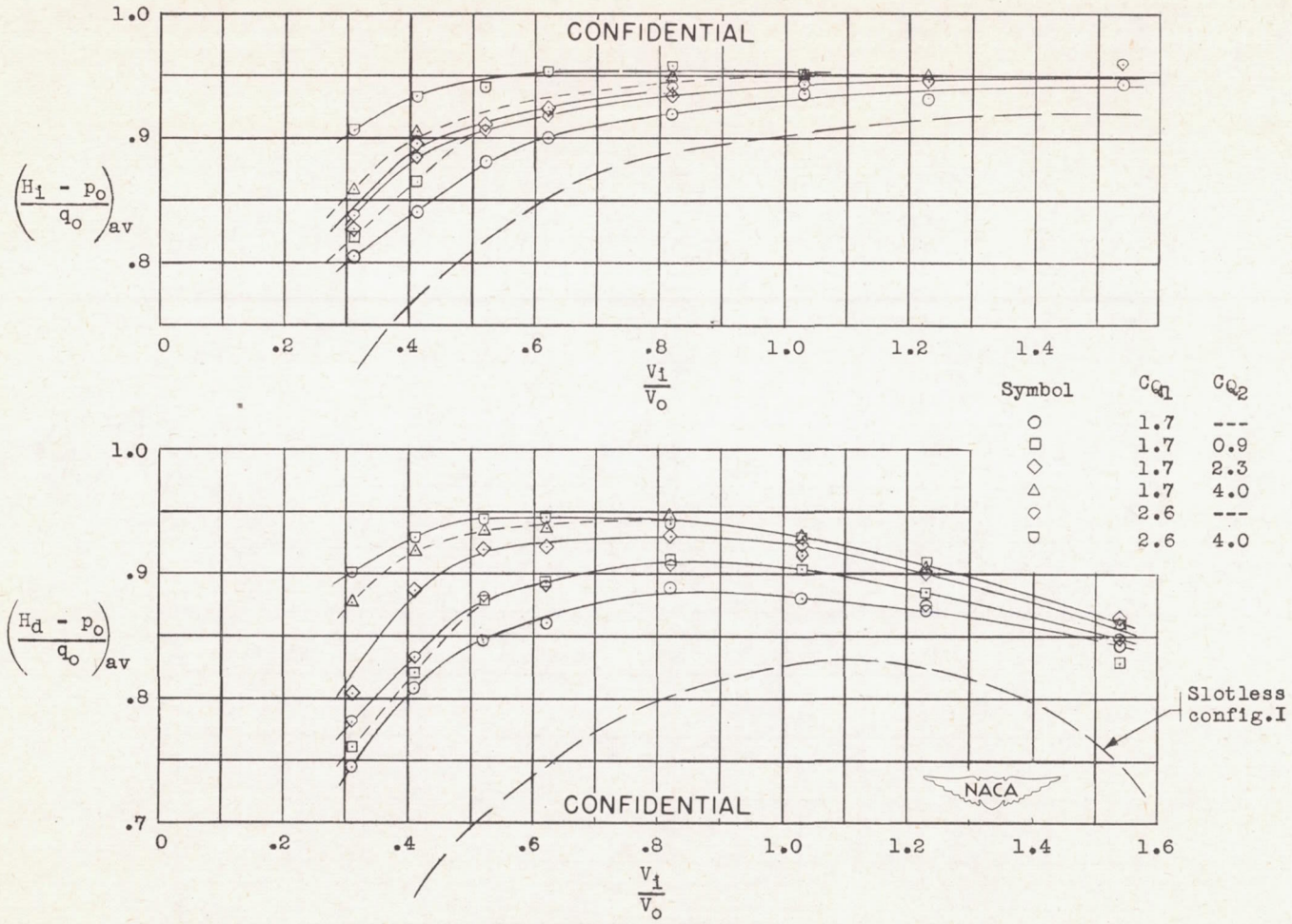

(b) Configuration V.

Figure 15.- Continued.

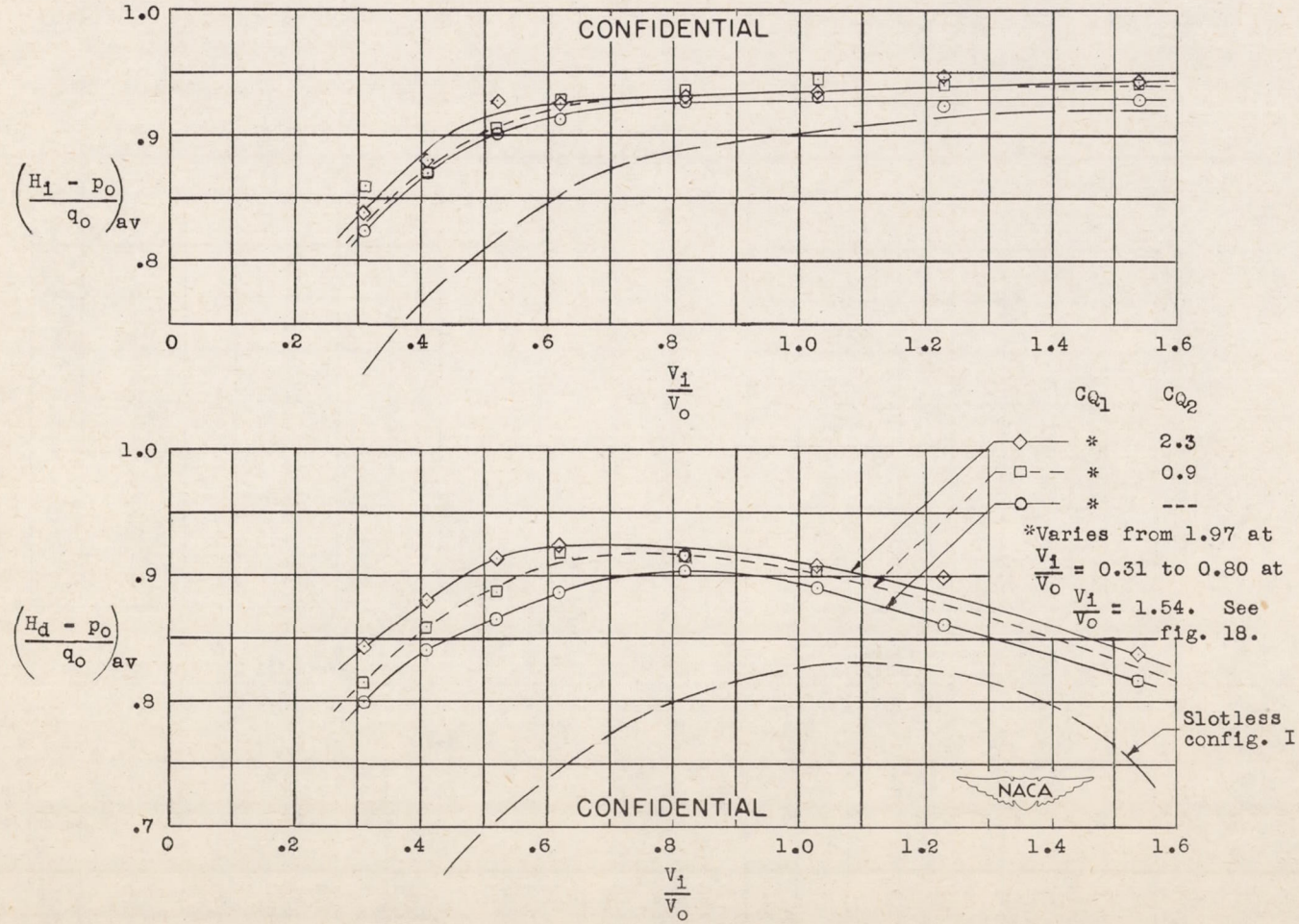

(c) Configuration VI.

Figure 15.- Concluded.

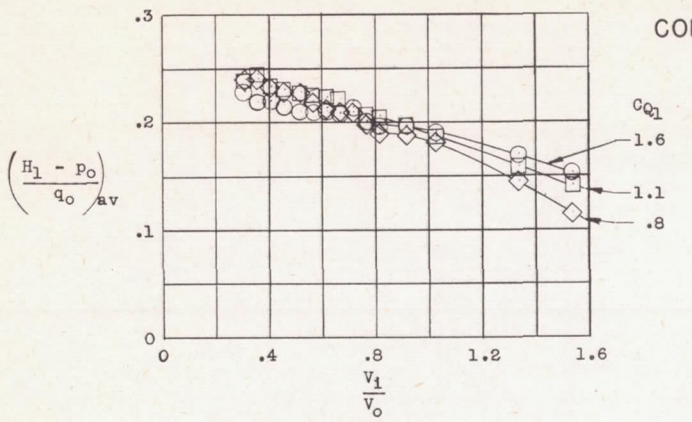

(a) Configuration III - Ramp slot.

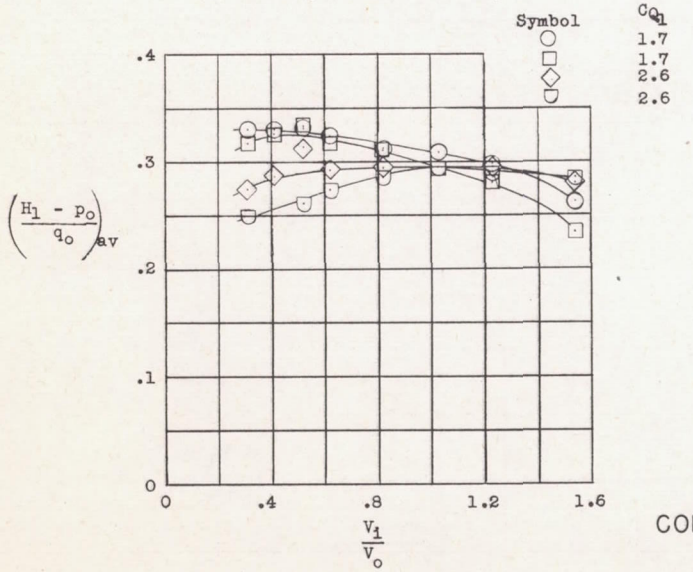

(b) Configuration V - Ramp slot.

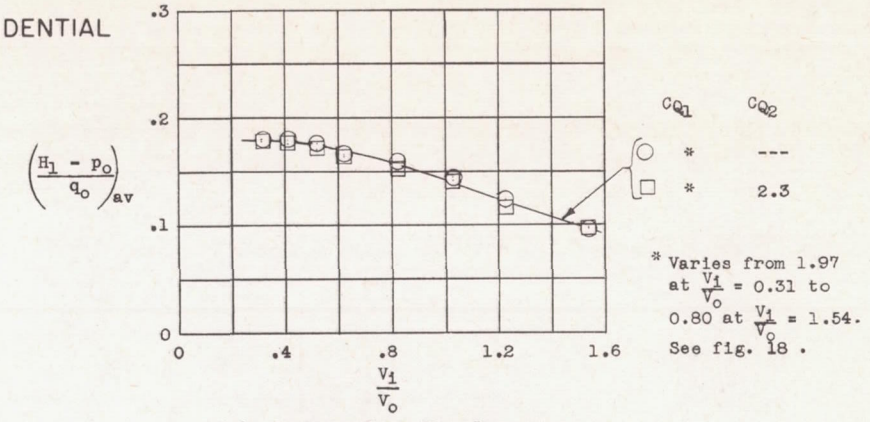

(c) Configuration VI - Ramp slot (measured at exit of bypass ducting).

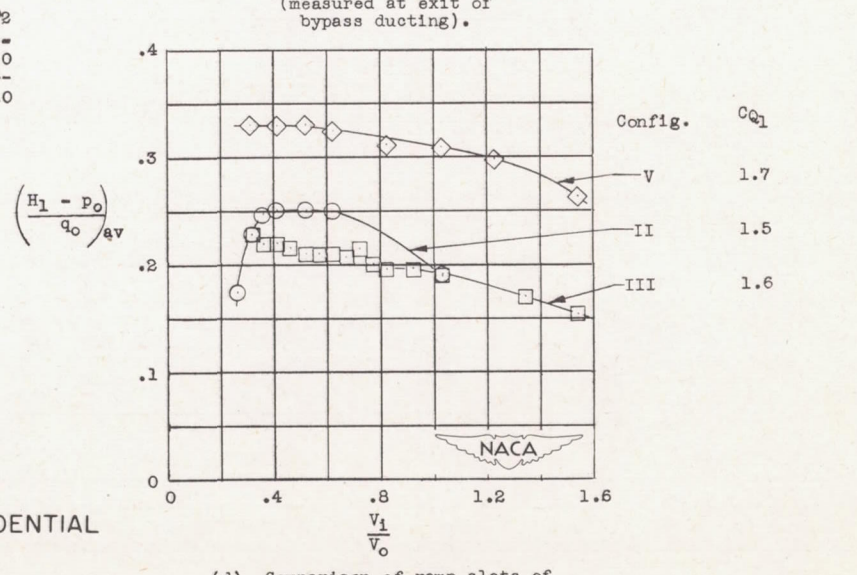

(d) Comparison of ramp slots of configurations II, III, and V.

Figure 16.- Average total-pressure recoveries in suction slots after diffusion. Boundary layer B.

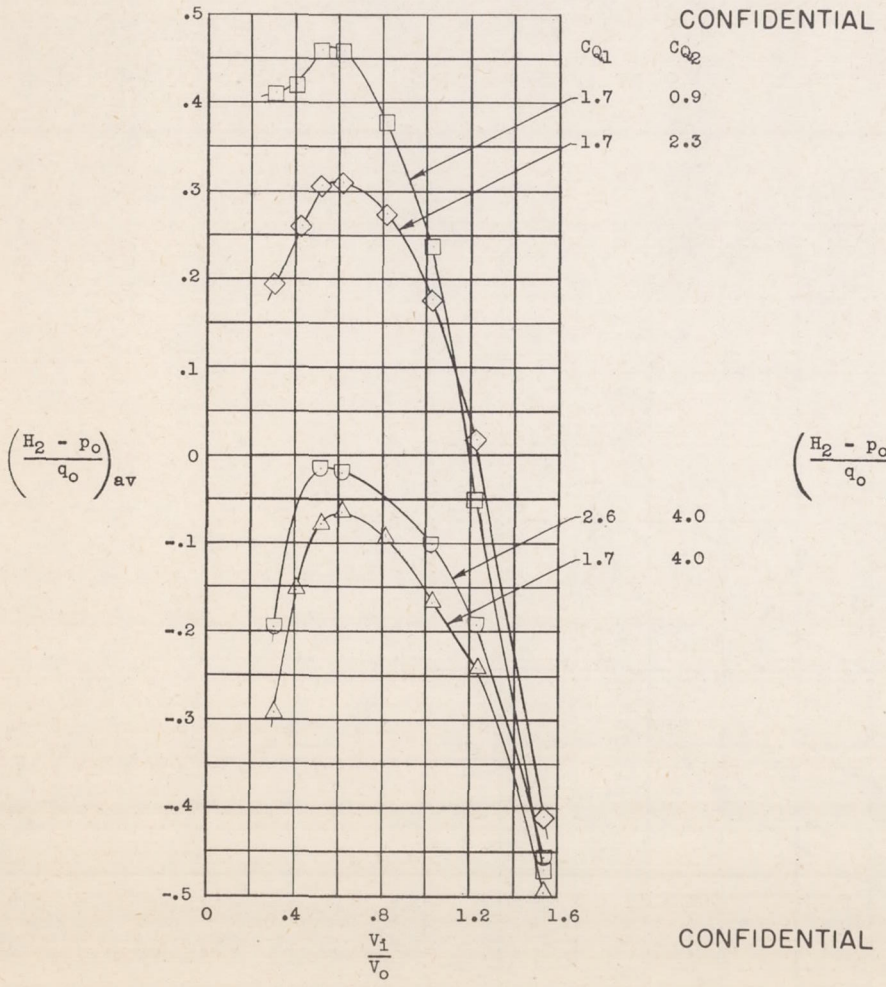

(e) Configuration V - Second slot.

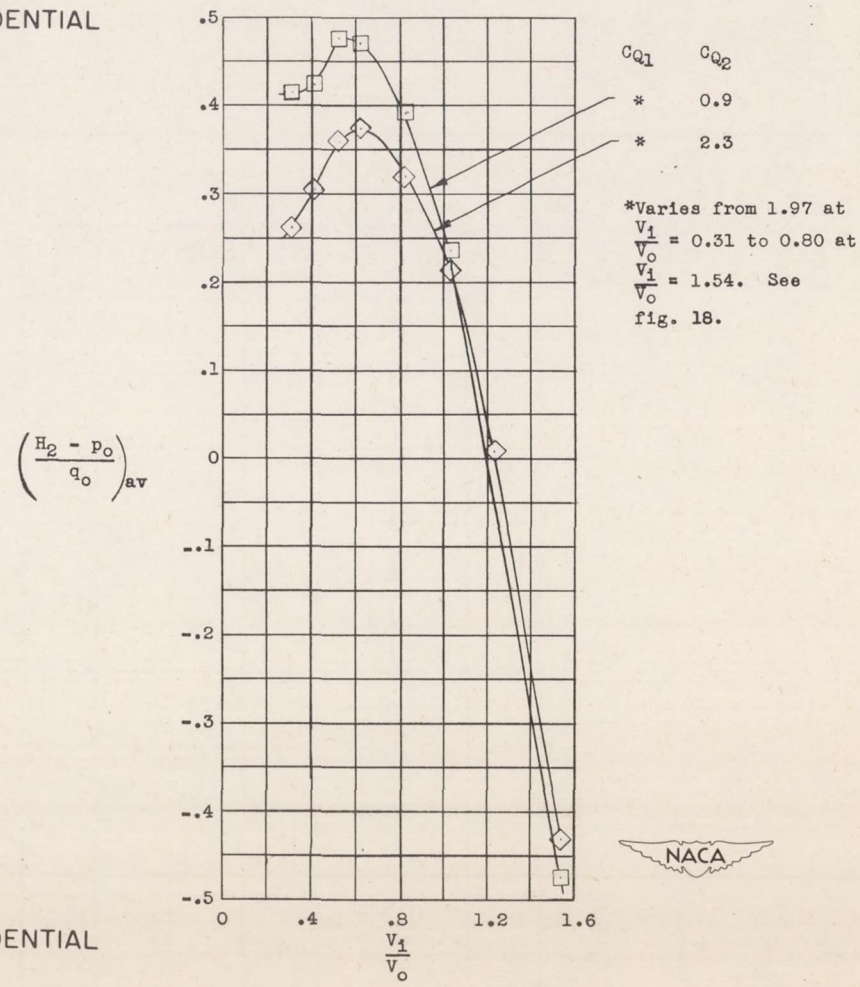

(f) Configuration VI - Second slot.

Figure 16.- Concluded.

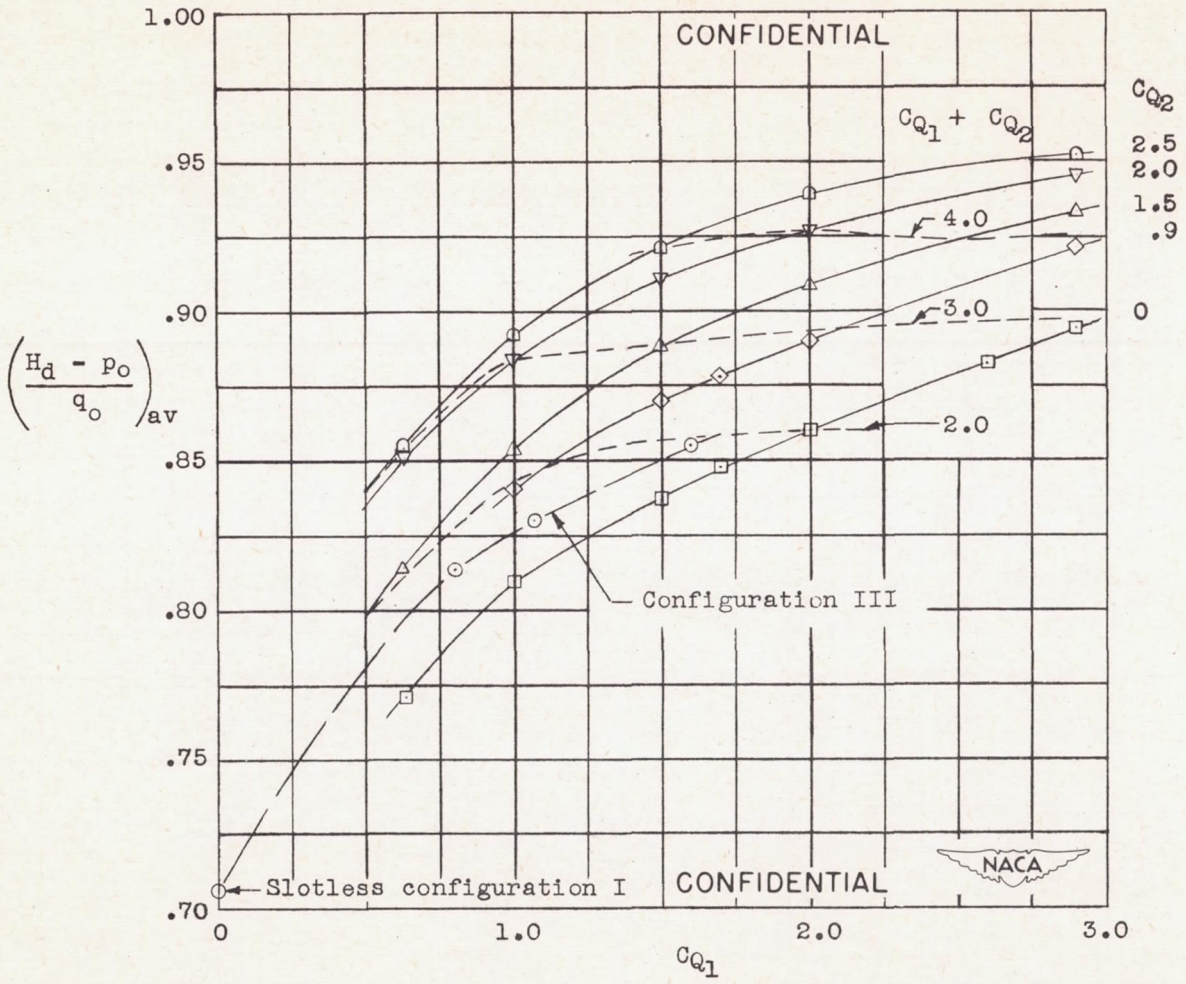

Figure 17.- Average total-pressure recovery at end of diffuser at $\frac{V_i}{V_o} = 0.52$ as a function of suction quantity and distribution of suction. Configuration V, boundary layer B.

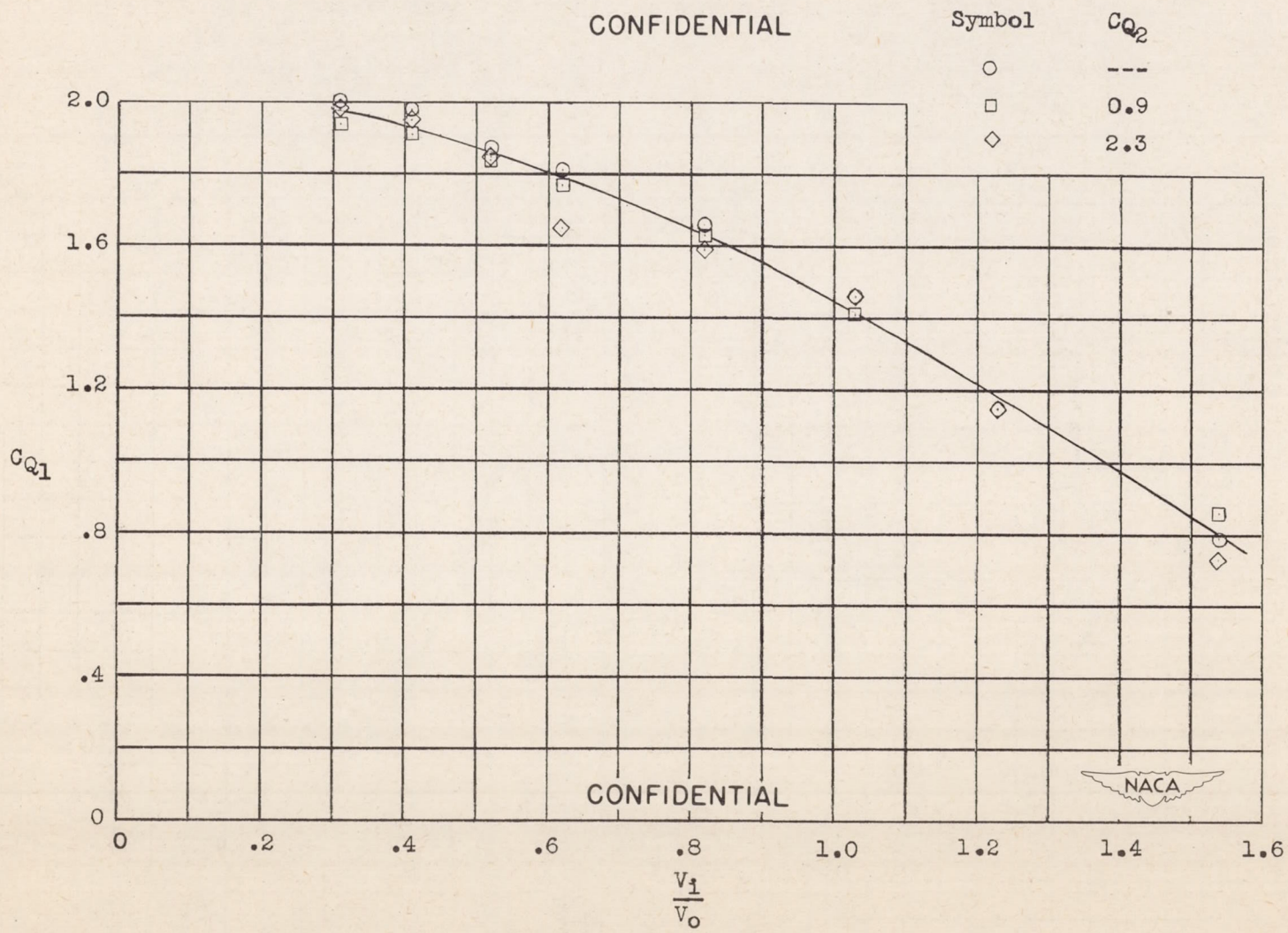

Figure 18.- Suction flow quantity provided by bypass of configuration VI. Boundary layer B.

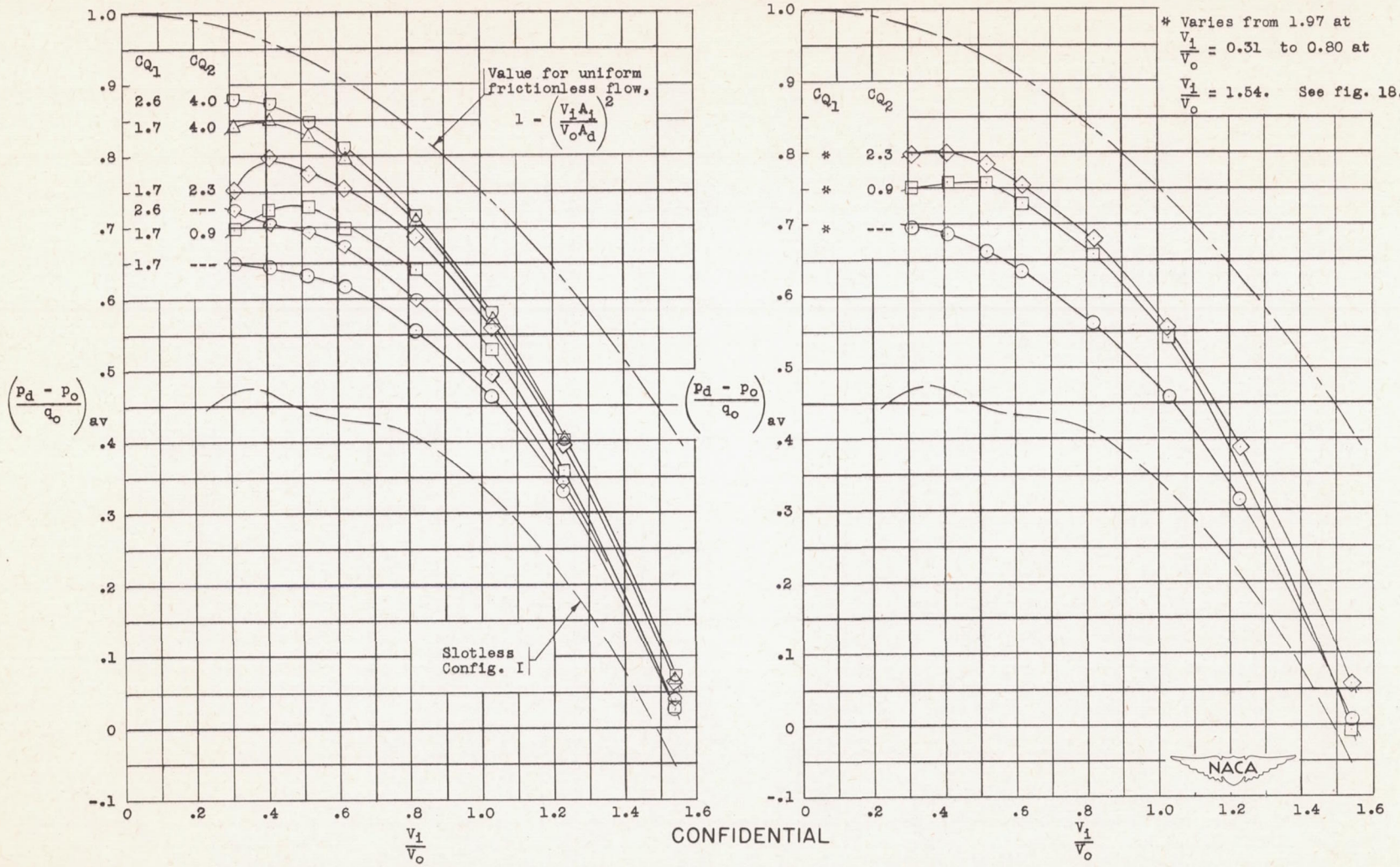

(a) Configuration V. (b) Configuration VI.

Figure 19.- Average static pressure at end of diffuser. Boundary layer B.

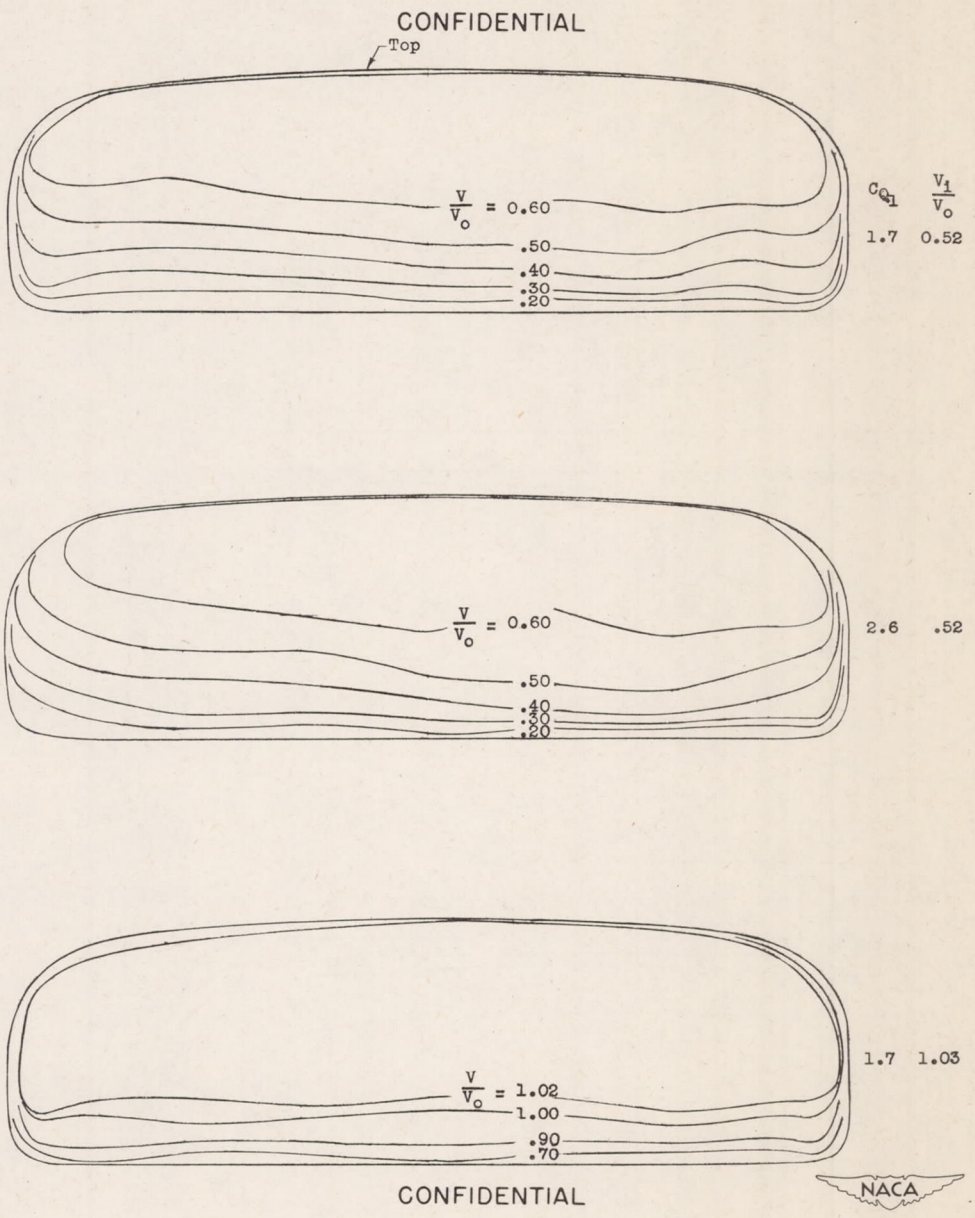

(a) At inlet.

Figure 20.- Velocity distributions in main duct of configuration V. Boundary layer B.

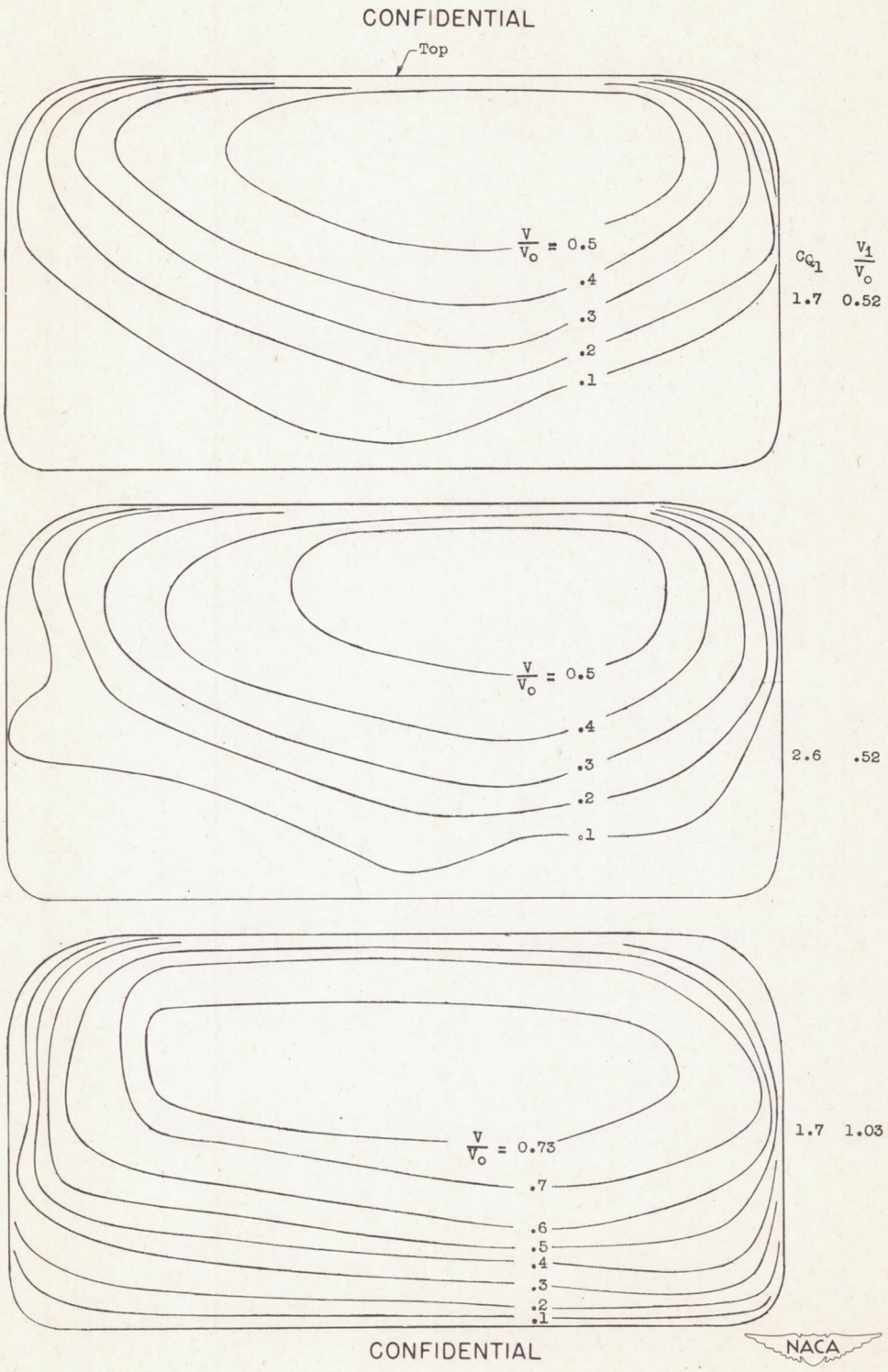

(b) At end of diffuser.

Figure 20.- Concluded.

CONFIDENTIAL

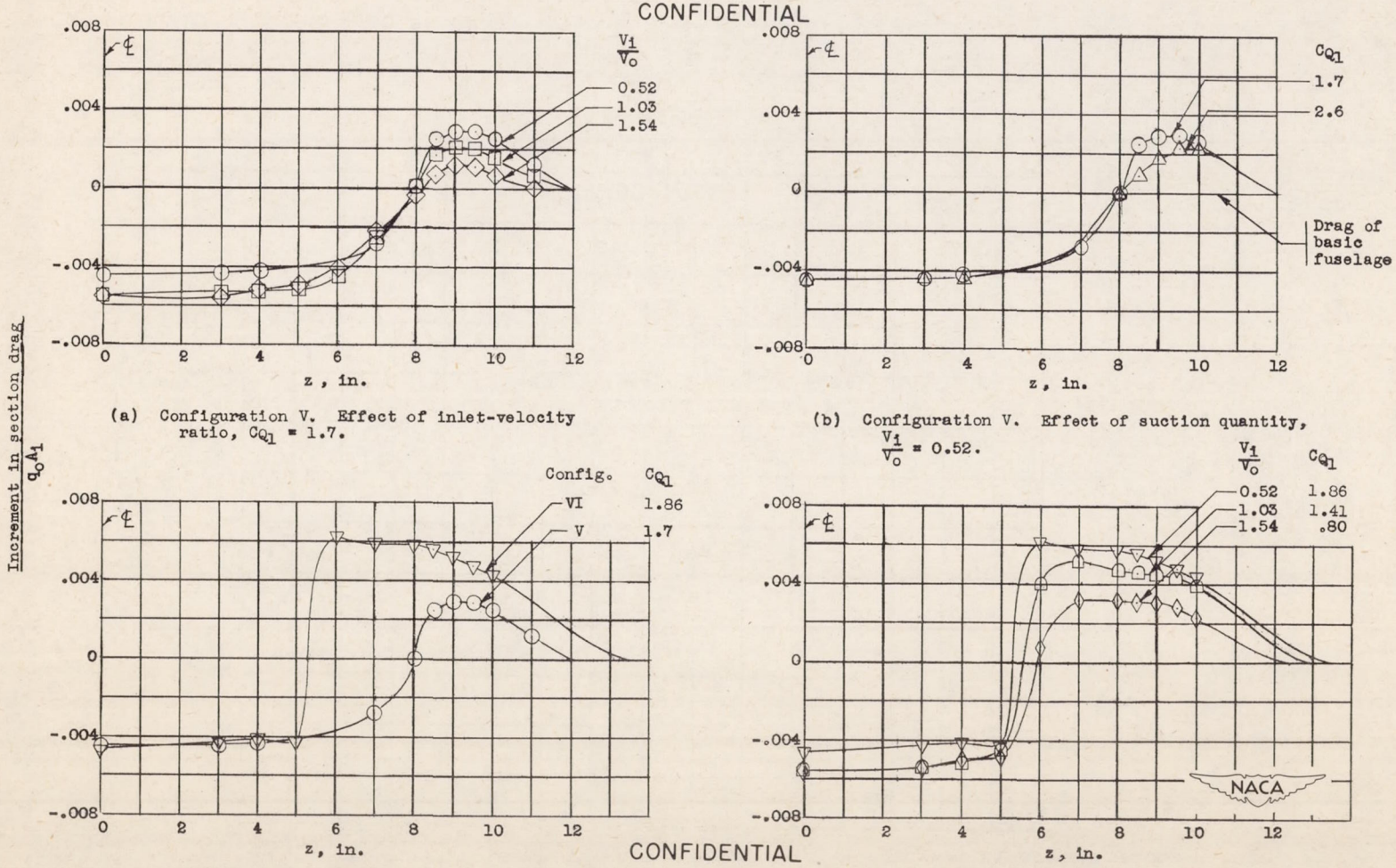

(a) Configuration V. Effect of inlet-velocity ratio, $C_{Q_1} = 1.7$.

(b) Configuration V. Effect of suction quantity, $\frac{V_1}{V_o} = 0.52$.

(c) Configurations V and VI. Effect of bypass installation, $\frac{V_1}{V_o} = 0.52$.

(d) Configuration VI. Effects of inlet-velocity ratio and suction quantity.

CONFIDENTIAL

Figure 21.- Spanwise distribution of section wake drag increment at station 8 caused by installation of scoop. Boundary layer B.

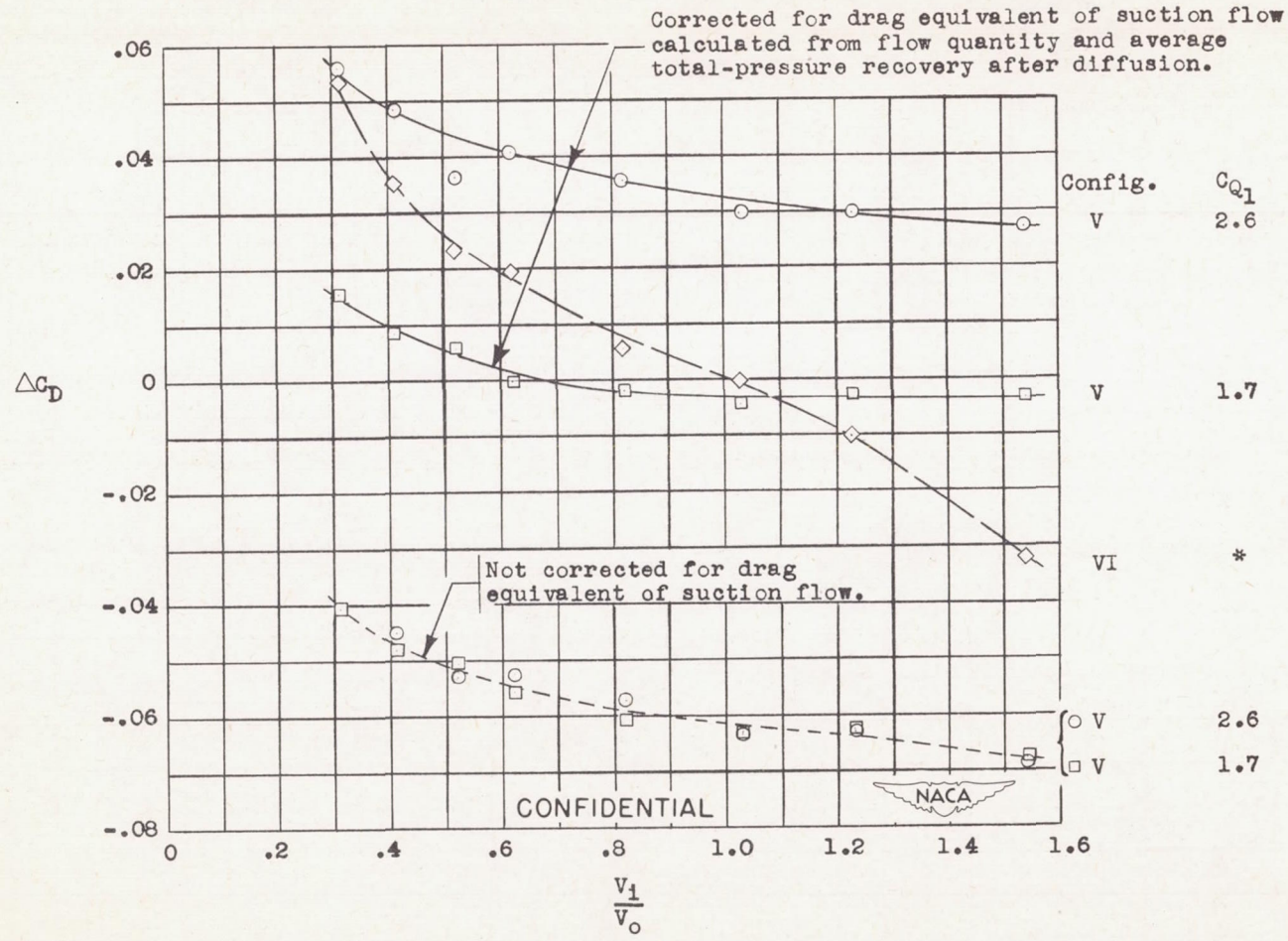

Figure 22.- Increase in external drag caused by installation of scoop. Boundary layer B.

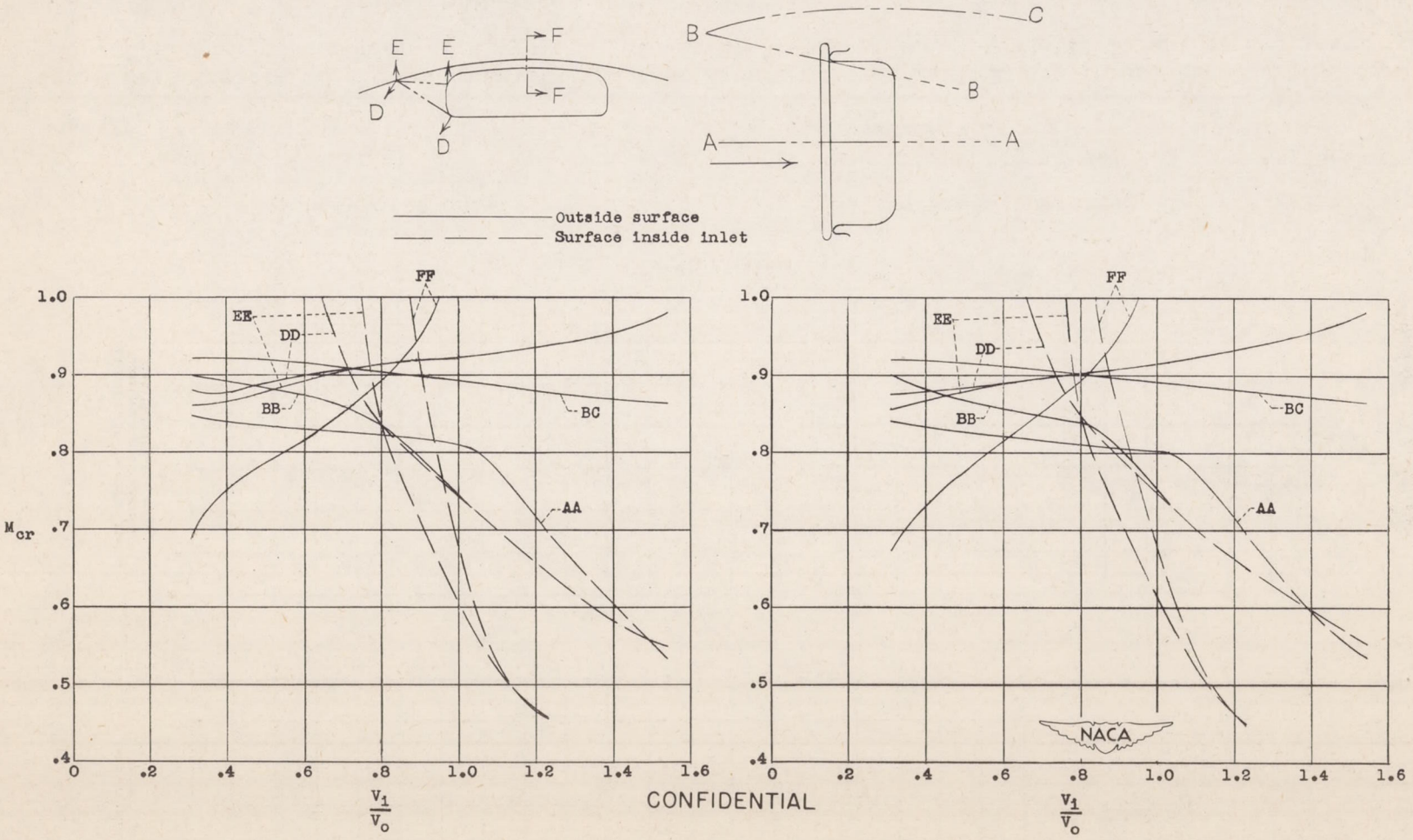

(a) $C_{Q_1} = 1.7$.

(b) $C_{Q_1} = 2.6$.

Figure 23.- Predicted critical Mach number characteristics of configuration V. Boundary layer B.

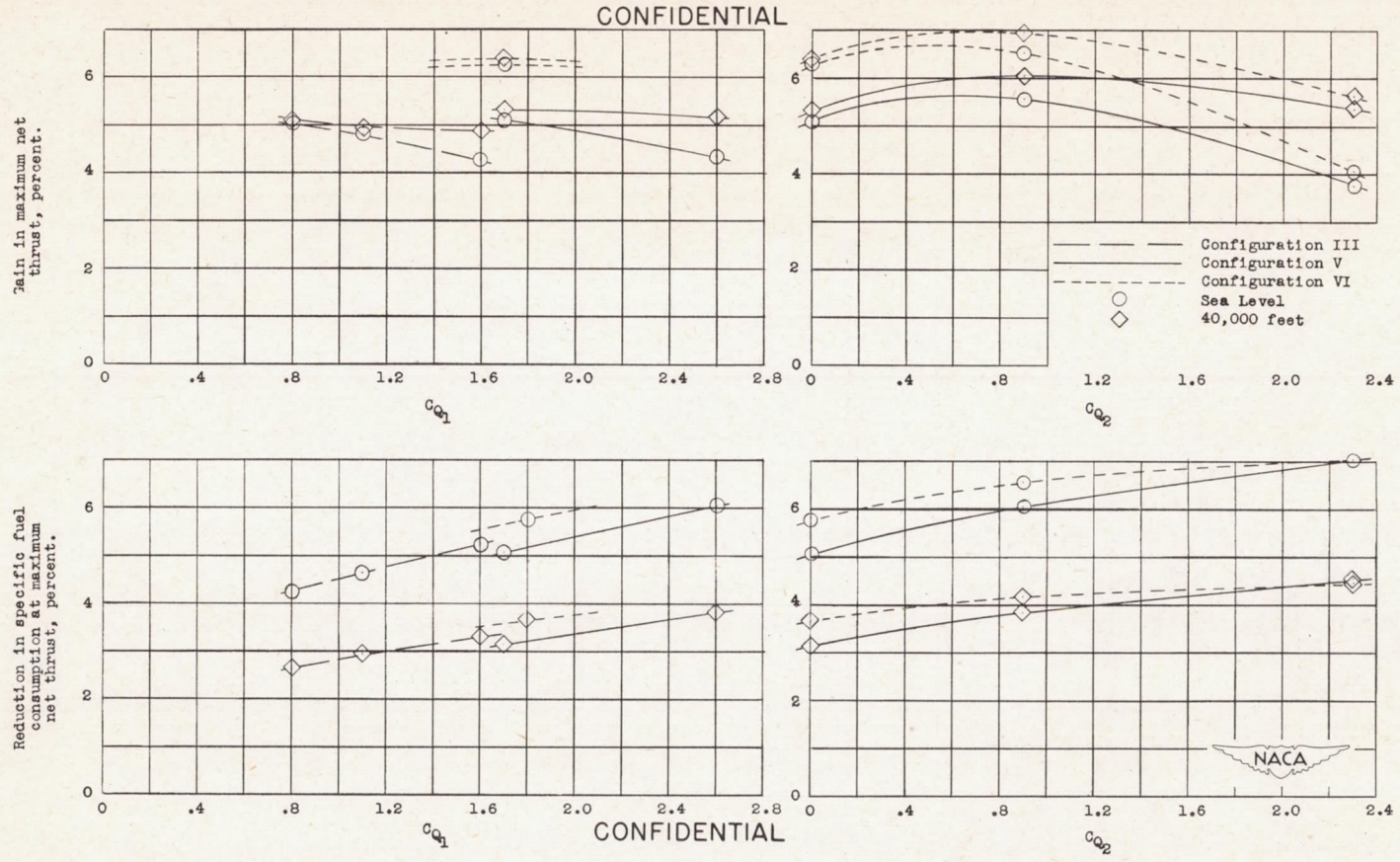

(a) Ramp slot only.

(b) Two slots operating, C_{Q_1} = 1.7 for configuration V and 1.8 for configuration VI.

Figure 24.- Effects of suction quantity and slot arrangement on maximum net thrust and corresponding specific fuel consumption of a typical jet engine (rated at 4000 lb static thrust at sea level at 7700 rpm) for a typical high-speed design condition. V_o = 600 mph, $\frac{V_i}{V_o}$ = 0.6, engine operating at rated rpm, boundary layer B.

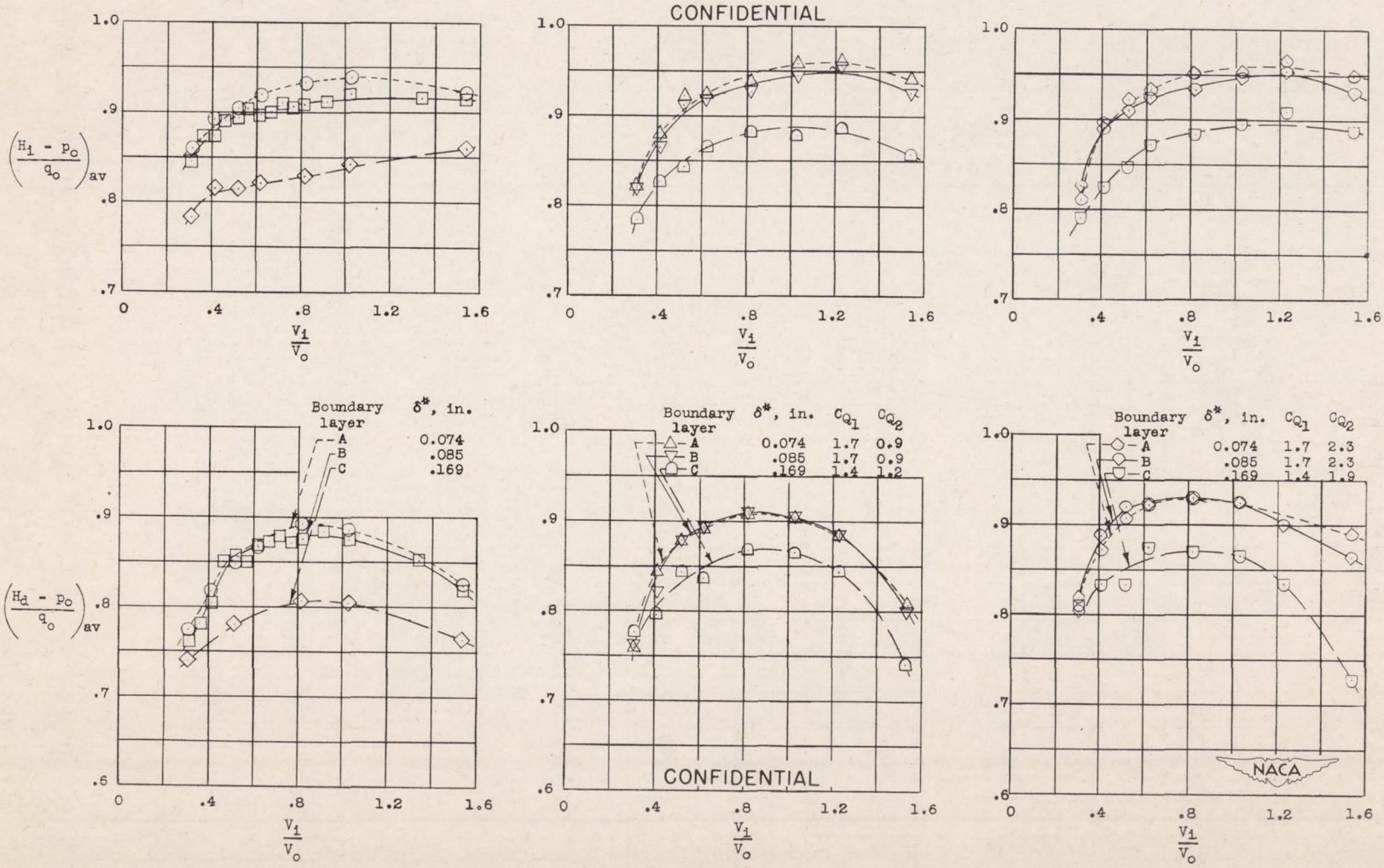

(a) Configuration III, $C_{Q_1} = 1.6$.

(b) Configuration V.

Figure 25.- Effect of boundary-layer thickness on average total-pressure recoveries at inlet and end of diffusers.

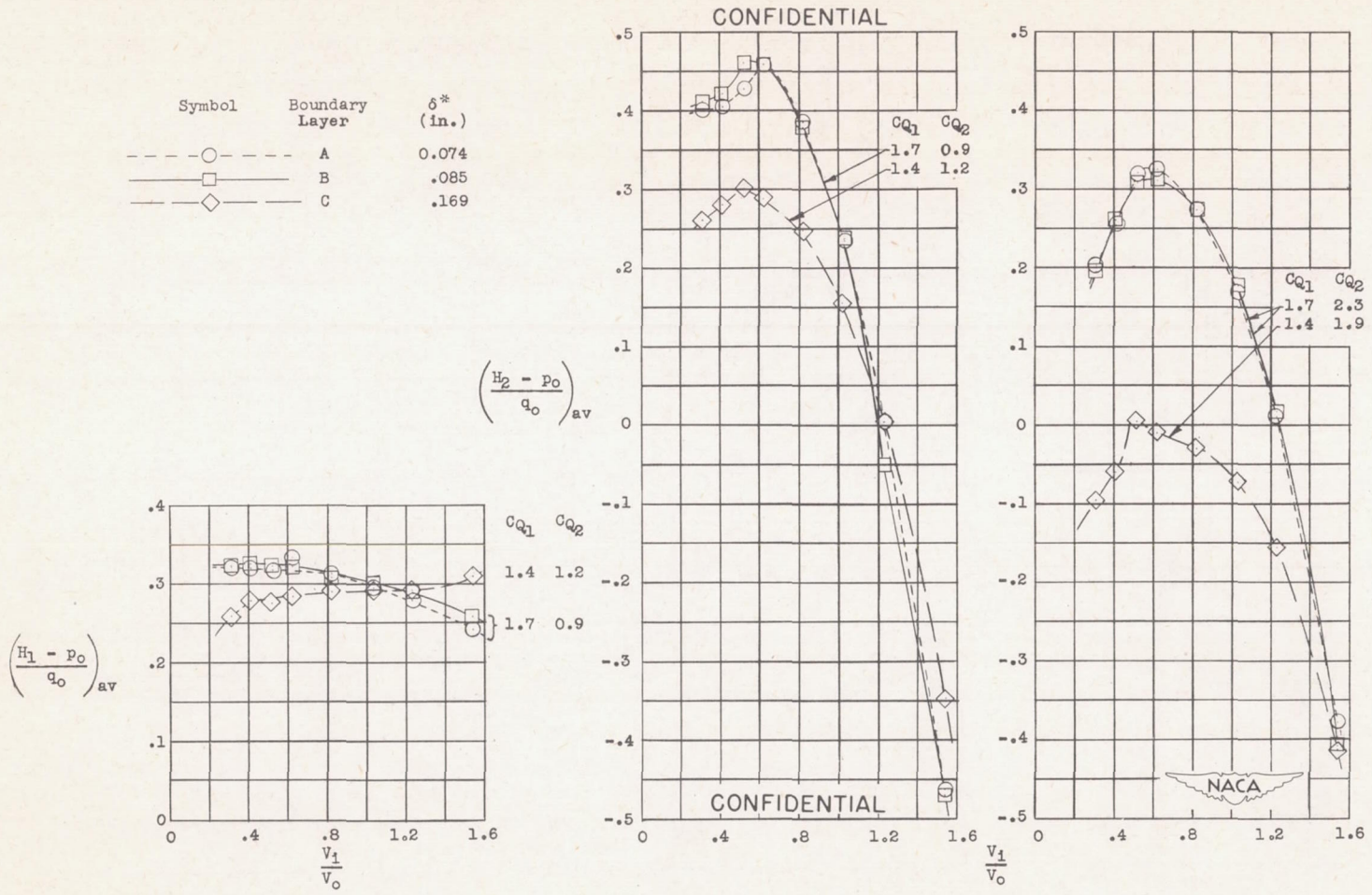

(a) Ramp slot.

(b) Second slot in duct floor inside inlet.

Figure 26.- Effect of boundary-layer thickness on average total-pressure recoveries at ends of diffusers of suction slots of configuration V.

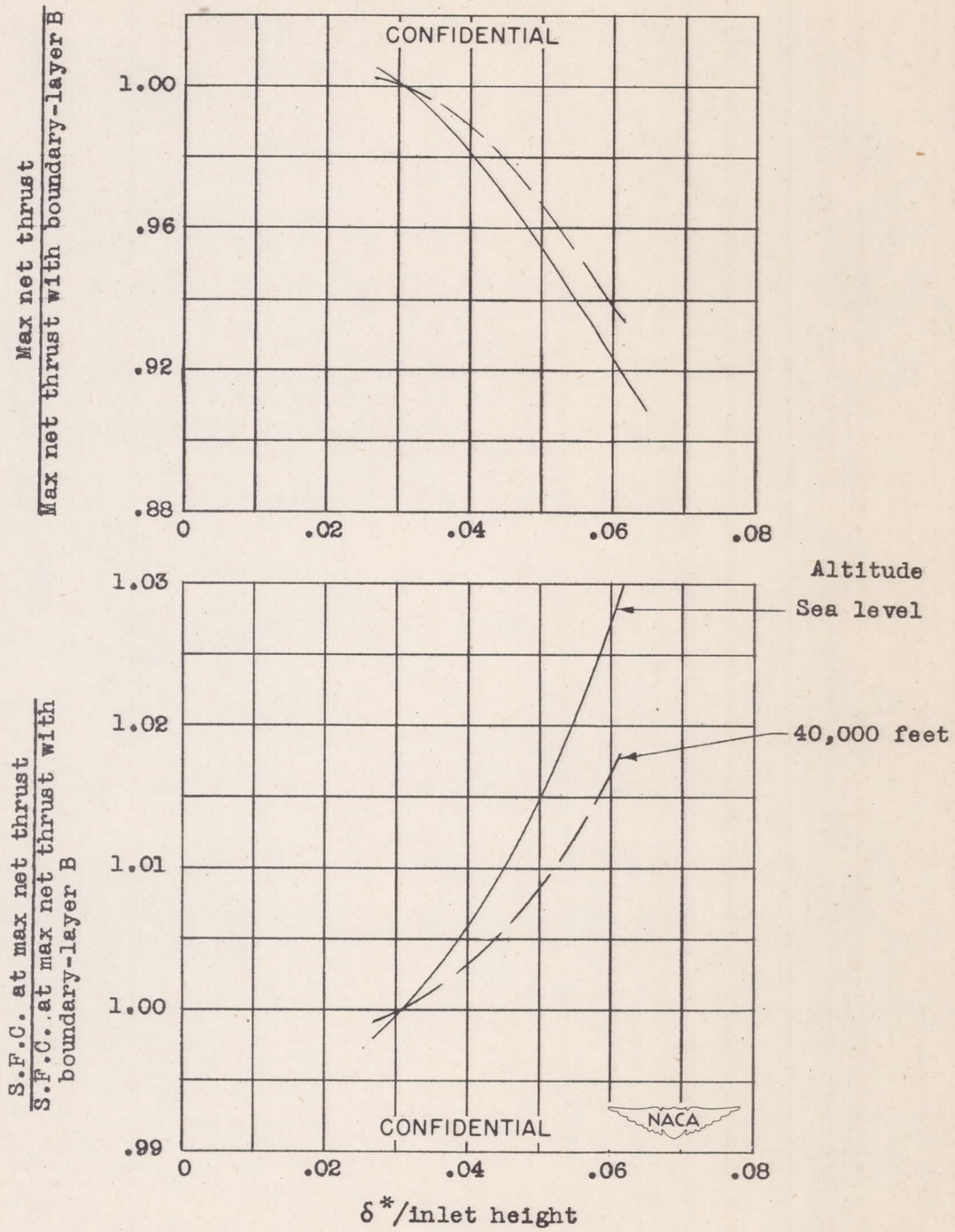

Figure 27.- Effect of boundary-layer thickness on maximum net thrust and corresponding specific fuel consumption of a typical jet engine for a typical high-speed design condition. V_o = 600 mph, $\frac{V_i}{V_o}$ = 0.6, C_{Q_1} = 1.6, configuration III.